



MSc in Electrical and Electronic Engineering -
Master Thesis

**Magnesium cycle-based CO₂
mineralization : Integration in Swiss
Energy-from-Waste plants**

Internship period : 03.01-01.07.22

Author:

Julie Rose DUTOIT

Supervisor at HZI:

Dr.Eng. Jaroslav HEMRLE

EPFL Supervisors:

Prof. François MARÉCHAL

PhD. Shivom SHARMA

Contents

1	Introduction	1
1.1	Background	1
1.2	State-of-the-art	2
1.3	Problem statement	3
1.4	Project background	3
1.5	Company overview : Hitachi Zosen Inova AG	4
1.6	Thesis outline	4
2	Methodology	5
2.1	Modeling with OpenModelica	6
2.1.1	Technologies library	7
2.1.2	Fixed investment cost estimation	9
2.1.3	Transport logistics	11
2.1.4	Life-cycle analysis approach	11
2.2	Process integration	12
2.2.1	Optimization with OSMOSE	12
2.2.2	Heat integration	13
2.2.3	Key performance indicators	14
3	CO₂ mineralization pathways overview	15
3.1	Rocks natural weathering	16
3.2	<i>In-situ</i> mineralization	17
3.3	<i>Ex-situ</i> mineralization	18
3.3.1	Direct mineralization	18
3.3.2	Indirect mineralization	20
3.4	Mineral source	22
3.4.1	Alkaline feedstock	22
3.4.2	Activation	27
3.5	Mineralization products	28
3.6	Logistics of supply chain	29

4	Plant process overview	31
4.1	Acid leaching	32
4.2	CO ₂ dissolution	33
4.3	CaCO ₃ precipitation	34
4.4	Magnesium salts regeneration	36
4.5	Resources and energy flows	39
4.6	Fixed-investment cost	41
5	Process integration into the Energy-from-Waste context	43
5.1	Energy-from-Waste plant	43
5.2	Utilities integration	44
5.3	Plant arrangement	47
6	Mineralization scenarios	50
6.1	Scenario 1 : Pure CaCl ₂ intake	51
6.2	Scenario 2 : Wollastonite-based mineralization	51
6.3	Scenario 3 : Industrial alkaline waste utilization	52
6.3.1	3a : Separated sites	53
6.3.2	3b : Unified site	54
6.4	Scenario analysis	54
6.4.1	Environmental performance	54
6.4.2	Economic performance	57
6.4.3	Key performance indicators	58
7	Discussion	59
7.1	Integration in the industrial landscape	59
7.2	Process optimization	60
7.3	Decarbonizing the Energy-from-Waste plant	60
7.4	Profitability analysis	61
7.5	Carbonfree Chemicals : process performance	62
8	Conclusion	64
A	<i>Carbonpathway</i> library documentation	i

Abstract

An *ex-situ*, indirect aqueous CO₂ mineralization pathway based on magnesium solvent cycling for precipitated calcium carbonate is studied for application in the Energy-from-Waste context in Switzerland. Necessary main equipment components, resources flows and energy requirements are determined for a mineralization plant capacity of 100 kt_{CO₂}/y. The options for input alkaline material are screened and a selection of scenarios are simulated using a library of models developed with the software OpenModelica.

Assessed with the platform OSMOSE, the process integration to the municipal solid waste incineration plant and a range of heat utilities enables the determination of heat recovery opportunities and the assessment of the plant configurations options. In particular, it is found that the EfW boiler steam typically provides half of the heat requirements for the mineralization before design optimization.

Three distinct scenarios for plant arrangement and calcium sourcing are defined, respectively assessing pure calcium salts, mined wollastonite ore and steel waste slags. The effective EfW plant decarbonization reaches 23.8% at best, but improvement on process efficiency and design may significantly increase this performance to achieve lower carbon intensities and EfW plant decarbonization potential of more than 64%. A profitability analysis of this decarbonization system shows that CO₂ capture costs are relatively high, but that the PCC retail price might play an important role in offsetting the mineralization plant total annual expenditures.

Keywords: Energy-from-Waste, Carbon Capture Utilization and Sequestration, Indirect CO₂ mineralization, Magnesium salts, Process Integration

Acknowledgments

My gratitude goes to Jaroslav, for being such a supportive, respectful, instructive and constructive supervisor at the company. Thank you for trusting me and my work, and for leaving so much freedom to it. Cheers to our brainstorming sessions and other more philosophical discussions !

To Shivom, Rafael Graf, Niccolò and Ayoung (last but not least, my dear), for the great collaboration and kindness all along the internship.

To Professor François Maréchal, for your support and good advice.

To Carbonfree Chemicals, in particular the CTO Joe Jones and CEO Martin Keighley, for valuable insights and interesting exchanges from the front line of the development of this important technology.

To all the dear colleagues I am grateful to have had, for the daily comfortable ambiance and passionate discussions around energy technologies, in so many different areas of application.

To the rowing team Belvoir Ruderclub, which gave me so much more than a sport to practice... I will always cherish you.

Julie

List of Figures

2.1	Study workflow, with specification of each tool used and its programming language. . .	5
2.2	Architecture of the OpenModelica environment, taken from OpenModelica, 2022. . . .	7
2.3	Developed OpenModelica library of technology models, called Carbonpathway in reference to its main purpose : supporting decarbonization pathways assessment.	8
2.4	Simple determined model for wollastonite grinding, with economic (rock costs, ground minerals revenues, power price, grinder investment cost, O&M costs, etc.) and environmental (CO ₂ footprint from power emission factor and other sources) accounting structure.	9
2.5	Classification of capital cost estimates, taken from AACE, 2005.	10
2.6	OSMOSE platform optimization methodology, as presented in Tock, 2013.	13
3.1	Material fluxes and process steps associated with the mineral carbonation of silicate rocks or industrial residues, taken from IPCC, 2005.	16
3.2	Bjerrum plot of carbonate speciation versus pH, taken from Yuen et al., 2016.	17
4.1	Scheme of the indirect, aqueous mineralization process based on hydrated MgCl ₂ regeneration to Mg(OH) ₂	32
4.2	Flow sheet of the main mass, power and heat flows per process unit.	39
4.3	Composite curves of the mineralization process hot and cold streams, before integration to the EfW plant.	40
4.4	Grand composite curve of the mineralization process, before integration to the EfW plant.	41
4.5	Purchased equipment cost breakdown for the main components of the whole mineralization plant infrastructure, including salt production site (fine grinding and leaching process).	42
5.1	Grand composite curves of the mineralization process sub-system and the utilities sub-system, composed of EfW steam, cooling water and NG boiler.	45
5.2	Grand composite curves of the integrated mineralization process, with heat pumping and DHN.	46
5.3	Grand composite curves of the total integrated system, when utilities are integrated to the process. <i>Left</i> : reference case with only EfW steam, cooling water and NG boiler. <i>Right</i> : environmentally improved case with addition of electrical fluid bed, DHN and HP.	47

5.4	The distinguishable blocks of the mineralization pathway, which can be clustered in different sites.	48
6.1	Scheme of the carbonation route using pure CaCl_2 as alkaline input.	51
6.2	Scheme of the wollastonite carbonation route.	52
6.3	Scheme of an industrial waste carbonation route in the case of separated sites.	53
6.4	Environmental impact of the mineralization plant for each scenario, without heat and cold utilities. The dashed line indicates the total amount of CO_2 taken up by the process (hence contained in the EfW flue gas, accounting for both biogenic and non-biogenic CO_2) : $126.7 \text{ kt}_{\text{CO}_2}/\text{y}$	55
6.5	Environmental impact of the whole plant for each scenario, accounting for heat and cold utilities.	56
6.6	Environmental impact of the whole plant for each scenario, considering indicatively the displacement of PCC production.	56
6.7	Operational expenditures of the whole plant for each scenario, accounting for heat and cold utilities.	57
6.8	Total expenditures (OPEX and annualized CAPEX) of the whole plant for scenarios 1, 3a and 3b, accounting for heat and cold utilities. Scenario 2 is omitted given its significantly higher annual OPEX.	58

List of Tables

2.1	Emission factor (activity-based approach) of transport modes, using average values from ECTA and CEFIC, 2011. <i>Note : values for diesel trucks are comparable to super B-train trailer tank trucks in Pootakham and Kumar, 2010.</i>	11
3.1	Magnesium, calcium and iron content of various igneous rocks, with corresponding mass ratio necessary for carbonation R_{CO_2} and experimental conversion efficiency of the Mg, Ca and Fe ions to carbonated form (Lackner et al., 1995, O'Connor et al., 2005). <i>Note : Basalts, composed of pyroxenes, olivines, magnetites and feldspars, have high ratio R_{CO_2} (>4.9) and low conversion efficiency η_{exp,CO_2} (ca. 15%). * indicate non-reported values.</i>	23
3.2	Chemical composition (in [wt.%]) and estimated sequestration potential (kg_{CO_2}/t_{waste}) of diverse industrial alkaline wastes, both approximate theoretical value ϵ_{th,CO_2} and experimentally determined ϵ_{exp,CO_2} range. <i>Note : BOF : Basic Oxygen Furnace, EAF : Electric Arc Furnace, AOD : Argon Oxygen Decarburization. Data gathered from : Shen and Forssberg, 2003, Ecke, 2003, Yadav et al., 2010, Jo et al., 2014, Sanna, Uibu et al., 2014, Ukwattage et al., 2014, L. Wang et al., 2019, Meng et al., 2021, W. Liu et al., 2021, Rausis et al., 2021, Xie et al., 2022.</i>	25
3.3	Estimated CO_2 sequestration potential of selected industrial alkaline wastes in Switzerland, based on national availability and experimental carbonation efficiency ϵ_{exp,CO_2} (taken from Table 3.2). <i>Note : Data gathered from Zucha et al., 2020, Tomohiro, 2021, NipponSlagAssociation, 2003, Schorcht et al., 2013, CemSuisse, 2022, PerlenPaperAG, 2022, Bajpai, 2015, AluSuisse, 2015, Y. Liu and Naidu, 2014, Renforth, 2019.</i>	26
4.1	Initial fixed capital expenditures (CAPEX), including direct and indirect costs, calculated with both the Lang estimation method and bare-module cost approach. Uncertainty ranges are based on error propagation from estimated unit components cost ranges.	42
5.1	Municipal waste incineration flue gas composition before and after state-of-the-art flue gas treatment. <i>Note : Heavy metals (HM) comprise Hg, Cd, Pb and Zn. * indicate unspecified values.</i>	44

5.2	Utilities sizes for the reference case of EfW steam, NG-fired boiler and cooling water tower for cold utility.	45
5.3	Utilities sizes for the improved case, when an electrically heated fluidized bed reactor (FB), HP and DHN connection are additionally considered. No NG-fired boiler is selected.	46
5.4	Utilities sizes when the fluidized bed reactor (FB) is gas-driven, and HP and DHN connection are considered. The heat equivalent for NG combustion is based on LHV basis.	47
5.5	Summary of the assumptions regarding resources transportation logistics. Transport types, related cost (computed from Bina et al., 2014 and) and assumed distances for the optimization are listed for the main resources flows, if the plant is subdivided. . . .	49
6.1	Sensitivity of the plant annual TOTEX on key commodities purchase/selling price increase of 1%, in percentage.	58
6.2	Key performance indicators for each scenario. <i>Note : here, the carbon intensity indicator does not take into account the displacement impact of PCC production.</i>	58

Nomenclature

Acronyms

APC	Air Pollution Control	IPESE	Industrial Processes and Energy Systems Engineering
BA	Bottom Ash	LCA	Life-Cycle Analysis
BF	Blast Furnace	LHV	Lower Heating Value
BOF	Basic Oxygen Furnace	MILP	Mixed Integer Linear Programming
CAPEX	Capital expenditure	MSWI	Municipal Solid Waste Incineration
CCUS	Carbon Capture Utilization and Sequestration	NG	Natural Gas
CIF	Cost, Insurance and Freight	OPEX	Operational expenditure
CKD	Cement Kiln Dust	ORC	Organic Rankine Cycle
CW	Cooling Water	PCC	Precipitated Calcium Carbonates
DETEC	Département fédéral de l'Environnement, des Transports, de l'Energie et de la Communication	PI	Process Integration
DHN	District Heating Network	TOTEX	Total expenditure
EAF	Electric Arc Furnace	UNCTAD	United Nations Conference on Trade and Development
EfW	Energy-from-Waste	VBSA	Verband der Betreiber Schweizerischer Abfallverwertungsanlagen
FA	Fly Ash	WtE	Waste-to-Energy
FB	Fluidized Bed	Symbols	
FG	Flue Gas	ϵ_{exp,CO_2}	Experimental sequestration efficiency of industrial alkaline waste, kg_{CO_2}/t_{waste}
FOB	Free On Board	ϵ_{th,CO_2}	Theoretical sequestration efficiency of industrial alkaline waste, kg_{CO_2}/t_{waste}
GHG	Greenhouse Gas	η_{th,CO_2}	Experimental conversion efficiency of the mineral ore alkaline content to carbonates, -
GWP	Global Warming Potential	R_{CO_2}	Mineral ratio of ore to CO_2 , kg_{ore}/kg_{CO_2}
HHV	Higher Heating Value		
HP	Heat Pump		
IPCC	Intergovernmental Panel on Climate Change		

Chapter 1

Introduction

1.1 Background

Climate change, one of the greatest environmental threats of our times, is originated by significant increase in atmospheric concentration of greenhouse gases from human activities. Following the Kyoto protocol of 1997 and the Paris Agreement in 2015 (Maizland, 2021), incentives and political efforts have started in many European countries in order to tackle reduction of carbon dioxide (or equivalents) released by industries, transports, agriculture, households through heating systems and other sectors. In particular, an international trading system for CO₂ emissions exists since 2005 : the Emission Trading System ETS (“Système d’échange de quotas d’émission de l’UE (SEQE-UE)”, 2022).

In Switzerland, Energy-from-Waste (EfW) plants are currently exempt from any carbon taxation : neither the CO₂ levy of 120 CHF/t_{CO₂} (FOEN, 2021) nor the ETS (FOEN, 2022a) is applied on their activity. Consequently, they have not yet deployed decarbonization technologies to reduce the CO₂ emissions of municipal solid waste (MSW) incineration flue gas. Together with special solid waste used as alternative fuel in Swiss industries, MSW incineration flue gases amounted to 6.8% of the total greenhouse emissions from all sectors in 2020, with industries (24.8% in total), transports (31.6%), agriculture (14.6%), households (16.4%) and others summing up to 11 Mt_{CO₂}/y (FOEN, 2022b). In March 2022, the Federal Department for Environment, Transport, Energy and Communication (DE-TEC) and the Association of Plant Managers of Swiss Waste Treatment Installations (VBSA) renewed and realigned their agreement *to reduce emissions from waste incineration, to create incentives for more efficient energy use and to promote the deployment of CO₂ capture in waste treatment installations* (FOEN, 2022a). This new agreement forces waste treatment installations to put at least one CO₂ capture plant of minimum nominal capacity of 100 kton_{CO₂}/y into operation by 2030. Should it not be the case by the end of that year, the agreement obligates the participation of EfW plants in the European Emission Trading System ETS (swissinfo.ch, 2020). It further incentivizes the operators to lay the foundations for carbon capture and storage (CCS) on a large scale in the medium to longer term, setting annual interim targets for this. To reach this target, Swiss incineration plants have to implement a decarbonization strategy and select technologies that fulfill the CO₂ capture goal.

1.2 State-of-the-art

The complex challenge of capturing or utilizing industrial CO₂ instead of rejecting it into atmosphere has been extensively investigated and reviewed (Mikkelsen et al., 2010, Bains et al., 2017, Osman et al., 2021). One of the potential decarbonization technologies for industrial application is mineral carbonation, reproducing natural weathering with faster kinetics and enhanced conversion efficiency on industrial scale. Since 1990, considerable efforts of research and development have been devoted to improve the technical feasibility of various different mineralization pathways. In the past decade, start-ups and companies have emerged in the field to tackle the energy use, operational considerations, product value and economics, in the aim to propose profitable business models. Mineralization of CO₂ has proven to be economically viable at industrial scale in the case of injection of CO₂ in the cement production process for improvement of concrete quality (curing, El-Hassan, 2020) or at the SkyMine plant in Texas for production of sodium bicarbonate (Walters, 2016). However, uncertainty remains about the potential of these 2 specific technologies as effective overall CO₂ sequestration technology due to specific high energy demand (Ravikumar et al., 2021) or suitability for larger scale application (Lee and Lee, 2021).

In general, it is claimed that the current global market for raw commodities produced by *ex-situ* mineralization pathways might easily be flooded if deployed on global scale (Sanna, Hall et al., 2012). Furthermore, 10–15% of the global CO₂ emissions are released by small/medium emitters, who represent a better target for carbon capture by mineralization in terms of logistics and technology effectiveness compared to large emitters (Sanna, Hall et al., 2012). Thus, indirect carbonation pathways may be implemented as niche application to non-displaceable important carbon emitters (Dwortzan, 2021), to facilitate the larger deployment by economic or environmental advantage. For instance, the integration of cement kiln dust mineralization in cement plants is shown to improve overall profitability of the plant (Pedraza et al., 2021). This type of industrial integration should include symbiotic network design between power generation, mining, manufacturing, and CO₂ capture plants to exploit the interdependencies between these sectors, as highlighted by Yuen et al., 2016. In fact, the environmental burden of mineralization process energy demand might be at least partly offset by the utilization of the carbonated material (Ostovari et al., 2022, Sanna, Hall et al., 2012). Beside the off-take of this main product, the consideration of reuse or disposal of by-products such as silicate residues, leached metal ions, salts, acids and bases, wastewater and waste heat is essential for the holistic approach of mineralization pathways (Sanna, Uibu et al., 2014).

In spite of the challenges related to mineral carbonation at industrial scale, motivation for further investigation stays, given the stable, leakage-free method with no long-term monitoring, and the large feedstock availability, namely Ca and Mg-based silicate minerals (Romanov et al., 2015). In Europe, Ostovari et al., 2022 show that the current available solid feedstock (considering currently active mines of natural minerals and steel slag from electric arc furnace (EAF) steel production) could already mitigate 4.8 Mt_{CO₂}/y, and that the mineralization supply chain could reduce the GHG emissions of industry in Europe by up to 160 Mt_{CO₂}/y. This figure may be compared to 877.31 Mt_{CO₂-eq} emitted by the industrial sector in the EU-28 in 2017.

1.3 Problem statement

This project has the purpose to understand and evaluate a specific magnesium-cycle based indirect CO₂ mineralization pathway in the context of Waste-to-Energy plants in Switzerland. There exist many options of integration in the industrial landscape, which shall be investigated and compared. The strategies to assess the research questions listed hereinafter are formulated in the objectives.

Research questions

- What are the interfaces of the indirect Mg-cycle based mineralization pathway for industrial process integration ?
- Under which conditions of clustering and available utilities does the integrated Mg-cycle based mineralization fulfil the sequestration purpose ?
- Which option(s) of alkaline input material and plant configuration - if any - is economically profitable in Switzerland ?

Objectives

1. Understanding of all processes involved in the mineralization pathway, determining the energy and mass balances and accounting for related CO₂-equivalent emissions.
2. Profitability assessment of the mineralization plant, estimating the total expenditures and revenues related to infrastructure components capital cost, commodities, utilities required and other operational costs, as well as transport cost.

1.4 Project background

This project is realized as Master Thesis within the Energy Technology and Science Master program at Ecole Polytechnique Fédérale de Lausanne (EPFL), during a 6-months internship at Hitachi Zosen Inova (HZI, Zürich). This thesis is created jointly within the laboratory of Industrial Process and Energy System Engineering (IPESE), under the supervision of Prof. François Maréchal and Dr. Shivom Sharma, and HZI company, under the supervision of Dr. Jaroslav Hemrle.

The internship is carried out in the Research & Development Department of the company, within the framework of the Renewable Gas research group. The project is linked to the collaboration of HZI and CarbonFree Chemicals Holding¹, jointly developing technologies to separate and mineralize CO₂ from flue gases of Energy-from-Waste (EfW) plants, following the signature of a Memorandum of Understanding (HZI, 2021) in November 2021.

¹<https://carbonfree.cc/>

1.5 Company overview : Hitachi Zosen Inova AG

The initial company was established in 1933 as “L. von Roll Aktiengesellschaft” in Switzerland, later known as Von Roll Inova. In 2010, it joined Hitachi Zosen Corporation, one of Japan’s larger industrial and engineering firms, creating the current Hitachi Zosen Inova AG. HZI has become a global leader in energy from waste (EfW) and renewable gas, with over 600 plants across the world.

The HZI Group is divided into 4 areas of activities :

- **Plant Engineering & Construction** : HZI is an Engineering, Procurement and Construction (EPC) supplier of energy-from-waste and renewable gas plants, providing technology and active in the project development process, with capabilities of providing Operation and Maintenance (O&M) during the plant lifetime.
- **Services** : This area of activity provides support for a broad range of plant infrastructures, such as incineration and boiler equipment, flue gas treatment equipment, energy recovery equipment and digester and biogas upgrading equipment.
- **Energy-from-Waste** : The state-of-the-art thermal treatment of the waste by incineration is developed at HZI with focus on effective combustion, energy recovery, flue gas treatment and recovery of valuable residues.
- **Renewable Gas** : HZI offers in particular 3 technologies to produce biogas, biomethane, hydrogen and synthetic natural gas. The Kompogas® anaerobic digestion produces natural fertilizers and raw biogas whilst managing biogenic waste, the BioMethan Gas Upgrading process treats raw biogas to produce high-grade biomethane, and hydrogen is produced through the EtoGas power-to-gas technology.

1.6 Thesis outline

The methodological approach for this thesis, including the presentation of the simulation tool OpenModelica and the optimization software OSMOSE, is described in Chapter 2. Chapter 3 reviews the existing pathways for CO₂ mineralization and lists the options for mineral sources. The specific mineralization route studied in this work is presented in detail in Chapter 4.

Chapter 5 assesses the integration of the mineralization pathway to an EfW plant in Switzerland, presenting the utilities considered, the heat integration performance and plant configuration analysis. Specific scenarios are assessed in Chapter 6, and key findings of all chapters are highlighted and put into perspective in Chapter 7.

Chapter 2

Methodology

This chapter presents the tools developed and used during the internship to assess the research questions and describes in detail the approach followed. The workflow is displayed in Figure 2.1, highlighting the working environment for each step of the study.

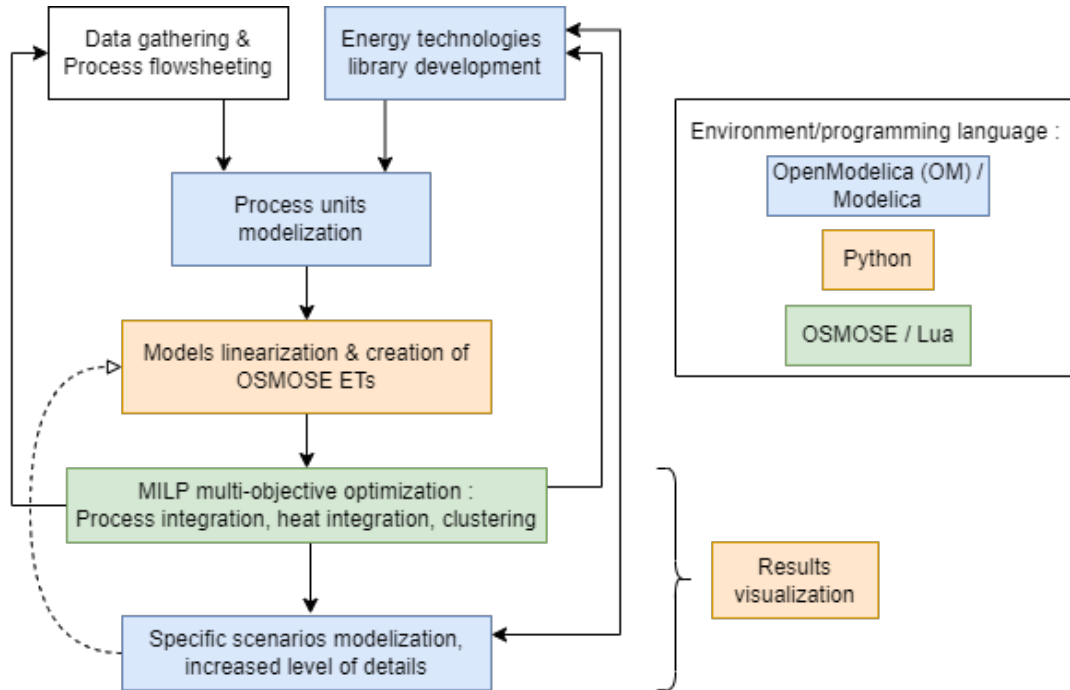


Figure 2.1: Study workflow, with specification of each tool used and its programming language.

The data gathering is done thanks to literature reviewing on the mineralization technologies status and access to the HZI company database for techno-economic parameters of resources, industrial reactor infrastructures (process units) and operating Energy-from-Waste plants. In parallel, a library of models on energy-related technologies is developed in the open-source simulation software OpenModelica, with which the process units of interest are modeled and linked in order to represent the mineralization pathway energy and mass balances.

In order to use the models in a linear programming optimizer, those have to undergo a linearization

process. For this step, two options were investigated : export of Functional Mock-up (FMU) Interfaces directly from the OpenModelica files, and utilization of the OMPython package in Python 3.9, for models simulation and access to optimized parser results that give control over every element of the output. The latter is the preferred solution for the present framework, given the increased constraints on OpenModelica models internal structure in the case of FMUs usage.

The linearized models are formatted in the programming language Lua and used with the OSMOSE optimization software for process integration in the industrial context and clustering regarding logistics and land price. Depending on the optimization results, defined scenarios are then implemented in the Modelica language for more profound analysis of specific case studies, enabling the use of non-linearity and eased implementation of specific contextual details and integration. The performance of the different pathway scenarios is eventually evaluated and compared on the basis of predefined metrics comprising economic, environmental and other useful indicators. Iterative development of this scenario definition is possible through repeated linearization and subsequent optimization of the Modelica models, for example in order to run the optimization around different operational points (depicted in the workflow as dotted arrow).

2.1 Modeling with OpenModelica

Modelica is an object-oriented, declarative, multi-domain modeling language for equation-based, component-oriented modeling of complex systems. It is available in various commercial simulation environments and one free, open-source environment, OpenModelica¹, developed and supported by Linköping University and the Open Source Modelica Consortium (OSMC) since 1998. It is chosen as simulation tool for this thesis as it offers good documentation and a large number of functionalities, enabling flexible use : debugging, optimization, visualization and 3D animation, web-based model editing and simulation, scripting from Modelica, Python, Julia, and Matlab, efficient simulation and co-simulation of FMI-based models, compilation for embedded systems, and more features described in Fritzson et al., 2020. The architecture of the environment is illustrated in Figure 2.2.

¹<https://openmodelica.org/useresources/userdocumentation>

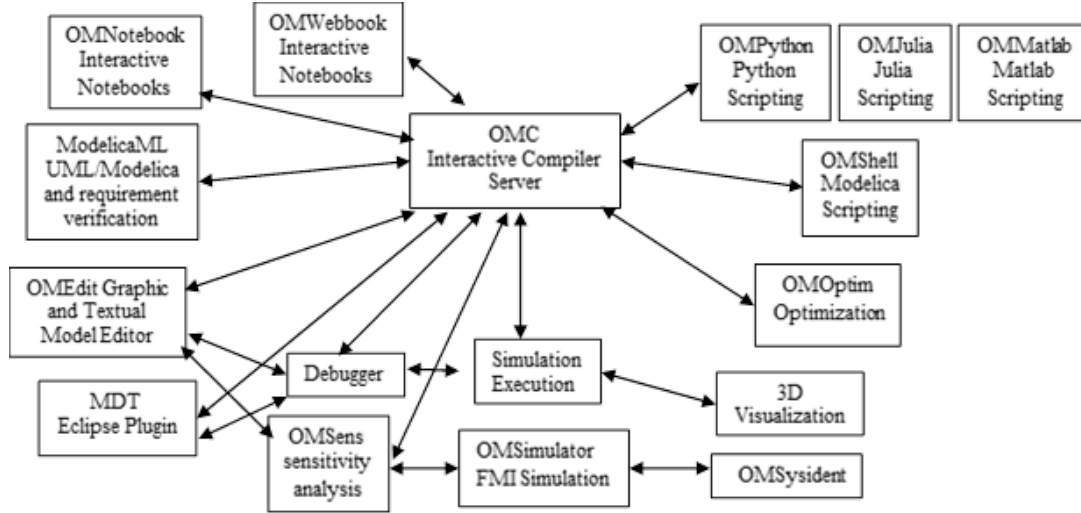


Figure 2.2: Architecture of the OpenModelica environment, taken from OpenModelica, 2022.

The models are developed using the OpenModelica Connection Editor (OMEdit), through which the Modelica Standard Library is available for free use. This default library is useful for modelization of mechanical (1D/3D), electrical (analog, digital, machines), magnetic, thermal, fluid, control systems and hierarchical state machines². Numerical functions, as well as functions for strings, files and streams, are also included. Many commercial, free or user-owned libraries can be added to the collection of libraries, as is done in the present study with the energy technologies library created from scratch, and with software packages for calculation of thermo-physical substances' properties.

2.1.1 Technologies library

Critical requirement and motivation for the development of a dedicated library of technologies models is the need to consistently handle not only general process and thermodynamic properties, but also properties highly specific to waste treatment, material and energy recovery, for example detailed composition of the complex streams. Developed during the internship and under continuous expansion and structural improvement, the library aims at providing support for assessment of energy-related process pathways in the Energy-from-Waste industry context. This library consists in models of process streams, units and whole-chain pathways, each with different possible levels of complexity depending on the users requirement for details.

²<https://github.com/modelica/ModelicaStandardLibrary>

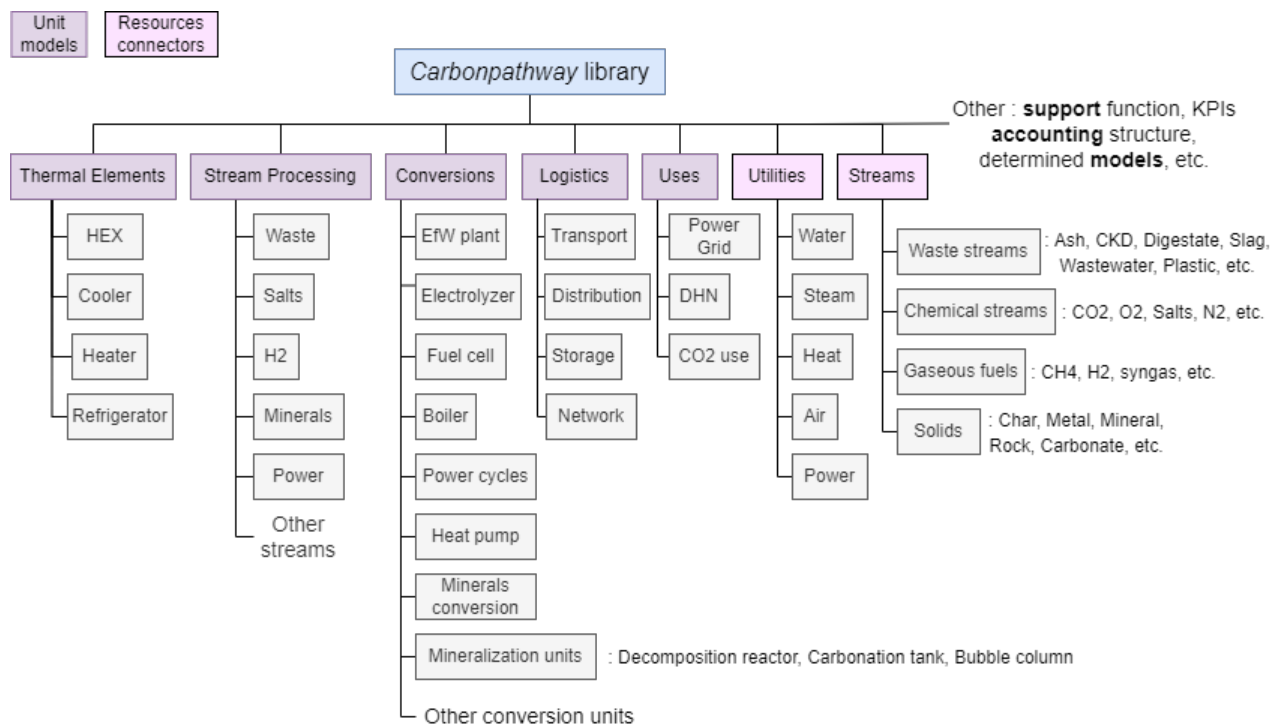


Figure 2.3: Developed OpenModelica library of technology models, called Carbonpathway in reference to its main purpose : supporting decarbonization pathways assessment.

The library is categorized as featured in Figure 2.3. Unit models are currently packaged into 5 main classes : *Conversion* (for processes transforming significantly the nature of the input streams), *Stream processing* (for processing, handling and logistics of specific resources), *Thermal Elements*, *Logistics* (generic distribution, transportation, storage and networking) and *Uses*. The *Utilities* package contain generic resources connectors relevant in most of industrial projects : water, steam, power, air and generic heat connectors. The *Streams* package lists all other resources connectors that are used in the unit models, each being defined through mass flow and varying number of attributes : composition, quality indication, temperature, pressure, etc. Support functions are available in a dedicated folder, and other packages are under development (e.g. control units). For user-friendly and efficient modeling of whole-chain pathways, the models are systematically commented, documented and versioned. For the same purpose, simple icons are designed for each unit and stream, as can be observed in the simple model of Figure 2.4. A flexible Key Performance Indicator (KPI) accounting structure is implemented for systematic and eased accounting of CAPEX (including capital investment, depreciation and salvage value), OPEX (resource costs and revenues, reactors operation and maintenance, taxes/subsidies), Net Present Value (NPV) and environmental impact (currently accounting for CO₂-equivalent emissions only).

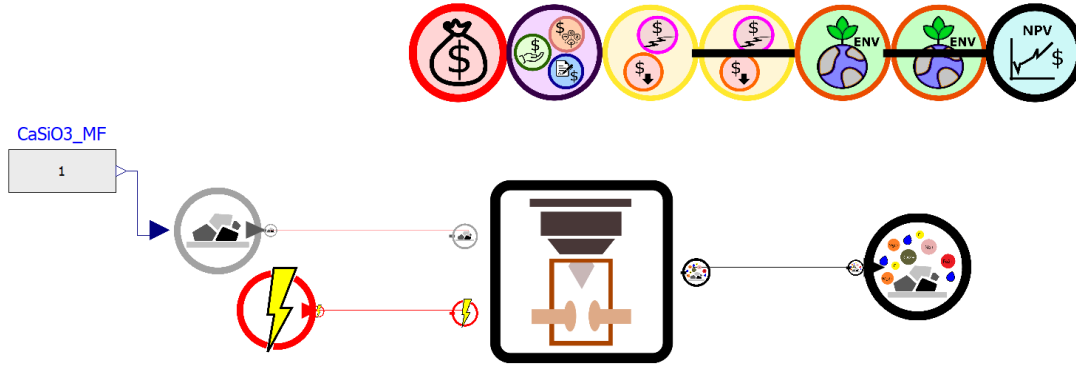


Figure 2.4: Simple determined model for wollastonite grinding, with economic (rock costs, ground minerals revenues, power price, grinder investment cost, O&M costs, etc.) and environmental (CO_2 footprint from power emission factor and other sources) accounting structure.

2.1.2 Fixed investment cost estimation

For this work, a capital costs database (property of the company HZI) of more than 340 industrial components is built and extended with data gathered from combined literature and business data available in the company. The approach for the capital cost estimation of the mineralization project infrastructure follows the state-of-the-art methodology based on unit process cost correlation to its sizing capacity or parameter, as presented in many process and chemical engineering reference documents (Uhlrich and Wiley, 1984). For instance, Turton et al., 2018 estimate the investment costs through a logarithmic law correlation: $\log_{10}(C_{reactor}^0) = k_1 + k_2 \cdot \log_{10}(L) + k_3 \cdot [\log_{10}(L)]^2$ where $C_{reactor}^0$ is the reference purchase price for a certain reference year of a component made of carbon steel and operating at atmospheric pressure, L is the sizing capacity or parameter and k_i are fitting coefficients. In this work, the components cost data is similarly fitted (for the coefficients a , b and c) to the power law $C_{reactor}^0 = a + b \cdot L^c$. The reference cost is then adapted to the year of simulation by taking into account a factor $\frac{I_t}{I_{t,ref}}$, where I_t is the cost index for the current year and $I_{t,ref}$ is the cost index for the reference year.

The purchased equipment cost $C_{reactor}^0$ represents only 15-40% of the total fixed-capital investment cost, as described in (Sari, 2014). All additional direct (piping, instruments and controllers, insulation, electrical wiring, etc.) and indirect (freight, insurances, taxes, construction overhead, engineering expenses, etc.) costs associated with equipment purchase and installation must be taken into account. Depending on the cost estimation level of detail desired, many estimation methods are available as reviewed in Couper, 2003. The Association for the Advancement of Cost Engineering (AACE International, Non-Profit-Organisation) (AACE, 2005) describes the accuracy of those estimates depends on the type of estimate, ranging from order-of-magnitude to detailed estimate. The classification shown in Table 2.5 indicates that the relevant class for the scope of this study is class 4, for which the accuracy range might span from -15% to +50%. The relevant capital cost estimation methods for this class are based on the purchased equipment price, applying a factor dependent either on the phase of the material used (solids/liquids, Lang method) or the type of the equipment

(Hand and Wroth, based on delivered equipment price, methods) to compute the total initial CAPEX of the plant.

Class	Type of Estimate	Description	Accuracy Ranges
5	Order-of-magnitude estimate (also Ratio/Feasibility)	Based on limited information. Concept screening.	Low: -20% to -50% High: +30% to +100%
4	Study estimate (also Major Equipment/Factored)	List of major equipment. Project screening, feasibility assessment, concept evaluation, and preliminary budget approval.	Low: -15% to -30% High: +20% to +50%
3	Preliminary design estimate (also Scope)	More detailed sizing of equipment. Budget authorization, appropriation, and/or funding.	Low: -10% to -20% High: +10% to +30%
2	Definitive estimate (also Project Control)	Preliminary specification of all the equipment, utilities, instrumentation, electrical and off-sites. Control or Bid/Tender.	Low: -5% to -15% High: +5% to +20%
1	Detailed estimate (also Firm/Contractor's)	Complete engineering of process and related off-sites and utilities required. Check Estimate or Bid/Tender.	Low: -3% to -10% High: +3% to +15%

Figure 2.5: Classification of capital cost estimates, taken from AACE, 2005.

For this work, this methodology is put into perspective with the bare module method (Turton et al., 2018), which consists of accounting for the influence of material and pressure level of reactor through their respective factor F_M and F_P when relevant, or through a more general bare module factor F_{BM} taking into account all direct and indirect costs associated with the equipment and installation labour in a radius of around 3 meters. The bare module cost C_{BM} is calculated with the relation :

$$C_{BM} = C_{reactor}^0 \cdot F_{BM} = C_{reactor}^0 \cdot (B_1 + B_2 \cdot F_M \cdot F_P) \quad (2.1)$$

where the coefficients B_i depend on the component type and the application.

Capital cost annualization

In order to compare initial capital costs to operational process costs spanning over the lifetime of an infrastructure, CAPEX can either be annualized or the Net Present Value (NPV) of the annual income generated initially by the investment can be computed. Both approaches are equivalent, and for this study the first approach is preferred.

The annualized CAPEX is computed by $C_{BM,ann} = \tau \cdot C_{BM}$, where the annualization factor τ considers the value of both the investment and subsequent annual income after a certain amount of years n , corresponding to the lifetime of the component, under a certain monetary interest rate i . The factor τ is computed with the following equation :

$$\tau = \frac{i \cdot (1 + i)^n}{(1 + i)^n - 1} \quad [y^{-1}] \quad (2.2)$$

For the scope of this work, the equipment lifetime is typically assumed at 20 years, and the interest rate is taken as 6%.

2.1.3 Transport logistics

As described in numerous literature on transport cost calculation methodology (Pootakham and Kumar, 2010, Bina et al., 2014), the assessment of transportation economics should take into account both fixed and variable transportation cost components. The former, independent of the type and size of the cargo, includes cost of ownership (including vehicle depreciation), annual sale taxes, license fees and taxes, handling fees (loading and unloading), management and overhead (central services, dispatching, etc.) cost, as well as insurance costs. The latter, dependent on the type and size of the cargo and on transport distance, includes fuel cost, labor cost, maintenance and repair cost, tire cost and other possible variable costs such as toll fees.

Although it is demonstrated that the transport distance alone is not the most determining factor in truck transport costs estimation (Martinez-Zarzoso and Nowak-Lehmann, 2007), the transport cost accounting is simplified for the scope of this study. The approach is to first assume a certain state-of-the-art mode of transport (amongst train, truck and sea shipping) for each resource, depending also on the options available on-site. A transport distance is then set by assuming the average distance to a plausible source/sink for a certain resource. Using the UNCTAD database (UNCTAD, 2022), the Cost Insurance Freight (CIF) value of the goods is compared to the Free-On-Board (FOB) value, and the corresponding shipping cost is derived. It is compared to and validated with the unit shipping costs across specific European countries, for a given distance of 500 km, calculated in Bina et al., 2014. In case of a railway transport possibility, the shipping cost is assumed to scale proportionately to the results reported for each country by Bina et al., 2014.

The specific emission factor of transport are systematically taken into account for tracking of the environmental footprint (ECTA and CEFIC, 2011), summarized in Table 2.1.

Transport mode	Specific CO ₂ emissions kg _{CO₂-eq} /(km · ton)
Train	0.022
Truck (diesel, heavy-duty : 40 tons)	0.062
Short-sea/barge	0.016-0.031

Table 2.1: Emission factor (activity-based approach) of transport modes, using average values from ECTA and CEFIC, 2011. *Note : values for diesel trucks are comparable to super B-train trailer tank trucks in Pootakham and Kumar, 2010.*

2.1.4 Life-cycle analysis approach

In an effort to assess the mineralization process in a holistic approach, the consideration of material input upstream activities and by-products off-take by disposal or reuse is essential. For resources to be exchanged with external sources and sinks, the scope boundary is taken at the gate of the plant. Hence, the related buying and selling prices are considered for delivery or off-take respectively at the plant location.

Concerning environmental impact, the present work considers the carbon dioxide emissions to atmosphere, accounted in CO₂-equivalent footprint. The Ecoinvent database (version 3.7.1, Wernet et al., 2016) is used for the environmental impact assessment of the main resources involved in each process. The Life-Cycle Impact Analysis (LCIA) method used for data extraction is IPCC 2013, GWP 100 years, based on the system model of allocation for multi-product activities and cut-off by classification for by-products. Whilst the present thesis does not target to fulfil to embody a systematic Life-Cycle Analysis (LCA) approach, the accounting of significantly impacting upstream or downstream activities enables to put the different pathways into perspective, in order to consider additional indirect benefits or impacts of the process. The environmental benefits of using a material which would have generated CO₂-equivalent emissions if used otherwise, or producing a material that represents a certain environmental burden when produced by state-of-the-art technologies, are denominated as displacement impacts.

2.2 Process integration

2.2.1 Optimization with OSMOSE

For the process integration, the software OSMOSE ("OptimiSation Multi-Objectifs de Systèmes Energétiques Intégrés") is used, developed by the IPESE laboratory (EPFL). In essence, this research tool aims at decision-making support for design, optimization and analysis of integrated industrial energy systems, supply chains and urban planning.

The OSMOSE platform links databases, such as thermodynamic properties tables (e.g. Coolprop) and Life Cycle Inventory (Ecoinvent³), simulation softwares (Aspen, Belsim Vali and other links in progress) to optimization solvers (e.g. cplex) and data visualization tools. It constitutes an optimization framework using combinations of meta-heuristic (genetic algorithms) and deterministic (Mixed Integer Linear Programming (MILP), Kantor et al., 2020) optimization approaches, showcasing fast conversion and a global optimum with well-defined solution methods. Figure 2.6 features the different iterations of the optimization problem. The physical model is defined through internal mathematical formulation appearing as black box for physical and chemical transformations and heat transfer requirement, using input parameters and output entities.

The Process Integration (PI) method of OSMOSE identifies processes and utilities which can be optimally integrated to achieve higher efficiencies at lower cost than conventional processes, thereby considering materials and energy flows with thermodynamic constraints imposed by formulation of the heat cascade within the MILP. The performance evaluation is done on economic (equipment sizing, capital investment estimation, etc.) and environmental (Life Cycle Assessment (LCA)) indicators for trade-offs assessment. In addition to the global problem framework, a multi-objective optimization loop might be implemented for determination of optimal decision variables values and resolution of Mixed-Integer Non-Linear problems.

³<https://ecoinvent.org/>

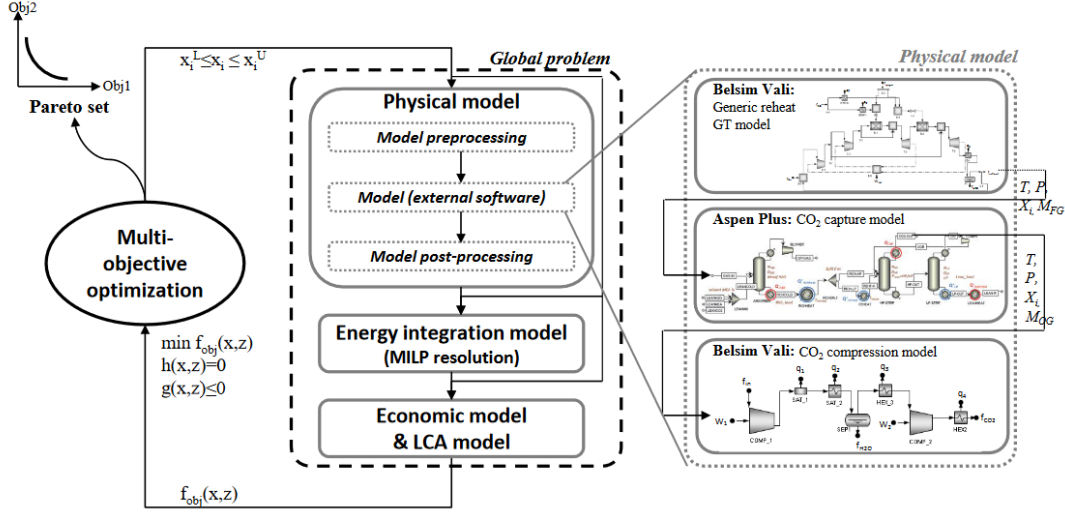


Figure 2.6: OSMOSE platform optimization methodology, as presented in Tock, 2013.

Even if the MILP formulation presents some drawbacks, for instance the requirement for model linearization, it has already been used often for system analysis and optimization as it presents a flexible and powerful method for solving large, complex problems, as is the case with industrial symbiosis and process integration. The OSMOSE framework has already well proven its effectiveness in numerous applications such as urban system design (Rager, 2015), biomass conversion systems (Peduzzi, 2015) and many industrial sectors : pulp and paper (Kermani et al., 2019), Kermani et al., 2018), chemicals (Bungener, 2016) and food industry (H. C. Becker, 2012).

2.2.2 Heat integration

As part of the process integration, heat integration is based on pinch analysis (developed initially by Linnhoff and Hindmarsh, 1983) and aims at recovering the maximum amount of heat between processes to minimize external supply of energy from cold or hot utilities. Heat and cooling loads are defined with corresponding temperature levels for each unit process : hot streams require cooling, and cold streams require heating. By cascading the heat between the relevant temperature levels, the Minimum Energy Requirement (or Maximum Energy Recovery, MER) and pinch point of the whole industrial process can be determined (Kemp, 2011). Although intermediate heat transfer systems might most probably be required due to physically restricted feasibility of some exchanges for safety, shutdown and other industrial constraints (H. Becker et al., 2010, Hu and Ahmad, 1994), implying energy penalties, the present study assesses the ideal case, assuming that any heat exchange between cold and hot streams is possible. For the integration of cold and hot streams, the minimum approach temperature considered in this work is $\Delta T_{min} = 5$ K, unless stated otherwise.

The computed heat cascade results are typically visualized in Composite Curves (CC) of hot and cold streams and Grand Composite Curves (GCC). CCs present a combination of hot (or cold) streams, respecting their associations to the relevant temperature intervals, which results in the hot (or cold)

composite curve. The temperatures are typically displayed in their *corrected* domain, by adding (or subtracting) the system minimum temperature difference at the pinch point divided by 2, $\Delta T_{min}/2$, to the hot (or cold) composite curve. As an alternative representation of the CCs, GCCs are built from a summation of hot and cold streams in the same temperature intervals and are more practical for determining the integration of utilities by graphical approach (Butun et al., 2018). François and Irsia, 1989 propose a mathematical programming methodology to address this optimal utility selection, which might be done considering also exergy efficiency through Carnot Composite Curve (CCC) computation (X. Feng and Zhu, 1997).

2.2.3 Key performance indicators

The definition of performance metrics allows to compare economic and environmental benefits or drawbacks of a given set of options, and provides useful indications on other operational variables of interest, such as process efficiencies and resource flows. The 6 performance indicators used for assessment of the scenarios results are listed hereafter. The annualized capital cost (CAPEX) is not directly compared, but its accounting is included through the TOTEX computation.

- **Environmental impact**, in t_{CO_2-eq}/y : Carbon dioxide (and equivalents) emissions caused by the mineralization process.
- **Carbon intensity**, $t_{CO_2,emitted}/t_{CO_2,FG}$: Ratio of the CO_2 emitted directly and indirectly for the whole process to the quantity of CO_2 taken up through the flue gas. *Note : For the process to be effectively sequestering CO_2 , this value needs to be below 1.*
- **OPEX**, in CHF/y : Annual operational costs for the project, mainly including resources costs and revenues, O&M costs of reactors and transportation costs. The potential costs related to carbon emissions taxation are excluded of this performance indicator.
- **TOTEX**, in CHF/y : Total annual expenditure for the project, computed as the sum of OPEX and annualized CAPEX.
- **CO_2 specific sequestration cost**, in CHF/ $t_{CO_2,mineralized}$: Total cost (OPEX + annualized CAPEX) per mineralized CO_2 , disregarding the direct and indirect emissions of the mineralization process.
- **PCC break-even price**, in CHF/ t_{PCC} : PCC selling price for achieving break-even of the mineralization plant TOTEX.

Chapter 3

CO₂ mineralization pathways overview

First mentioned in 1990 (Seifritz, 1990), the CO₂ carbonation as a carbon sequestration pathway is a phenomenon occurring already naturally, when atmospheric CO₂ dissolves into water and becomes available for reacting with mineral ions (Ca, Mg, Na, Fe, Al, etc.) released from their host rock, producing carbonates. This natural weathering is spontaneous and overall exothermic, but has very slow kinetics (Prigiobbe, Hänchen et al., 2009) - thus insufficient as CO₂ sink to cope with the current extent and growth of worldwide carbon intensive industries, as the reaction happens over geological timescales (Romero-Mujalli et al., 2019).

Driven by increasing interest for CO₂ sequestration methods in an effort to reduce the rise of its overall atmospheric concentration, many mineralization pathway options have evolved through considerable forced acceleration of reaction rates. The reaction can happen either *in-situ*, also called "mineral trapping" (Mazzotti et al., 2005), as an underground geologic sequestration in which a portion of the injected CO₂ reacts with alkaline aquifers or silicate rocks present in the target formation to form solid carbonate species, or *ex-situ*, in a designed reactor or industrial process above ground. The latter can be subdivided further into two categories of processes :

- Direct or indirect (multiple steps) carbonation
- Aqueous or gas-solid process

This chapter particularly reviews an indirect, aqueous mineralization process : the magnesium-cycle based pathway producing precipitated calcium carbonates (PCC), as patented by the company Carbonfree Chemicals (J. D. Jones and St, 2012, J. D. Jones, 2014, J. D. Jones and Yablonsky, 2016, J. Jones and Yablonsky, 2020, J. D. Jones and Yablonsky, 2021).

In addition to the carbonation process type, the resource streams involved in mineralization pathway can also vary significantly. Figure 3.1 presents a schematic overview of the mineral carbonation options. The gaseous CO₂ stream to be cleaned can either be concentrated or mixed to other compounds, as typically the case in industrial flue gas. The alkaline minerals input can be provided either by industrial products or wastes, or by mined minerals - all differing notably in composition, sequestration potential, availability and price. Depending on its composition and stability in atmosphere, the final carbonated product can be commercialized or landfilled, with differing correspond-

ing product quality requirements. Logistics of supply chain related to the material displacements between distant locations, given the distributed nature of the industrial sites involved, are a critical aspect of the industrial integration of such a process (Ostovari et al., 2022) and must be taken into account.

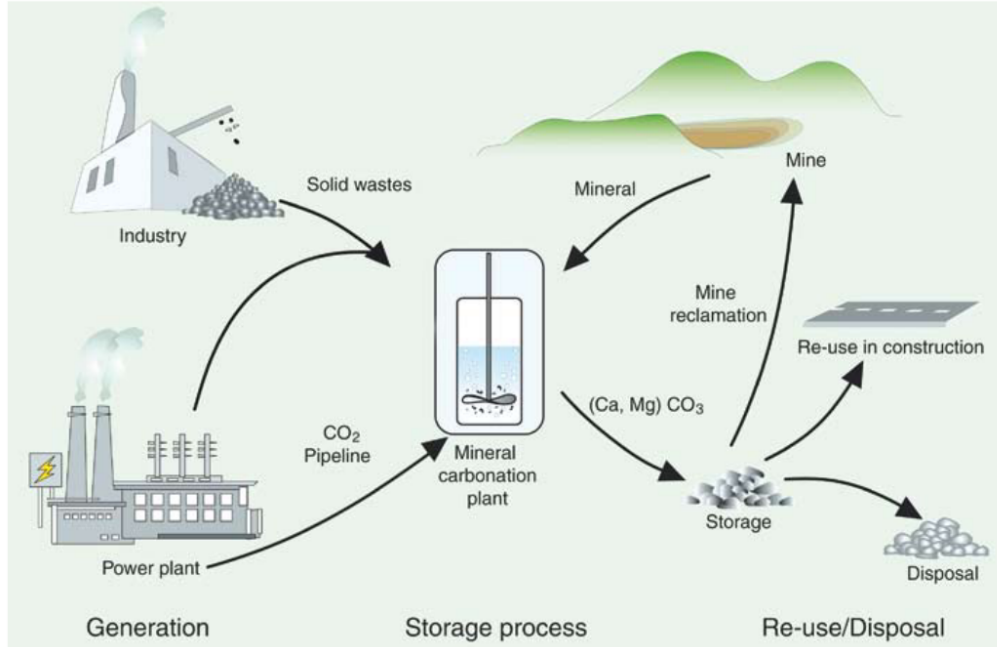
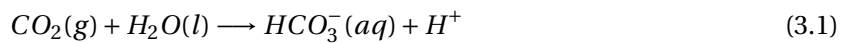


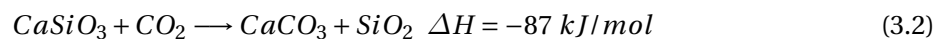
Figure 3.1: Material fluxes and process steps associated with the mineral carbonation of silicate rocks or industrial residues, taken from IPCC, 2005.

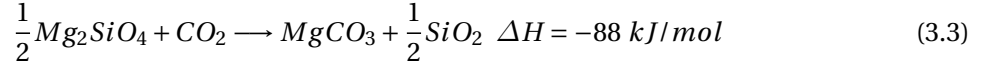
3.1 Rocks natural weathering

During natural weathering, atmospheric CO_2 is dissolved in water, acting as catalyst (Fricker and Park, 2013), and reacts to produce carbonic acid :



Under standard conditions and in aqueous solutions, carbonic acid finds equilibrium with carbonate species (HCO_3^- , CO_2 and others) and water, according to pH. The dissolved CO_3^{2-} ions are the only form that can react spontaneously with alkaline-earth oxides to precipitate carbonates such as calcite (CaCO_3), magnesite (MgCO_3) and siderite (FeCO_3). The alkaline-earth metals, among which magnesium and calcium are most reactive, are typically contained in silicate minerals such as wollastonite (CaSiO_3), olivine ($(\text{Mg, Fe})_2\text{SiO}_4$), ortho- or clinopyroxene ($(\text{Mg, Fe})_2\text{- or } (\text{CaMg, CaFe})\text{Si}_2\text{O}_6$) and serpentine ($(\text{Mg, Fe})_3\text{Si}_2\text{O}_5(\text{OH})_4$, originated by olivine hydration) (Sanna, Uibu et al., 2014). The overall carbonation reactions typically follow exothermic reactions 3.2 and 3.3 (Lackner et al., 1995) :





Despite the favourable thermodynamics, the kinetics of these reactions are considerably slow. One reason is the availability of free CO_3^{2-} ions in the water : as can be seen in Figure 3.2, the ambient pH allows only <1% of the carbonate species to be in this form.

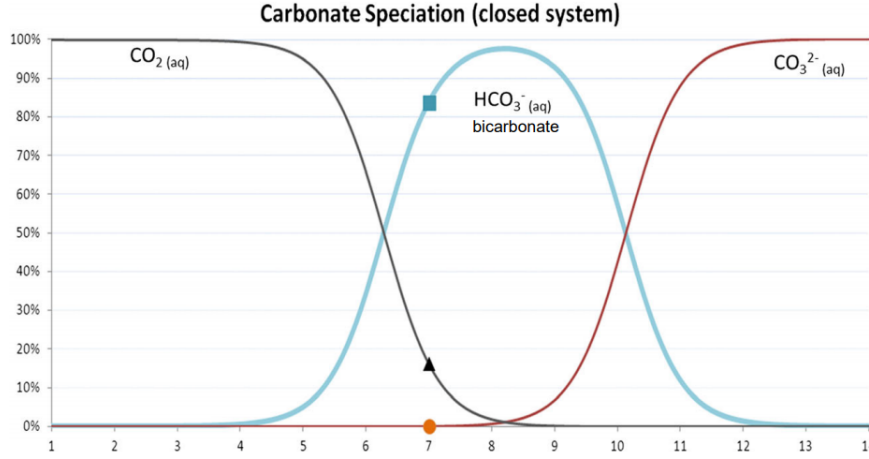


Figure 3.2: Bjerrum plot of carbonate speciation versus pH, taken from Yuen et al., 2016.

Furthermore, the low rate of mass transfer of CO_2 species into the water is due to the relatively low partial pressures and concentrations of CO_2 in the atmosphere (Assima et al., 2013), the low exposed surface-area-to-volume ratios of existing mineral ore veins (Oskierski et al., 2013) and the existence of inert barriers such as silica layers over active Mg/Ca oxides in the minerals (Teir, Revitzer et al., 2007). Another factor contributing to the slow reaction kinetics of mineralization is the lack of sufficiently alkaline environments to encourage rapid formation of carbonates (Highfield et al., 2012). Because of all these factors, the naturally occurring mineralization does not represent a carbon sequestration option without being sped up (Van Pham et al., 2012).

3.2 *In-situ* mineralization

For purposes of permanent carbon sequestration, mineralization can be enhanced underground (*in-situ*) by injection of CO_2 -bearing fluids, typically water or supercritical CO_2 , into porous ultramafic and mafic geological formations. The most reviewed host rocks are basalts (both on- and offshore (Sanna, Uibu et al., 2014)), mantle peridotites (composed by olivin and pyroxenes, Kelemen et al., 2018) and shale caprock (Romanov et al., 2015), which all feature much higher reactivity than sedimentary basins and consequently require less monitoring against leakages (Gislason and Oelkers, 2014). Kelemen et al., 2018 report that *while most rock materials undergo passivation and decreasing reaction rates with increasing reaction progress, in most cases experimental olivine carbonation rates are approximately constant to more than 90% completion. This may be due to “reaction-driven*

cracking”, formation of etch pits, and/or other processes that continually renew olivine reactive surface area.

The attractiveness of the *in-situ* mineralization relies in the great potential for sequestration volumes : 60'000'000 Gt_{CO₂} worldwide if the resource is economically accessible and ultimately fully carbonated (Kelemen et al., 2019). However, only few projects have up-scaled, all being focused on injection in basalt host rocks. In 2013, the pilot project in Wallula (Washington, USA, McGrail et al., 2014) injected ca. 1 kton_{CO₂} between 828 and 887 m depth. Modeling results claim that 60% of the injected CO₂ is sequestered via mineralization within two years, with the resulting carbonates occupying ca. 4% of the available reservoir pore space (White et al., 2020). Another project at demonstration plant scale is the CarbFix project¹ in Iceland (Snæbjörnsdóttir et al., 2017), with a current annual injection capacity of 12 kton_{CO₂}/year (2022), demonstrating the feasibility of carbon storage in basaltic rocks. Nevertheless, the applicability of such methods to other sites is claimed to be dependent on the availability of suitable host-rocks and sufficient water to dissolve the CO₂ during its injection. As a consequence, the largest geological storage potential for CO₂ is reported to be offshore, where the mid-oceanic ridges contain permeable basaltic layers and the oceans provide an unlimited reservoir for the required water requirements (Snaebjornsdottir et al., 2020).

Generally, the limits of *in-situ* mineralization are the economic considerations related to the artificial ways of enhancement of the chemical reactions, which require a large amount of energy (Sanna, Uibu et al., 2014). The estimated transport and storage cost for this technology are reported to be 17 USD/t_{CO₂}, which is about double of the cost associated to geological storage in sedimentary basins. The cost of carbon capture must be added to this cost, which brings the cost of this technology to the range of 72–129 USD/t_{CO₂} (Ragnheidardottir et al., 2011).

3.3 *Ex-situ* mineralization

For sites located far from potential geologic storage sites, mineral carbonation processes above ground have been extensively considered as alternative. In order to accelerate the mineralization kinetics, Yuen et al., 2016 review thoroughly the methods based on two types of approaches : physical and mechanical activation for increased molecular collisions, and pseudo-chemical catalysis, in which the catalysts need an additional regeneration cycle.

3.3.1 Direct mineralization

Direct mineralization designates the processes which react the CO₂ stream directly with the mineral source, development of which was motivated by the exothermic character of the overall carbonation reaction that can be done either in dry or in aqueous conditions. The main advantage of the dry method is the simplicity of heat recycle from the exothermic reaction (Romanov et al., 2015), and the first direct solid-gas carbonation process is described by Lackner et al., 1997, carbonating Mg(OH)₂ powder by flowing gaseous CO₂ on it in a reactor at 450°C. The magnesium hydroxide is produced

¹<https://www.carbfix.com/>

from leaching magnesium ions from peridotites with HCl, which forms magnesium chloride MgCl_2 that is ultimately thermally decomposed. In reported optimal conditions of 500°C and 340 bar pressurized CO_2 , full conversion of $\text{Mg}(\text{OH})_2$ is achieved in a minimum reaction time of 2 hours. The authors raise attention to the need for reaction catalyst, and Zevenhoven et al., 2002 investigate NaCl, NaHCO_3 and Al_2O_3 , without noticeable improvements. Air Pollution Control (ARC, untreated fly ash composed of calcium species) residues dry carbonation is investigated by Prigiobbe, Polettini et al., 2009, who find conversion rates of 60-80% (in less than 10 minutes) at atmospheric pressure for carbonation temperatures above 350°C and CO_2 concentration above 10%. These encouraging results are explained by the increased reactivity to carbonation of calcium hydroxides (and others, such as magnesium hydroxides) contained in the residues, with regards to silicates thereof. The natural or industrial occurrence of hydroxides is however very limited (see the availability of fly ash resources in Section 3.4.1), and generally the direct dry carbonation reaction kinetics are reported to be too slow for industrial CO_2 sequestration purposes (Huijgen, 2007).

To accelerate and improve the conversion, aqueous mineralization processes take advantage of the water acting as catalyst for the carbonation. The direct aqueous process most advanced yet is the route developed by NETL (O'Connor et al., 2005), which investigates carbonation of wollastonite, olivines (of different grades), serpentines (lizardite and antigorite) and steel slags using different carrier solutions (NaCl , NaHCO_3 , Na_2CO_3). For wollastonite, the maximum carbonation degree achieved is 69% (at 200°C, p_{CO_2} of 20 bar and average particle size $<38\text{ }\mu\text{m}$) for an energetic energetic CO_2 sequestration efficiency of 75% (Huijgen et al., 2006). For steel slags, the energetic efficiency reaches only 69%. In order to improve the respective carbonation rates, Gerdemann et al., 2007 explore the alteration of reactor pH, considering that lower values enhance metal dissolution kinetics but penalise the carbonate precipitation. The authors find optimal carbonation conditions (CO_2 partial pressure, temperature, carrier solution composition) for wollastonite, olivine and thermally activated serpentines, with respectively 81.8, 49.5 and 73.5% conversion (extent of reaction). Other trade-offs between reaction parameters exist due to both the dissolution of ions and the precipitation of carbonates happening in the same media : for instance, the authors highlight the effect of reaction temperature, which improves dissolution kinetics, but reduces CO_2 solubility and thus precipitation rate.

Given the natural availability of olivines and their reduced thermal activation as compared to serpentinites (see Section 3.4.1), several research investigate the enhancement of their aqueous mineralization kinetics. Jarvis et al., 2009 determine that the most effective bicarbonate additive for carbonation rate increase at 185°C and 13.5 MPa is a 5.5 M KHCO_3 solution. For an applied temperature of 120°C, Prigiobbe, Costa et al., 2009 find that additives do not have a measurable effect on dissolution rate. However, the latter is verified to be log correlated linearly and negatively with pH (range tested : 2 to 8), and decreases with increasing particle sizes (range tested : 90 to 355 μm). In particular, Eikeland et al., 2015 highlight the importance of reduced particle size for efficient conversion, reaching 70% in 2 hours for particle size of 10 μm and addition of NaHCO_3 and NaCl to catalyze the reaction under supercritical conditions. The conversion extent depends on reaction time (100% conversion

reached in 4 hours) and the carbon sequestration rate is significantly linked to temperature, pressure and additives. Assima et al., 2014, Daval et al., 2013 and Sanna et al., 2013 investigate the kinetics of direct aqueous carbonation of serpentines (more specifically : lizardite, chrysotile and brucite) and raise discussions around its technical feasibility on large scale, as high pressure and temperature are required, as well as long residence time for relatively low reaction rates.

Curing is another direct aqueous mineralization pathway, in which gaseous CO₂ is used as curing agent for concrete slabs, forming a membrane to reduce cracking and dusting, thus providing enhanced strength of the concrete (Zhan et al., 2016). The curing process might also be used to react with various alkaline-containing wastes, such as slags (Nguyen et al., 2020) for manufacture of building material, pellets, clinkers, etc. Though carbon dioxide emission reduction is reported given the possibility to utilize recycled CO₂ (El-Hassan, 2020), the energy use and injection losses seem to prevent the process from being an effective direct carbon sink (Tanzer et al., 2021, Ravikumar et al., 2021). This carbon utilization is industrially the most advanced direct aqueous mineralization pathway, being currently developed by several companies. For instance, Carbstone Innovation NV² (Belgium) applies curing on steel slags for production of tiles, clinkers, building blocks and briquettes in a pilot plant since 2013 (patented process : Van et al., 2020). O.C.O. Technologies³ (United Kingdom, previously called *Carbon8 Aggregates*) carbonates lime-based reactants in 3 commercial facilities, to form aggregates pellets for construction. Carbon Upcycling Technologies⁴ (Canada) injects recycled CO₂ for an enhanced supplementary cementitious materials (SCMs) fabrication method, increasing cement strength and durability (patent application : Sinha, 2020).

3.3.2 Indirect mineralization

In order to circumvent trade-offs around several reaction parameters in the direct carbonation pathways and thereby improve conversion efficiency and kinetics, indirect routes which separate the ion extraction and carbonate precipitation in at least two stages have evolved. Similarly to direct processes, they can be performed in dry or aqueous conditions but feature overall proven favored kinetics, enhanced ease of by-products separation and higher commercial product purity (Sanna, Lacin-ska et al., 2014, Hemmati et al., 2014). Ongoing researches focus most on aqueous processes, often referred to as pH-swing methods, given the preferential acidic conditions for the ion extraction step and the optimal carbonation pH of 10 for precipitate purity, as recalled by Azdarpour et al., 2015. The authors extensively review the pH-swing mineralization pathways for calcium and magnesium carbonates production from Ca- and Mg-rich minerals. This section presents an outline of the research groups in indirect aqueous mineralization, which mostly assess magnesite (MgCO₃) mineralization, due to the greater availability of magnesium-containing rocks naturally (see Section 3.4.1).

²<https://www.orbix.be/en/technologies/carbonation>

³<https://oco.co.uk/>

⁴<https://carbonupcycling.com/>

Laboratory scale

Since over a decade, a research group at Åbo Akademi University (ÅAU, Finland) investigates solid-solid extraction of reactive magnesium from serpentines with ammonium sulfate $((\text{NH}_4)_2\text{SO}_4)$ as solvent (Romão et al., 2012). Fagerlund, 2012 optimizes a fluidized bed reactor for the carbonation stage at elevated temperature and pressure, and show that for a flue gas pressure at 50 bar and reactor temperature at 550°C, carbonation kinetics of $\text{Mg}(\text{OH})_2$ are much faster than for MgO . Wet and dry carbonation are compared in Zevenhoven et al., 2016, and current research focuses on the optimization of reaction conditions, integration in the industry as well as 100% recovery of the ammonium sulfate, ammonia, and sulfur dioxide byproducts.

Maroto-Valer et al., 2005 chemically activate serpentines with ammonium sulfate (H_2SO_4), hydrochloric acid (HCl), and nitric acid (HNO_3) at ambient temperature and find that over 70% of the Mg ions are extracted with H_2SO_4 , also confirmed by Teir, Revitzer et al., 2007 to be the most efficient acid for Mg extraction (followed by HCl , HNO_3 , formic acid (HCOOH) and acetic acid (CH_3COOH)). The dissolution efficiency with ammonium salts is further investigated by X. Wang and Maroto-Valer, 2011a, revealing full extraction of magnesium (and 17.6% of silica, 98% of iron) for NH_4HSO_4 concentration of 1.4 M (3 h of reaction at 100°C). The authors add sodium hydroxide to the produced magnesium sulfate to precipitate $\text{Mg}(\text{OH})_2$.

Sanna, Lacinska et al., 2014 investigate the dissolution and carbonation of olivine, pyroxene and amphibole-rich rocks using an ammonium salt, studying the effect of temperature (50, 70 and 100°C) and time (range : 5 to 180 minutes). They find that temperature has direct effect on the rates of mineral dissolution reactions, and that highest dissolution efficiency (77%) is achieved using olivine with particles 75–150 μm (3 h at 100°C, with a limitation due to product layer diffusion). Too low Mg extraction efficiencies (<30%) make amphibole and pyroxene-rich rocks an unviable resource for this process.

Calcium ions extraction efficiency from recycled concrete aggregate and steel slag using NH_4HSO_4 is studied by Dri et al., 2013. The tested temperature range is 25–90°C, resulting in a maximum extraction efficiency for Mg and Fe of respectively 85% and 90%, with CaSO_4 precipitating after 3 hours at 90°C. In particular, the extraction of calcium from steel slags is assessed by Said, 2017 using NH_4Cl and Eloneva, 2010 using CH_3COOH . Teir, Eloneva, Fogelholm et al., 2007 compare the dissolution efficiencies and kinetics of Si, Ca, Mg, Al and Fe of wollastonite, steel converter slags and blast furnace (BF) slags in CH_3COOH at 50°C. For each mineral source, the dissolution efficiency after 1 h reaches 51% (wollastonite), 88% (steel converter slags) and maximum dissolution (BF slags).

Industrial scale

Two-stage mineralization pathways are developed in several companies. Operating since 2015, the SkyMine technology from Carbonfree (formerly Skionic, USA, Walters, 2016) is the world's first and largest industrial-scale carbon mineralization facility, with up to 50 $\text{kton}_{\text{CO}_2}$ /year captured from cement plant flue gas, forming commercialized baking soda (sodium bicarbonate NaHCO_3). The patented process developed by Blue Planet (USA) uses calcium-containing industrial wastes and am-

monium salts for the mineralization cycle (Constantz and Bewernitz, 2019), with a commercial facility planned in San Francisco⁵. The Cambridge Carbon Capture (UK) technology (CO₂LOC⁶, patented in the US : Priestnall, 2018) is based on magnesium silicates (olivine or serpentine) for MgCO₃ production using industrial exhaust gas : a pilot plant is currently projected (Scialom, 2020).

3.4 Mineral source

The range of input material options for CO₂ mineralization is large : alkali (Na, K), alkaline earth (Ca, Mg) and other (Al, Fe, Cu, Co, Ni, Zn, etc.) metals are all potential candidates for carbonation. However, most of these elements are either too rare, too valuable (e.g. iron) or unstable over long-term time frames in atmosphere (alkali bicarbonates). Given their natural availability and stability in the carbonated form, calcium and magnesium are the most investigated elements in the literature, and this section reviews the options for sources and required preliminary ion activation.

3.4.1 Alkaline feedstock

Pure alkaline earth salts

Alkaline ions might be supplied by alkaline earth salts, either mined or generated as industrial by-products. Hydroxides (Mg(OH)₂, Ca(OH)₂) are naturally too rare and commercially too expensive to be considered for large-scale mineralization (Eloneva, 2010), but alkaline chlorides (MgCl₂, CaCl₂) might represent an opportunity for mineralization, for example in industrial waste brines (Simonetti et al., 2019, Azdarpour et al., 2015). Indeed, upon spontaneous and exothermic dissolution (-80 kJ/mol_{CaCl₂} (Kustov et al., 2007), -800 kJ/mol_{MgCl₂} (Shin and Criss, 1979), ions are readily available for carbonation without further activation.

If chlorides have to be industrially synthesized, their upstream environmental burden must be taken into account. In the case of CaCl₂, the Solvay process is used : $2NaCl + CaCO_3 \rightarrow CaCl_2 + Na_2CO_3$. Given that this process is separating carbonates for the production of CaCl₂, it is not relevant for a holistic approach, and the attributed environmental impact (GWP100a) is 0.467 kg_{CO₂}/kg_{CaCl₂-dry} (European context : allocation method, cut-off by classification, Wernet et al., 2016). MgCl₂ is typically extracted from sea water on an industrial scale by precipitating it as magnesium hydroxide, then converting it to the chloride by adding hydrochloric acid (Zohdy et al., 2013). Its environmental impact is not referenced in Ecoinvent, but reportedly close to the environmental burden associated to CaCl₂ due to the similarities in manufacturing processes. At lower purity grade, it is also a waste brine of a large number of processes involving washing of chlorine-contaminated material. Nevertheless, the technical suitability of magnesium brines is limited due to high energy-demand for seawater evaporation (Sanna, Uibu et al., 2014).

⁵<https://www.sfbayaggregates.com/>

⁶<https://www.cacaca.co.uk/>

Mined rocks

Largely discussed alkaline sources for CO₂ mineralization are mined mafic or ultramafic igneous rocks, in which Ca and Mg content are the highest and mainly present in the form of silicates. Magnesium silicates exist in the form of dunites (consisting mainly of olivine (Mg, Fe)₂SiO₄), peridotites (olivine and pyroxene) and serpentinites ((Mg₃Si₂O₅(OH)₄). These rocks have typically high trace element contents, such as nickel (Herzberg et al., 2016). They are often by-products of asbestos, metal ore or more precious minerals mining operations, thus widely available throughout Europe (Consortium, 2013) and especially in Finland, Sweden and Norway (Ostovari et al., 2022).

Calcium silicates, less widespread, are found in basalts and wollastonite (CaSiO₃). Basalts have low calcium concentration (Eloneva, 2010) and contain significant amounts of potassium and sodium, which consume part of the acid used in the leaching process by reacting with it, complicating its regeneration (Lackner et al., 1995). The iron content is reportedly not causing this type of problem. Wollastonite is a relatively minor industrial mineral, with worldwide crude ore production of ca. 1'200 kton/year, excluding USA production (Survey, 2020). China is its first producer (51%), followed by India (24%), USA (12%) and Mexico (9%) (Maier et al., 2015). Finland is the largest European producer (11 kton/year in 2019), with two deposits exploited : Ihalainen in Lappeenranta and Perheniemi in Iitti. Sarapaa et al., 2003 report the wollastonite deposits location in South Finland, and estimate the reserves of 2 specific location, yet not in mining operation : 2 Mt_{ore} (14.7% wollastonite) in Kalkkimäki and 5.8 Mt_{ore} (13% wollastonite) (later corrected in Peltonen, 2006), which represent together a wollastonite content of 1 Mt. Czech Republic, as well as Spain, Sweden and Norway in much smaller production quantities, also have wollastonite quarries (Consortium, 2013).

	Mineral	Mg, wt.%	Ca, wt.%	Fe, wt.%	R _{CO₂} , kg _{ore} /kg _{CO₂}	η _{exp,CO₂} , %
Ultramafic	Wollastonite	0.3	31.6	0.5	2.8	82
	Talc	15.7	2.2	9.2	2.8	15
	Forsterite (Olivin)	27.9	0.1	6.1	1.8	81
Serpentines	Antigorite	24.6	<0.1	2.4	2.1	92
	Lizardite	20.7	0.3	1.5	2.5	40
	Anorthite (Feldspar)	4.8	10.3	3.1	4.4	9
Peridotites	Dunite	29.7	0.2	*	1.8	*
	Harzburgite	27.2	0.5	*	2	*
	Lherzolite	16.9	5.2	*	2.7	*

Table 3.1: Magnesium, calcium and iron content of various igneous rocks, with corresponding mass ratio necessary for carbonation R_{CO₂} and experimental conversion efficiency of the Mg, Ca and Fe ions to carbonated form (Lackner et al., 1995, O'Connor et al., 2005). *Note : Basalts, composed of pyroxenes, olivines, magnetites and feldspars, have high ratio R_{CO₂} (>4.9) and low conversion efficiency η_{exp,CO₂} (ca. 15%). * indicate non-reported values.*

Table 3.1 lists the candidate minerals for CO₂ mineralization with their alkaline content, the mass

ratio of mineral ore to CO_2 necessary for the carbonation R_{CO_2} , determined on stoichiometric basis strictly, and the experimental conversion efficiency of Mg, Ca and Fe ions to their carbonated form (O'Connor et al., 2005).

The carbonation reactivity of the minerals is dependent on various factors, including the mineral composition, pre-treatment, and solubility at the specific carbonation conditions of time, temperature, and pressure. As can be concluded from previous research, serpentines (especially antigorite), olivines (forsterite) and wollastonite feature the biggest potential for carbonation, and have thus most often been retained as mineralization input materials (Giannoulakis et al., 2014). The alkaline ions activation potentially required by the minerals is reviewed in Section 3.4.2.

Industrial alkaline by-products or wastes

Given the economic challenge of mining operations (Gerdemann et al., 2007), alternative feedstocks such as industrial alkaline residues have been investigated. Many options exist, reviewed in particular by Mattila and Zevenhoven, 2014, Sanna, Uibu et al., 2014 and W. Liu et al., 2021 : municipal solid waste incineration (MSWI) ashes (Ecke, 2003, Bertos et al., 2004, Rendek et al., 2006), cement kiln dust (CKD, Kodama et al., 2008, Huntzinger et al., 2009, Mun et al., 2017), metallurgical slags (Kodama et al., 2008, Eloneva, 2010, Sun et al., 2011, Zappa, 2014, Mun et al., 2017), coal ash (bituminous coal or others, ashes possibly retrieved from landfills; Ji et al., 2017), bauxite residues (also called red mud) from the alumina production process (Bayer process, Yadav et al., 2010, Han et al., 2017), phosphogypsum waste (Kang et al., 2022), carbide (T. Zhang et al., 2022) and argon oxygen decarburization (AOD) slags (Salman et al., 2014), mixtures of alkaline brine wastes from paper production plants (Perez-Lopez et al., 2008, Spinola et al., 2021) or sludge ashes thereof (Kim and Kim, 2018), as well as many other industrial waste brines or mines tailings. Most of these wastes contain very low magnesium (0 to 15% MgO content) compared to calcium (often 25 to 70% CaO content) (Meng et al., 2021), hence the mineralization product discussed for industrial waste carbonation is generally CaCO_3 . The main mineral content of interest and the carbon dioxide sequestration potential per ton of waste, both approximated theoretical value and experimentally determined range, are reported in Table 3.2.

Waste type	MgO	CaO	Fe ₂ O ₃	SiO ₂	ϵ_{th,CO_2}	ϵ_{exp,CO_2}
MSWI fly ash	2-3	21-37	2-5	20-41	270	32-100
MSWI bottom ash	2.8	32-53	1-7.9	4-30	250	32-40
Steel slag (EAF)	4-15	25-47	1.6	27	552	120-180
Steel slag (BOF)	1.5-10	34-55	-	0.8	402	90-290
Blast furnace slag	8-11	15-41	0.5-0.9	34-36	413	70-230
AOD slag	5.8	60.7	0.2	27.6	410	150-270
Cement kiln dust	1-2	34.5-46.2	2.9	16.4	530	100-180
Coal fly ash	1-3	1.3-10	10-40	20-60	73	20-70
Bauxite residue	<1	1-20	28-43	3-18	128	41-72
Papersludge alkaline waste	1-5	45-82	<0.1	<0.1	500	100-260
Air Pollution Control (APC) residue	8	50-60	0.5-1.5	10	540	70-250
Gypsum waste	<1	27-33	<0.1	ca. 1	-	200-340

Table 3.2: Chemical composition (in [wt.%]) and estimated sequestration potential ($\text{kg}_{CO_2}/\text{t}_{waste}$) of diverse industrial alkaline wastes, both approximate theoretical value ϵ_{th,CO_2} and experimentally determined ϵ_{exp,CO_2} range. *Note* : BOF : Basic Oxygen Furnace, EAF : Electric Arc Furnace, AOD : Argon Oxygen Decarburization. *Data gathered from* : Shen and Forssberg, 2003, Ecke, 2003, Yadav et al., 2010, Jo et al., 2014, Sanna, Uibu et al., 2014, Ukwattage et al., 2014, L. Wang et al., 2019, Meng et al., 2021, W. Liu et al., 2021, Rausis et al., 2021, Xie et al., 2022.

For the United Kingdom, Sanna, Dri et al., 2012 review the benefits and drawbacks of using mineral wastes for carbon capture and storage, and their potential in CO₂ sequestration. The authors find that mineral wastes have the potential to capture only 0.1–1 Mt_{CO₂}/y in the UK, considering that currently, recycled concrete aggregate (RCA), steel slag (SS) and blast furnace slag (BFS) are not available for carbonation reuse. On the global scale, Renforth, 2019 quantifies the CO₂ carbonation potential of industrial alkaline wastes until 2100 for the 5 shared socioeconomic pathways (SSPs). As of 2020, absorption of CO₂ in the cement production represents more than half of this 1.5 Gt_{CO₂}/y potential, followed by steel slags, CKD and mine wastes carbonation. These wastes might alternatively be reused for other purposes than carbonation : agriculture, cement industry, construction/road material, wastewater treatment, etc., which application are reviewed by Elbaz et al., 2019 and Yi et al., 2012.

The regional availability of alkaline industrial wastes varies, and specifically for Switzerland, some are not produced by the inland industry (e.g. coal ashes). Table 3.3 lists the average reported amount of waste generated in Switzerland (based on the national production capacity of the main product and the waste-to-product ratio) and the corresponding CO₂ sequestration potential, computed systematically based on the upper bound on ϵ_{exp,CO_2} . Specifically in Switzerland, treatment and recovery of valuable resources from these waste have been investigated, instead of disposal by landfill. For in-

stance, metal recovery from fly ash by the FLUWA process (and extended method (FLUREC), Weibel et al., 2021) is nowadays state-of-the-art by law as landfill is prohibited since 2021 (Council, 2015). The unique processing plant on the Swiss territory is located in Hinwil (Syc et al., 2020), in operation since the beginning of the year 2017, designed to treat 200 kt/y of incineration bottom ash (IBA) by the horizon 2025 (Boni, 2020). The post-treatment and washing effectively separates not only heavy metals but is also claimed to predominantly leave CaCl_2 -brines, desirable for the mineralization process, as reported by Quina et al., 2018.

Waste type	Swiss production Mio. $\text{ton}_{\text{waste}}/\text{y}$	Sequestration potential $\text{kt}_{\text{CO}_2}/\text{y}$
MSWI fly ash	0.08	14-21.6
MSWI bottom ash	0.8	18-25.6
Iron slag	0.259-0.373	59.6-86
Steel slags (EAF)	0.041-0.067	7.3-12.2
Steel slags (BOF)	0.09-0.095	26-27.8
Cement kiln dust	0.27-0.49	49-87
Bauxite residues	0.021-0.06	1.5-4.3
Paper sludge alkaline waste	0.017-0.034	4.4-8.8

Table 3.3: Estimated CO_2 sequestration potential of selected industrial alkaline wastes in Switzerland, based on national availability and experimental carbonation efficiency $\epsilon_{\text{exp},\text{CO}_2}$ (taken from Table 3.2). *Note : Data gathered from Zucha et al., 2020, Tomohiro, 2021, NipponSlagAssociation, 2003, Schorcht et al., 2013, CemSuisse, 2022, PerlenPaperAG, 2022, Bajpai, 2015, AluSuisse, 2015, Y. Liu and Naidu, 2014, Renforth, 2019.*

These potential input materials for mineralization do not bear indirect environmental impact for the upstream activities, given that they are considered as wastes (Wernet et al., 2016). However, the assessment of their downstream impact is not straightforward. Indeed, depending on the off-take, which might vary substantially for different sites and types of waste, the impact may be either positive or negative. Boesch et al., 2014 establish an LCA model for waste incineration enhanced with new technologies for metal recovery, applied in Switzerland and report the burden associated to bottom and fly ash End-of-Life management, as well as displacement impact thanks to metal recovery from the ashes. Similarly, the LCA approach of Renforth, 2019 for a broad range of alkaline materials estimates the carbon offset through recycling or reuse. Dusts (from cement kiln, blast furnace, air pollution control, etc.) and steel slags are commonly reused, typically in supplementary cementitious materials (SCMs, Wernet et al., 2016 and GlobalCement, 2011). Alternatively, displacement impact might be discussed if waste treatment is avoided. The assumptions for this work are detailed in Chapter 6, when presenting specific scenarios.

3.4.2 Activation

The pre-treatment of the mineral ore enhances its reactivity for ion extraction, and is often described as key for reaching overall reasonable mineralization process efficiencies (Gerdemann et al., 2007). The activation can be realized in different ways, combinable or not, in the aim to increase the specific surface area :

- Chemically : using additives such as acids, steam or supercritical water
- Mechanically : through grinding to reduce the mean particle size. This process typically includes preliminary crushing, beneficiation (ore concentration) through gravity separation at low energy cost (O'Connor et al., 2005) and possibly multi-stage grinding
- Thermally : by removing chemically-bound water, thereby increasing the porosity

The type of treatment depends on the mineral source used in the mineralization. Some industrial alkaline wastes with fine sizes (cement kiln dust, ashes or brines) already feature good ion reactivity and might only need reduced activation, whereas minerals from rocks or metallurgical slags typically necessitate activation in order to be considered viable for mineralization. Additionally, O'Connor et al., 2005 argues that calcium silicates may require less ionic concentration or gaseous CO₂ activity compared to magnesium silicates for the same carbonation rates, given the higher precipitation rates of CaCO₃ compared to MgCO₃ (up to 4 orders of magnitude reported). Hence, the authors find that reduction of olivine particle size from 106-150 µm to <38 µm increase the carbonation conversion of their experiments from 10 to 90% (corresponding mechanical energy requirement : 300 kWh/ton), with a linear relationship between mechanical energy input and conversion efficiency gain. This relation plateaus for lower grinding energy input (150 kWh/t) in the case of 50%-grade wollastonite, which improves its carbonation efficiency from 50 to 80%. Lower grinding energy requirements (56 kWh/ton) for wollastonite size reduction to <38 µm are found by Huijgen et al., 2006, and only 31 kWh/ton is reported for steel slags of 0.02 m, which does not require beneficiation and can thus be ground in a single step. Apart from conventional grinding, other types of grinding have been investigated for feedstock activation. During attrition grinding, the mineral is stirred in a chamber filled with small stainless steel balls to induce imperfections into the crystal lattice, which results in a higher conversion than size reduction to the same diameter using conventional grinding (Huijgen, 2007). More recently, wet extractive grinding methods have been investigated, for instance using ball mills (Owais et al., 2021).

For serpentine, O'Connor et al., 2005 detect negligible activation with sole grinding, which is confirmed by Maroto-Valer et al., 2005. The authors report that thermal activation increases most the specific surface area of serpentines (antigorite, forsterite and magnesium oxide) at 650°C, consequently significantly lowering the carbonation temperature (185°C to ambient temperature) and pressure (125 to 45 atm) required. The heat requirements amount to respectively 293 and 326 kWh_{th}/t for antigorite and lizardite, as calculated in Gerdemann et al., 2007. Thermal and chemical activation, notably by sulfuric and hydrochloric acid, is also compared by the authors.

3.5 Mineralization products

In addition to being a potential carbon sequestration option, the mineralization process can also be considered as an industrial manufacturing process of valuable resources streams, which nature depends on the selected mineralization process and the alkaline feed. Hills et al., 2020 review the technology readiness level (TRL) of selected direct mineralization technologies for construction material production : concrete blocks, aggregates, tiles (e.g. for roof application), construction fillers, carbonated concrete, etc. Alternatively, using indirect mineralization pathways, precipitated calcium carbonate (PCC, CaCO_3), hydromagnesite ($\text{Mg}_5(\text{CO}_3)_4(\text{OH})_2\cdot 4\text{H}_2\text{O}$) or a mixture thereof is synthesized. Both carbonates are largely found in the Earth mantle and stable at atmospheric conditions (Teir et al., 2006, Ballirano et al., 2010). In addition, silica (SiO_2) and metal (Fe, Al, Mn, Zn, Ti, Cr, Ni) oxides can be separated to obtain >90% grades (Teir et al., 2010), with a possible incurred penalty on energy consumption and carbon footprint if the quality requirements of the products are increased, but potentially enhanced profitability (Chu et al., 2019). The applications and related market for these products are reviewed by Sanna, Hall et al., 2012 and Woodall et al., 2019.

Precipitated calcium carbonate (PCC)

PCC is a form of crystallized CaCO_3 powder, widely used in the industry as filler for painting and coating. Its most common manufacturing method is through hydration of lime with carbon dioxide, a high-temperature and energy-intensive process, implying a significant environmental burden. For this state-of-the-art process in Europe, the Ecoinvent database reports thus a carbon intensity of $1.4269 \text{ kg}_{\text{CO}_2-\text{eq}}/\text{kg}_{\text{PCC}}$ (impact assessment method IPCC 2013, GWP 100a), from cradle (i.e. with all upstream activities) to the raw material ready for utilization. Alternatively, it is synthesized as a by-product of poorer quality in the lime-soda process for NaOH production or in the Solvay process for Na_2CO_3 production. The European market represents a consumption over 2 Mt/y with around 75% of it only in the pulp and paper industry (Zappa, 2014), from which paper sludge waste can also be recycled for reuse of filler material. Quality requirements for this application are typically a purity higher than 98%, low manganese and iron contents since these elements have a very negative influence on the brightness of the product, and its iron content should be lower than approximately 0.1% (Mattila and Zevenhoven, 2014). The particle size for filler pigments should distribute between 0.2 and $2 \mu\text{m}$ (for more than 70% of the particles), as it affects paper smoothness, gloss and printing characteristics. Amongst the three anhydrous crystalline polymorphs calcite, aragonite and vaterite, the preferred crystal morphology for fillers is prismatic, rhombohedral or scalenohedral calcite, each conferring different desirable characteristics to the paper (Eloneva, 2010). For coatings and other applications in plastics and pharmaceuticals industries, most recurrent forms are rhombohedral calcite and orthorhombic acicular aragonite (crystals in the form of fine needles, rarer), in some cases with lower CaCO_3 purity grades constraints (>96%) (Zappa, 2014).

Alternatively, the precipitated calcium carbonates can be commercialized as equivalent to ground calcium carbonate (GCC). It is of lower purity grade and greater average particle size than PCC (up to

>50 μm for coarse GCC, Lehtinen et al., 2000), but may still be used in some applications for paper fillers, paint/coating or rubber application or as aggregate in the construction sector. For the U.S. market, GCC and PCC prices vary from 12 USD/ton for the cheapest GCC (crushed stone used as aggregate, Woodall et al., 2019), 26 USD/ton for coarse GCC (coarse) and up to 550 USD/ton for high-quality, coated PCC (Zappa, 2014).

Mineralization PCC product quality performances may differ depending on the calcium-containing input material. When synthesizing PCC from steel slags, Zappa, 2014 find particle size distribution between 10 and 100 μm , which does not satisfy requirements for high quality fillers and coatings, but might suit GCC-equivalent applications. Using blast furnace slags in a two-step indirect carbonation route, Chu et al., 2019 achieve 92.04% CaCO_3 purity, but relatively high by-products quality grades : 99.59% for SiO_2 and 97.7% for the hydrated solvent $(\text{NH}_4\text{Al}(\text{SO}_4)_2 \cdot 12\text{H}_2\text{O})$. Velts et al., 2011 characterize the PCC precipitates crystallized from oil shale ash leachates, and find high brightness with up to 96% CaCO_3 content, mean particle sizes ranging from 4 to 10 μm and controllable morphology, such as rhombohedral calcite, or coexisting calcite and spherical vaterite phases.

Hydromagnesite (MgCO_3)

Using serpentine as Mg-rich silicate mineral source, the research group at Åbo Akademi University in Finland produces silica sand of 82–88% purity, iron oxides and hydromagnesite $(\text{Mg}_5(\text{CO}_3)_4(\text{OH})_2 \cdot 4\text{H}_2\text{O})$ of 99% purity, with uniformly sized and spherical crystals with a lamellar structure. X. Wang and Maroto-Valer, 2011b find similar results, and particle size ranging from 5 to 100 μm . Despite these reasonably good product quality performance, there is currently not a sufficient market demand for Mg-based carbonates. Woodall et al., 2019 mention the research on magnesia cements, yet not implementable at large scale due to significantly higher costs and technical feasibility issues (e.g. long-term properties), and the potential application of hydromagnesite as flame-retardant mineral fillers.

3.6 Logistics of supply chain

The carbon dioxide source, solid feedstock (alkaline minerals and make-up salts) and markets for mineralization products are typically not present at the same location. Therefore, the logistics assessment of the supply chain involved is essential and must entirely be part of the process integration, given that the related costs generally represent a critical element of the cost structure (Camison-Haba and Clemente-Almendros, 2020).

Several studies investigated the potential of a supply chain for CO_2 capture, transport, and geological storage in Europe (d'Amore et al., 2021, d'Amore and Bezzo, 2017), and more recently, including CO_2 utilization (d'Amore and Bezzo, 2020, S. Zhang et al., 2020). In particular, Ostovari et al., 2022 optimize the supply chain for large-scale CO_2 mineralization in Europe, taking into account the location and amount of solid feedstock available for extraction, utilization of the mineralization products (where it is notably assumed that carbonates are not commercialized but returned to mines, and silicates are partially re-used in cement plants), location and amount of available CO_2 sources which

can be equipped with CO₂ capture, network required for CO₂ transport and carbon footprint of energy supply along the supply chain. The European supply chain could avoid 130 Mt_{CO₂-eq}/year in Europe (24% reduction of the industry sector's GHG emissions), requiring at least 5% expansion of existing infrastructure (road freight transportation and current energy supply), or new infrastructure building in the future (CO₂ pipeline network, Direct Air Capture (DAC), and renewable electricity system). The authors state that *One promising transition path is to start small and flexible, i.e., using the existing energy system to capture CO₂ from the industrial point sources, and transport the captured CO₂ by the currently available truck road transportation infrastructure. The supply chain for CCUS by mineralization could, thus, be gradually developed and fully implemented in the future to provide negative emissions on a large scale via direct air capture.*

Chapter 4

Plant process overview

This chapter presents an indirect aqueous carbonation pathway based on a magnesium chloride (MgCl_2) cycle for precipitated calcium carbonate (PCC) production using different types of calcium sources. This pathway is selected for the present work given the proven kinetics and conversion efficiencies of process reactions, large range of available calcium resources, selectivity in the precipitation stage (as opposed to Mg-based carbonates, Woodall et al., 2019) and the potential for end-product commercialization.

The four major aspects related to the CO_2 mineralization process design, with corresponding fixed-capital cost, are taken into account : pre-treatment of the mineral source (as reviewed in Section 3.4.2), purification for ion selectivity, carbonation stage, and reagent recycling operations. The three latter steps are illustrated in Figure 4.1, displaying the magnesium-cycle based mineralization core process as considered in this study. It takes as input a calcium-containing solution produced either from pure commercial calcium chloride or from a rock or industrial waste leaching process (also referred to as salt production site in this work). The calcium is carbonated when entering in contact with a magnesium brine containing dissolved HCO_3^- ions from the absorption of gaseous CO_2 in a $\text{Mg}(\text{OH})_2$ - MgCl_2 slurry. The gas is injected pressurized either pure or through industrial flue gas, and decarbonized gas exits the absorption column. After precipitation of the CaCO_3 , the remaining solution of MgCl_2 hydrates must be regenerated to retrieve the $\text{Mg}(\text{OH})_2$ - MgCl_2 slurry. This is done by preliminary concentration of the solution (evaporation), crystallization of $\text{MgCl}_2 \cdot 6\text{H}_2\text{O}$ and dehydration of the crystals to $\text{MgCl}_2 \cdot 2\text{H}_2\text{O}$. The $\text{Mg}(\text{OH})_2$ is eventually synthesized by further dehydration and dehydroxylation in a decomposition tank, producing thereby water and HCl vapor. Part of the magnesium hexahydrates may by-pass this regeneration, to substitute part of the water input in the $\text{Mg}(\text{OH})_2$ - MgCl_2 slurry.

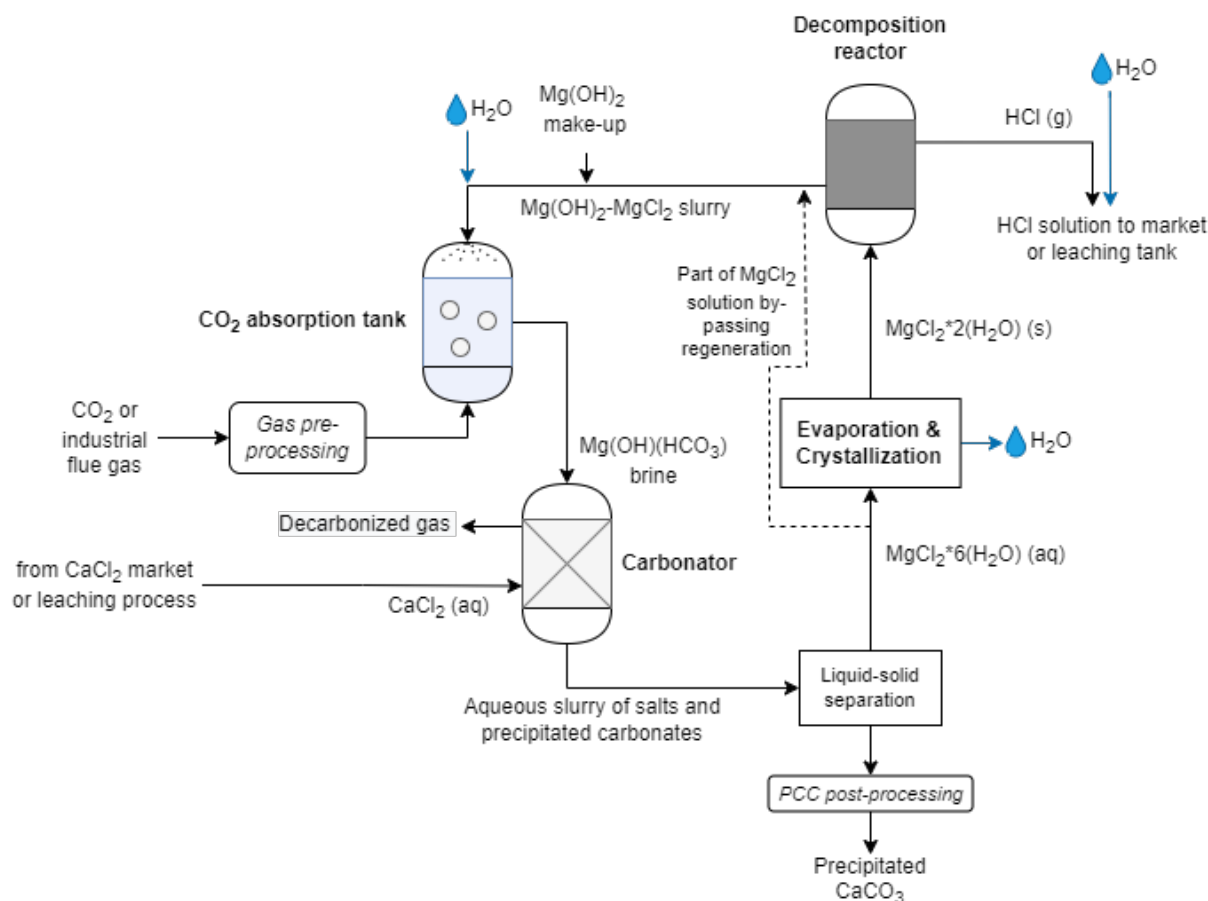


Figure 4.1: Scheme of the indirect, aqueous mineralization process based on hydrated MgCl_2 regeneration to Mg(OH)_2 .

4.1 Acid leaching

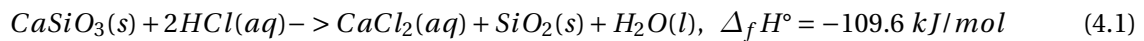
For the scope of the present study, the leaching of calcium ions takes place in acidic pH, through heap leaching or in a stirred leaching tank. It is supplied by the fine calcium-rich material (particle size $<75\ \mu\text{m}$), potentially pre-activated beforehand by grinding (see 3.4.2). The mineral dissolution can be fulfilled by a number of strong acids, typically most performing for ion extraction : hydrochloric acid (HCl) (Arce et al., 2017, Mun et al., 2017), nitric acid (HNO_3) (Teir, Revitzer et al., 2007, Doucet, 2010, and sulfuric acid (H_2SO_4) (Q. Zhao et al., 2015). Weaker acids such as acetic acid (CH_3COOH) (Mun et al., 2017), formic (HCOOH) (Teir, Revitzer et al., 2007), ammonium chloride (NH_4Cl) (Mun et al., 2017) and ammonium bisulfate (NH_4HSO_4) might also be used, as they generally present better selectivity for metal elements (Z. Chen et al., 2021). HCl is selected for the leaching process given its coherence with the process studied : it is regenerated in the decomposition reactor, jointly with Mg(OH)_2 .

The claimed drawbacks of HCl-based extraction are mainly its lower leachate selectivity (Arce et al.,

2017) and its high energy penalty for regeneration through electrodialysis of NaCl, for which Hemmati et al., 2014 develop a much more efficient process (bipolar electrodialysis (-60% of energy penalty). The difficulties around selectivity of Ca ions seem to be overcome by Jo et al., 2017, who study the carbonation of steel slags with calcium ions extraction based on HCl dissolution. The authors investigate the removal of leached impurities by gradual increase of the pH in a neutralization tank and report a complete removal (by precipitation) of Al and Fe ions at pH = 7 and Mg ions at pH = 11 from the nano-particles of the CaCO₃ precipitated (80-120 nm, 98.5% purity). An exception appears to be potassium, which stays dissolved in the solution : as mentioned by Lackner et al., 1995, potassium and sodium react with the HCl and are only hardly separable afterwards. The stepwise increase of pH is also applied in Bang et al., 2016, removing successfully the undesired Mg, Al and Ti. Using 0.5 M HCl on cements, Mun et al., 2017 report an extraction selectivity for calcium of 99%, the remaining being magnesium, silicate and traces of Fe₂O₃ and SO₃, achieved when the final solution pH is between 8.5 and 10.

The calcium ions dissolution rate and efficiency are influenced by particle size of the solids, solid-to-liquid ratio, acid concentration and reaction temperature (Jo et al., 2017). The HCl leaching performs better at lower solid-to-liquid ratio, and optimal leaching temperature range from 60 to 100 °C (Teir, Revitzer et al., 2007, J. Zhang et al., 2010). Nevertheless, even if the reactor is not thermally activated (so with initial ambient reactor temperature), the leaching media temperature naturally raises by as much as 20-30°C due to the exothermic reaction (Arce et al., 2017), thus almost reaching optimal temperature. For this reason, no heating demand is considered for the leaching process in the present study. The two most important factors for dissolution efficiency are average particle size of 75 to 125 µm, which show a significantly enhanced extraction efficiency as compared to bigger diameters (Teir, Revitzer et al., 2007), and high acid concentration. Specifically, Mun et al., 2017 show a linear relationship between acid concentration (studied range : 0.1 to 0.5 M HCl) and maximum extraction ratio of calcium ions from steel slags and cement wastes. High acid concentration may compensate high solid-to-liquid ratio with regards to reaction kinetics (Mattila et al., 2012).

For steel slags, Jo et al., 2017 find a full extraction of the calcium ions after 1 hour (30°C, S/L = 50 g/l, 1 M HCl). For wollastonite, J. Zhang et al., 2010 reach 96.1% Ca ions leaching efficiency after only 10 minutes (30°C, CaO/HCl molar ratio = 0.5, 4 M HCl), following the exothermic leaching reaction :



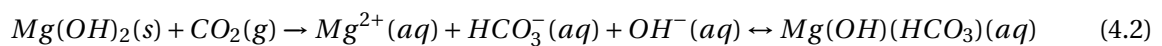
For the present work, no additive (e.g. EDTA) is used as recovery of pure products is more complicated and expensive (Mun et al., 2017). For the reactor, it is assumed that the molar ratio of CaO/HCl is 2 (J. Zhang et al., 2010), and that respectively 3% and 10% of SiO₂ and K are leached (Jo et al., 2017).

4.2 CO₂ dissolution

The gaseous CO₂ to be mineralized is typically carried by industrial exhaust gas, differing substantially in composition and impurities content depending on its origin. For direct aqueous wollastonite

carbonation, Yan et al., 2013 claim a conversion reduction by about half of the value for a purified CO₂ stream (60%, at 40 bars and 200°C), if the flue gas is composed of N₂ (ca. 82%vol), CO₂ (15%vol), O₂ (3%), SO₂ (0.1%vol) and NO (0.05%vol). This efficiency loss is attributed to an increased acidity in the solution, hindering the calcium carbonate precipitation, and competitive reaction of gypsum (CaSO₄·2 H₂O) production. When studying the effect of impurities (Na⁺, K⁺, Mg²⁺, Al³⁺ and anions SO₄²⁻, NO₃⁻ on the couple reaction-extraction-crystallization of industrial waste CaCl₂-brines from ammonium production plants, Dong et al., 2018 emphasize the importance of SO₄²⁻ removal before mineralization, as CaSO₄·2H₂O precipitation on the carbonate surface reduce significantly mass transfer. For fly ash direct carbonation, Rausis et al., 2021 find 25% conversion efficiency for pure CO₂ stream, whereas for a mix of 84% N₂, 15% CO₂ and 1% H₂O, the conversion is below 16% : this gap is lowered for increased gas pressure (7 bar), and conversion efficiencies reach 36 and 32% respectively.

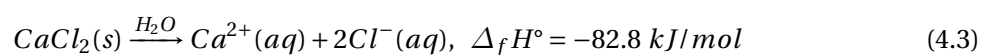
In the CO₂ absorption tank, the Mg(OH)₂ flakes contained in the slurry reacts spontaneously with the gaseous CO₂ molecules following the reaction 4.2. The enthalpy of reaction computed from the heat of formation of reactants and products is $\Delta_f H^\circ = -68.4 \text{ kJ/mol}$ at STP.



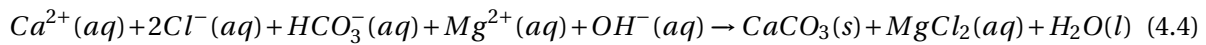
T. Li et al., 2014 study thoroughly the CO₂ removal using Mg(OH)₂ in a bubble column, selected due to its high heat and mass transfer, compactness, and lower operating and maintenance costs. The effects of inlet gas flow rate, gas temperature, diameter and height of the column, and solution concentration are analyzed. In particular, the CO₂ removal efficiency is shown to be independent of absorbent concentration, since it is restricted by the Mg(OH)₂ dissolution rate. Increase in flow gas velocity is shown to overall reduce the CO₂ removal efficiency due to decreased Mg(OH)₂:CO₂ molar ratio, and for the same reason, there is a trade-off on the gaseous CO₂ concentration (12% is shown to be more efficient than the other values tested : 4, 8 and 16%). The optimal absorption efficiency of 75-80%, the reactor temperature range is 35 to 45°C, for which the reaction is neither limited by dissolution rate nor MgCO₃ formation. The authors notably predict the carbon and magnesium speciation at the bottom of absorber depending on the input Mg(OH)₂ solution concentration, and study the absorption equilibrium (in particular, pH) and kinetics along the column. Following this review, the assumed temperature of the absorption column is 35°C, for a capture efficiency of the gaseous CO₂ of 80%.

4.3 CaCO₃ precipitation

The Mg(OH)(HCO₃) brine is fed to the carbonation tank, mixing with dissolved calcium chloride CaCl₂. If calcium chloride is supplied in crystalline form, its dissociation happens spontaneously when entering in contact with water, following the exothermic reaction 4.3.



The dissolved calcium ions react with the bicarbonate ions following reaction 4.4, releasing additional heat of $\Delta_f H^\circ = -29.9 \text{ kJ/mol}$ at STP.



B. Feng et al., 2007 bubble directly the CO_2 in a $\text{Ca}(\text{OH})_2$ slurry and investigate the effect of various operating parameters on the carbonation reaction, including the use of additives (EDTA, torpineol, etc.), CO_2 bubble size, gaseous flow rate and concentration, as well as temperature (25 and 80°C). The authors find that PCC particle size is decreasing with decreasing CO_2 concentration and decreasing bubble size. For their experiment, the average crystal diameter at ambient temperature ranges typically between 1 and 3 μm . J. Zhang et al., 2010 compare the carbonation efficiency for varying CO_2 pressure (20-50 bar), CaCl_2 concentration (1.3-2.4 M) and solvent/ CaCl_2 molar ratio. For Ca ions leached from waste cement and blast furnace slags, Mun et al., 2017 quantify the conversion ratio depending on pH for the range 9 to 12, for which the carbonation increases in both cases (e.g. for slags : 11% at pH 9, 22% at pH 12). X. Zhang et al., 2021 study the CaCO_3 precipitation kinetics in the CaCl_2 - CO_2 - $\text{Mg}(\text{OH})_2$ - H_2O system when mixing a CaCl_2 solution (0.5-1.5 M) with MgO powder. In particular, higher temperature is shown to increase the reaction kinetics, but does not influence final conversion rate as >99.5% is achieved for both 50 and 65°C.

Regarding crystallization mechanism, Dickinson et al., 2002 study the kinetic and thermodynamic control of CaCO_3 crystals growth, and show that carbon dioxide partial pressure p_{CO_2} and calcium ion concentration are the most important factors for determination of the precipitation reaction. In particular, the authors find that rhombohedral calcite is preferentially grown if the carbon dioxide partial pressure does not exceed a certain threshold (which depends on the calcium concentration), after which vaterite formation is favoured. Zappa, 2014 review the effect of additives (EDTA, amines, etc.) and impurities (ZnCl_2 , ions favouring aragonite formation, etc.), and at 40, 60 and 70°C, L. Li et al., 2021 find that calcite is the preferred precipitation form of carbonates. Chang et al., 2017 assess thoroughly the polymorphism of CaCO_3 precipitation, reviewing the effect of reactor temperature, pressure, pH of the solution, reaction time, degree of supersaturation, ion concentration and ratio, ionic strength, stirring, type and concentration of additives, and feeding order.

In the present work, it is assumed that carbonation efficiency is 95% for reactor residence time of 20 minutes, at 45°C. After liquid-solid separation, in which it is assumed that all impurities precipitate with the carbonate (thus no carbonated products enter the magnesium salt regeneration cycle), PCC crystals require purification from salts residues in order to reach commercial quality. Teir et al., 2016 assess the performance for separation processes of PCC produced from steel slags (using ammonium chloride), and find residual chloride content dropping from 10'000 to 10 ppm in a single-stage washing and filtration step. Washing water amounts range from 0.5 to 2 $\text{l/kg}_{\text{dry-solids}}$, and filtration rates are considered fast. A final PCC drying step is required to evaporate the remaining cake moisture (10-20%), for which typical temperature levels are 70-80°C (Beigi et al., 2015).

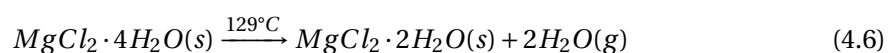
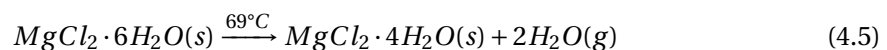
With regards to the particle size distribution (described in 3.5) achieved currently for PCC from mineralization pathways and assuming the costs reported by Zappa, 2014 for a large range of PCC and

ground calcium carbonates (GCC) quality, a PCC retail price of 100 CHF/t is assumed.

4.4 Magnesium salts regeneration

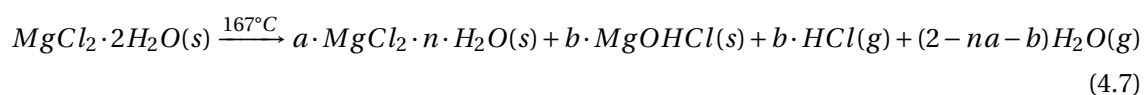
The CO₂ absorption tank requires important flows of Mg(OH)₂-MgCl₂ slurry supply and MgCl₂ hexahydrate off-take, which implies the need for a regeneration loop in order to avoid high resource buying and disposal costs. The regeneration occurs in 3 main steps : first, the solution is concentrated (saturated) in an evaporator. Then, under further heating, MgCl₂ · 6H₂O crystals are formed and dehydrated to yield MgCl₂ dihydrates. These crystals are eventually thermally decomposed to Mg(OH)₂ solid flakes, gaseous hydrochloric acid (HCl) and water vapor. According to Huang et al., 2011, the thermal decomposition mechanism for regeneration of MgCl₂ · 6(H₂O) to MgO follows the chemical reactions 4.5 to 4.10, enabled each by different temperature levels (displayed indicatively for each reaction). The enthalpy of these reaction depends significantly on reaction conditions : the influence of exact reaction temperature, heating rate and gaseous media composition (N₂ or water vapor) is reported in Xu et al., 2021 and Rammelberg et al., 2012 (see also Seeger et al., 2011 and Kirsh et al., 1987).

- **Concentration** of the magnesium chloride solution in an evaporator
- **Crystallization** of the MgCl₂ hexahydrate solids and **dehydration**, occurring in two steps respectively enabled theoretically (see (Huang et al., 2011)) by temperatures of 69°C (reaction range : 50-117°C reported by (W. Chen et al., 2018), limited by MgCl₂ · 6H₂O fusion above) and 129°C (reaction range : 90-167°C) :



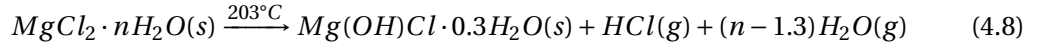
As reported by Kelley, 1945, the dehydration rate is expected to increase with increasing vapor pressure at the higher temperatures, and enthalpy of reaction is not significantly impacted by the temperature level. Practically, it appears that 402-407 K is the lowest temperature possible for carrying out both dehydration reactions, and the dehydration is thus considered at a temperature of 135°C (Xu et al., 2021 and Rammelberg et al., 2012). The corresponding enthalpy for both reactions is 1208 kJ/kg_{MgCl₂ · 6(H₂O)} (245 kJ/mol, Adham et al., 2012).

- Further **dehydration and thermal hydrolysis**, occurring simultaneously in the temperature range 167 to 400°C :



with $1 \leq n \leq 2$, $a + b = 1$ depending on reaction conditions.

(Klammer et al., 2020) states that *although stoichiometries of $Mg_x(OH)_yCl_z$ other than $x, y, z = 1$ are known, [our] results indicate that $MgOHCl$ is the predominant stoichiometry and that other magnesium hydroxychloride compounds can be neglected*. This implies for the present study the preferential choice of parameters $a = 0$, $b = 1$, $n = 1$ for reaction 4.7, with a reaction enthalpy of 1025 kJ/kg $_{MgCl_2 \cdot 2(H_2O)}$ (134 kJ/mol) at ca. 425°C, estimated from thermodynamic heats of formation (Kelley, 1945). Note that for the production of the intermediate compound $Mg(OH)Cl \cdot H_2O$, (Rammelberg et al., 2012) reports an enthalpy of reaction of 383 kJ/kg $_{MgCl_2 \cdot 2(H_2O)}$.

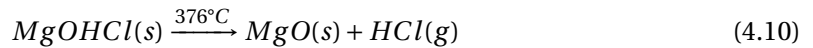


with $1 \leq n \leq 2$



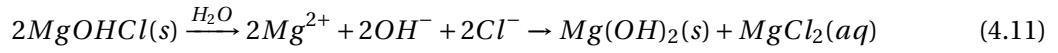
Several literature documents claim lower temperature required for partial fulfilling of Reactions 4.7 to 4.9 : temperatures from 250°C are mentioned in the molten salt process described by Wendt et al., 1999, J. Zhang et al., 2010 and Xu et al., 2021. However, Klammer et al., 2020 and Y. Zhao and Vidal, 2020 show that the majority of the magnesium chloride species react to $MgOHCl$ when the reaction temperature is above 400°C.

- **Dehydroxylation** or dehydrochloridization, for which the activation temperature was reported as low as 376°C (Kashani-Nejad et al., 2005), but is more recently re-evaluated to values higher than 400°C : 533-568°C in Y. Zhao and Vidal, 2020 (see also Klammer et al., 2020 and Bakker et al., 2013). The gaseous HCl partial pressure influence on the equilibrium of this reaction is addressed in particular by Kelley, 1945.

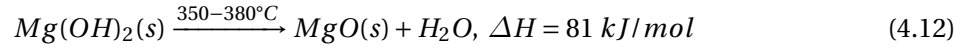


Note that an alternative mechanism is described by Huang et al., 2011 for the decomposition of $MgCl_2 \cdot H_2O$ to MgO , for which the reported minimum reaction temperature required is lower (360°C) due to more reactive intermediate products. Other decomposition pathways involving hydrated magnesium hydroxychlorides as intermediates are discussed in Bakker et al., 2013, reporting a minimum temperature of 446 and 560°C respectively for the 2-form ($2MgO \cdot MgCl_2 \cdot 6H_2O$) and 3-form ($3MgO \cdot MgCl_2 \cdot 11H_2O$) for full dehydroxylation. At such high temperatures, the complete decomposition reaction only takes ca. 1 minute.

The complexity of this MgO - $MgCl_2$ - H_2O system is particularly assessed in Klammer et al., 2020. The authors assume a stoichiometric speciation of $MgOHCl$ when dissolved in water, following reaction 4.11, and conclude that the assumption is plausible given the experimental results.



Given the higher reactivity for carbonation of $Mg(OH)_2$ compared to MgO (Fagerlund and Zevenhoven, 2011), the dehydration following reaction 4.12 (see Pan and Zhao, 2015 and Seeger et al., 2011) is in effect not required.



The aqueous dissolution of $MgOHCl$ is spontaneous at temperatures above $400^\circ C$, as it is the competitive reaction (w.r.t. MgO production by the thermal activation of reaction 4.10) described by Kashani-Nejad et al., 2005. Computed on the basis of enthalpies of reaction listed in Kelley, 1945 and reaction 4.12, the enthalpy for the overall reaction 4.11 at $425^\circ C$ is 13.2 kJ/mol , thus slightly endothermic.

In practice, reaction 4.11 is done after the decomposition reactor, when the aqueous $MgCl_2 \cdot 6(H_2O)$ solution is mixed with the regenerated $MgOHCl$ crystals, precipitating magnesium hydroxide crystals which are not soluble in water at normal conditions. The magnesium species form a concentrated slurry sprayed in the absorption tank, closing the regeneration loop. The piping and conveying of $MgOHCl$ solids must be done under dry conditions and with corrosive-resistant material, as emphasized by Kashani-Nejad et al., 2005.

4.5 Resources and energy flows

The main resources and energy requirements of the mineralization process are quantified and displayed in Figure 4.2. Dependent on alkaline material input, the salt production site is not detailed, except for the required CaO content and HCl make-up (due to losses in effluent mineral residues and potential wastewater). The principal water consuming stages are the bubble column and the PCC washing steps : they amount together to ca. 168 m³/h. The evaporation and crystallization reactor produce ca. 110 m³/h. The simulated decarbonized flue gas contains 2.2%vol. CO₂, and the carbonated product is of commercial grade (98.56% CaCO₃ purity) for a yearly output of 231.6 kt_{PCC}.

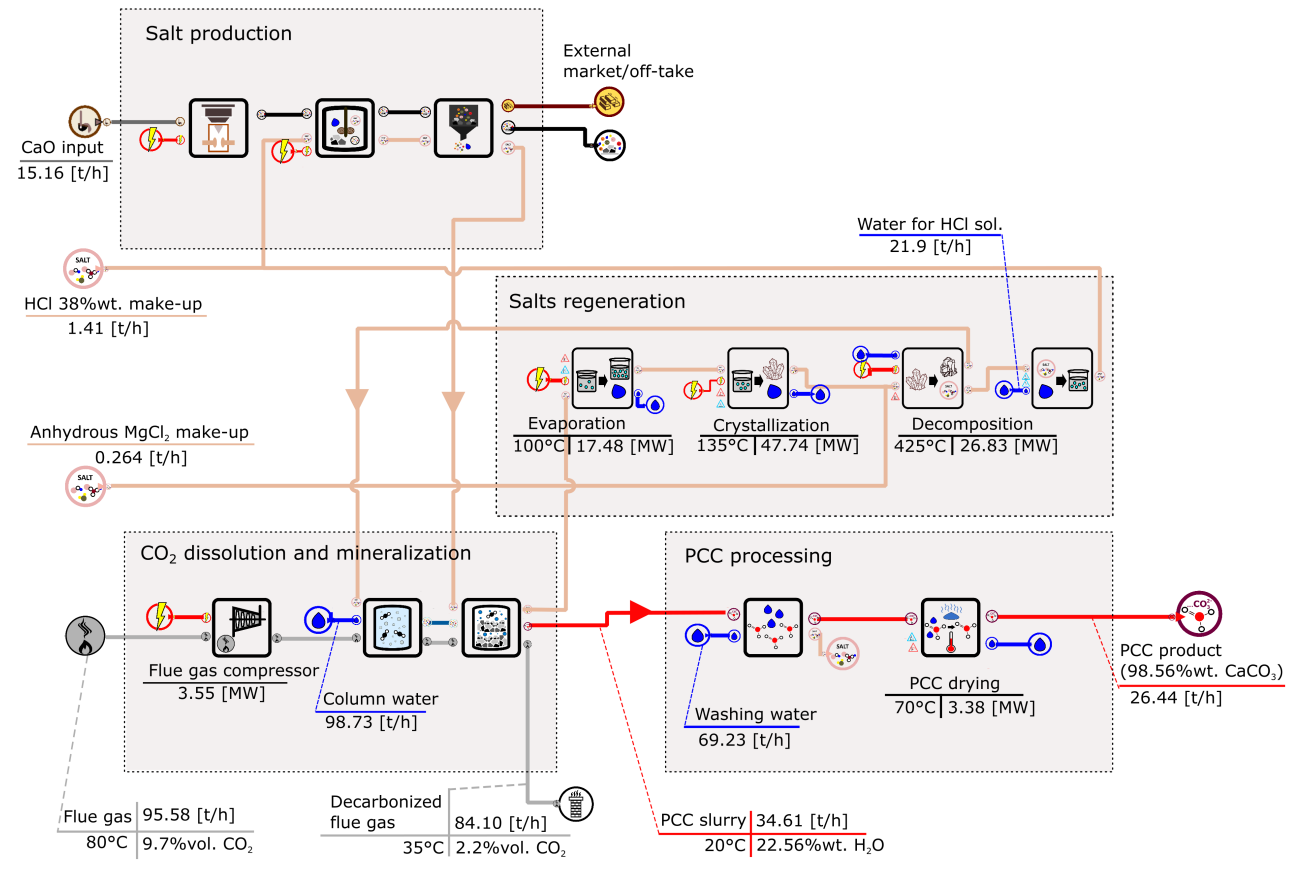


Figure 4.2: Flow sheet of the main mass, power and heat flows per process unit.

Hot and cold streams of the whole mineralization process can be visualized in the composite curves of Figure 4.3. The 3 largest heat requirements come from the MgCl₂·6H₂O-brine concentration stage in the evaporator (54.1 MW_{th}), followed by the crystallization heat (40 MW_{th}) and MgCl₂·2H₂O crystals decomposition heat demand at 430°C (23.3 MW_{th}). These high regeneration heat loads are heavily impacted by the salt decomposition efficiency of 50%, assumed given Reaction 4.11. Indeed, as a consequence, the preliminary evaporation and crystallization loads are also doubled.

The main cold requirement of the process lies in the latent and sensible heat in the evaporated water (steam just above the boiling point). The cold demand for HCl vapor cooling is relatively small, but spans over a large range of temperatures.

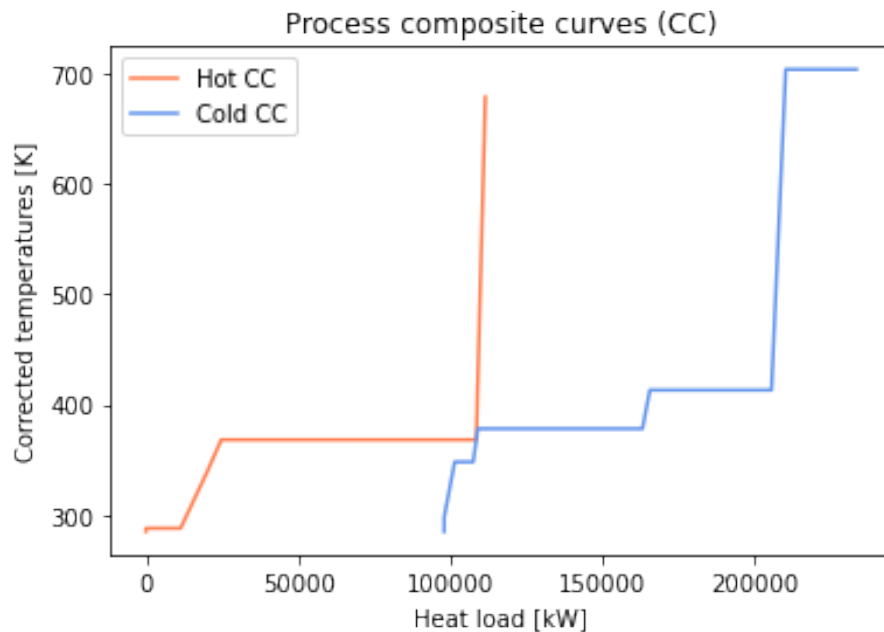


Figure 4.3: Composite curves of the mineralization process hot and cold streams, before integration to the EfW plant.

In order to improve the energy efficiency of the mineralization process, heat recovery between unit processes is key. If this recovery is optimally done, the Minimum Energy Requirement (MER) for the whole process, computed by the dedicated minimization problem in OSMOSE, amounts to :

- Cold utility requirement : 98.072 MW_{th}.
- Hot utility requirement : 121.884 MW_{th}.

This result is also graphically displayed in the grand composite curves of Figure 4.4. A unique self-sufficient pocket is observed between 348.15 and 368.15 K, as waste heat from the magnesium salts evaporation and crystallization can partially be reused for the drying of precipitated calcium carbonates. The process pinch point is at T = 378.15 K (105°C).

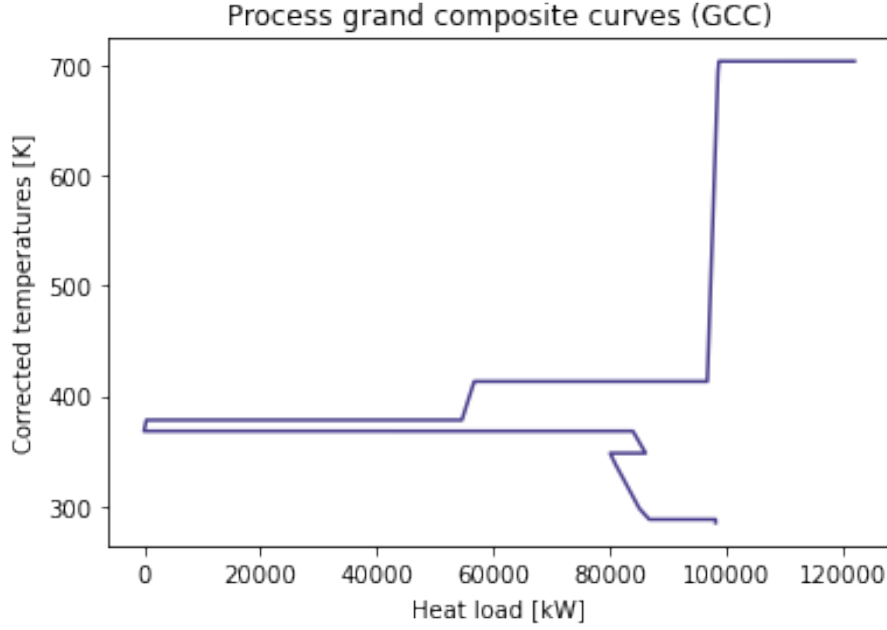


Figure 4.4: Grand composite curve of the mineralization process, before integration to the EfW plant.

4.6 Fixed-investment cost

The estimation of fixed-investment cost for a CO₂ mineralization plant with nominal capacity of 100 kton_{CO₂}/y in Switzerland is done following the methodology presented in Section 2.1.2. The total purchased equipment cost computed is 26.6 Mio CHF, excluding the heating and cooling utilities as those depend on the integration of the plant. The breakdown into main components cost is displayed in Figure 4.5. The predominant components in the CAPEX are the units required for salts regeneration : the crystallizer, evaporator and decomposition tank represent 58.7% of the mineralization plant purchased equipment costs. This share rises when considering the installed cost, particularly due to the relatively high bare-module factor of the decomposition tank. Indeed, the latter consists of heat- and corrosion-resistant materials for handling of HCl vapor, for which Turton et al., 2018 report F_{BM} higher than 5. These high cost might however be reduced if better decomposition efficiency are achieved : although reactor cost may increase for higher fluidized bed temperature, crystallizer and evaporator sizes may decrease significantly. Carbonation tanks represent the least significant cost as the reactor technology is comparatively simpler and fast precipitation kinetics are assumed (tank residence time of 20 minutes).

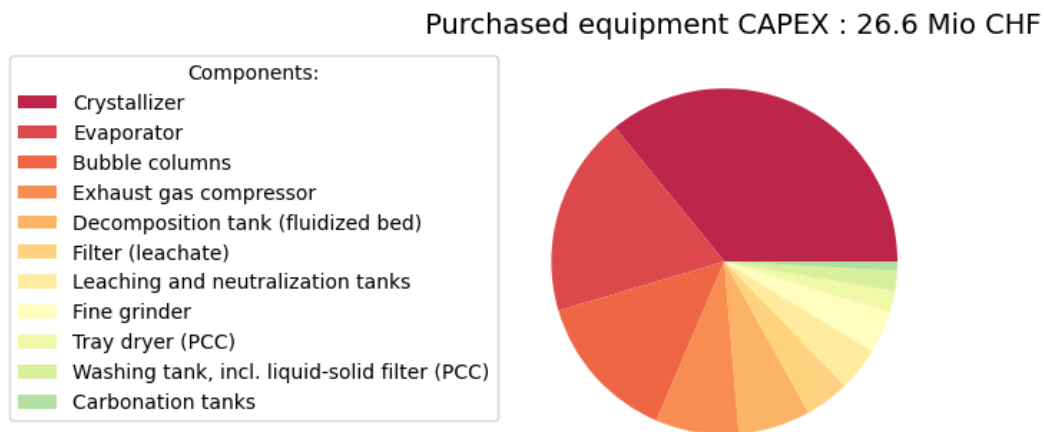


Figure 4.5: Purchased equipment cost breakdown for the main components of the whole mineralization plant infrastructure, including salt production site (fine grinding and leaching process).

For accounting of installation, as well as all other direct and indirect costs, the Lang methodology is selected. Given the mixed solid-fluid processing character of the mineralization plant, the multiplication factor of the purchased equipment to compute the total fixed-investment cost is 3.63. Table 4.1 presents the estimated CAPEX and corresponding uncertainty range when using the bare-module cost computation (accounting for contingencies and contractor fees of 35%) and the Lang method. Given the large uncertainty on exact cost correlation of reactors (specifically on the crystallizer and fluidized bed for decomposition), the estimations uncertainty ranges are overlapping in the range 53.3 to 134.8 Mio CHF, which already provides a reasonable indication of the fixed-capital cost for this stage of project assessment.

Method	Estimated CAPEX [Mio CHF]	Uncertainty range [%]
Bare-module cost	76.2	[-18.1, +76.9]
Lang method	96.8	[-44.7, +83.8]

Table 4.1: Initial fixed capital expenditures (CAPEX), including direct and indirect costs, calculated with both the Lang estimation method and bare-module cost approach. Uncertainty ranges are based on error propagation from estimated unit components cost ranges.

More detailed CAPEX estimates could include finer assessment of cost breakdown, as presented for instance in Lemmens, 2016 for an Organic Rankine Cycle (ORC) system. The authors compute the total fixed-capital cost based on an estimated delivered equipment cost percentage of on-site, off-site, indirect costs and other outlays. In order to make this further analysis relevant, remaining uncertainties around exact reactor types, dimensions and materials should be reduced in parallel for a more accurate computation of the purchased equipment cost.

Chapter 5

Process integration into the Energy-from-Waste context

The mineralization process described in the previous chapter is integrated to the Waste-to-Energy context in Switzerland, including the implementation of a set of energy supply utilities. In addition, several possible plant configurations are investigated, taking into account transport logistics.

5.1 Energy-from-Waste plant

Given the Swiss agreement between DETEC and ASSED described in Section 1.1, targeting one CO₂ capture plant of 100 kton_{CO₂}/year nominal size per waste treatment installation operator by 2030, this is the chosen reference size for the present study. Accounting for 80% absorption efficiency of the flue gas carbon dioxide, this corresponds to an Energy-from-Waste plant of nominal waste throughput of approximately 11.5 t_{MSW}/h. Several key figures and assumptions are necessary for setting the scope of this study :

- The biogenic fraction of the municipal solid waste combusted varies between regions and countries in the range 0.4-0.7 (Rosa et al., 2021). Following a research campaign applied on 5 Swiss plants (Bretscher et al., 2018), the biogenic carbon in the waste is in average 52.3% (2018). This biogenic part is not considered in the results analysis and discussion, given that the same effort on reducing the mineralization process carbon intensity has to be done, whether it is accounted for or not.
- The EfW plant produces superheated steam at 410°C and 41 bar (outlet of the boiler). This energy might be utilized for power generation (for own consumption or supply to the grid), heating and/or steam supply (e.g. to industrial partners for specific processes). For instance, and indicatively for comparison purposes, the HZI EfW plant in Perlen (Luzern, CH) produces 0.725 MWh_{el}/t_{MSW} by turbine power generation, 0.955 MWh_{th}/t_{MSW} in the form of steam (165°C, 4.5 bar) and 1.247 MWh_{th}/t_{MSW} are provided by steam leaving at 118°C, 0.8-1.8 bar for District Heating Network (DHN) (Renergia, 2020).

- Although few weeks of regular plant maintenance per year are typical, 8760 hours of operation per year are considered as reference.

The scope of the present study takes the flue gas just before its emission to atmosphere at the chimney stack, after state-of-the-art flue gas treatment. It generally includes several of the following stages : dry sorption with Na- or Ca-based additives for acidic pollutants (HF, HCl, SO_x) removal, fabric filtering and electrostatic precipitation for dust removal and selective reduction (catalytic or not) for NO_x removal. As baseline, no additional flue gas purification or pre-capture is considered for the present study. Therefore, the CO₂-containing gas taken up by the mineralization process has the composition as usually emitted to atmosphere by the incineration chimney stacks, described in Table 5.1.

	Gas composition [%vol.]				Impurities content [mg/Nm ³]							
	N ₂	CO ₂	O ₂	H ₂ O	Dust	HCl	SO ₂	NO _x	HF	NH ₃	HM	Dioxine
Boiler outlet	67.6	10	6	16.4	30	850	550	400	30	*	6	1
Chimney stack	68	9.7	6.4	15.9	<2	<4	<8	35	<0.5	<1	<0.1	<0.02

Table 5.1: Municipal waste incineration flue gas composition before and after state-of-the-art flue gas treatment. *Note : Heavy metals (HM) comprise Hg, Cd, Pb and Zn. * indicate unspecified values.*

5.2 Utilities integration

Besides the EfW plant, the integration of the mineralization plant is evaluated with other heat and electricity utilities, relevant for the system requirements calculated in Section 4.5. The options considered and corresponding key assumptions are listed hereafter.

- National power grid : Connection to the Swiss power grid, with an assumed power price of 0.2 CHF/kWh_{el} and emission factor of 0.108 kg_{CO₂-eq}/kWh_{el}, average for electricity consumption in Switzerland, including imports, for the year 2017 (Ruedisueli et al., 2022).
- Natural gas (NG) boiler : State-of-the-art methane combustion boiler, 97% internal efficiency, assuming a CH₄ purchase price of 70 CHF/MWh_{th} (on LHV basis).
- Cooling water (CW): Cooling tower (air-water) for water supply at 10°C, returning to the cooling tower at 20°C. Pumping, fan and other power requirements are taken into account, corresponding to an assumed power demand of 0.02 kW_{el}/kW_{th} (D'Antoni et al., 2014).
- Electrical heater : Electrically-coiled fluidized bed reactor (FB) for thermal decomposition of salts at temperature of 400 to 600°C, assuming a thermal efficiency of 0.95 (conversion of electric to thermal energy).
- Heat pump (HP) : Heat pumping for temperature levels ranging from ambient to above 130°C (Wallerand, 2018), with various options for working fluid : R12, ammonia, R141b, R32, CO₂, methane, etc. The minimum temperature difference inside the HP components is $\Delta T = 2$ K.

- District Heating Network (DHN) : Connection to a medium-temperature heating network for heat supply at 80°C ($T_{return} = 60^\circ\text{C}$) (Oppermann et al., 2020).

To give an insight into the optimized technology selection, specific power and fuel consumption or heat supply are reported. The corresponding environmental burden and economics are assessed in Chapter 6. Note that the EfW plant own requirements for utilities are out of the scope for this analysis.

Reference case : EfW, NG boiler and CW

If only the EfW plant (with corresponding steam supply), the NG boiler and the cooling tower are available, the heat is not efficiently provided. As can be observed on Figure 5.1, the EfW steam is not enough to cover the evaporation/crystallization loads, and does not provide at sufficiently high levels to be used for the decomposition tank. Moreover, as no other cold utility is considered below the pinch point, the cooling water tower duty is significant : the utility loads are summarized in Table 5.2.

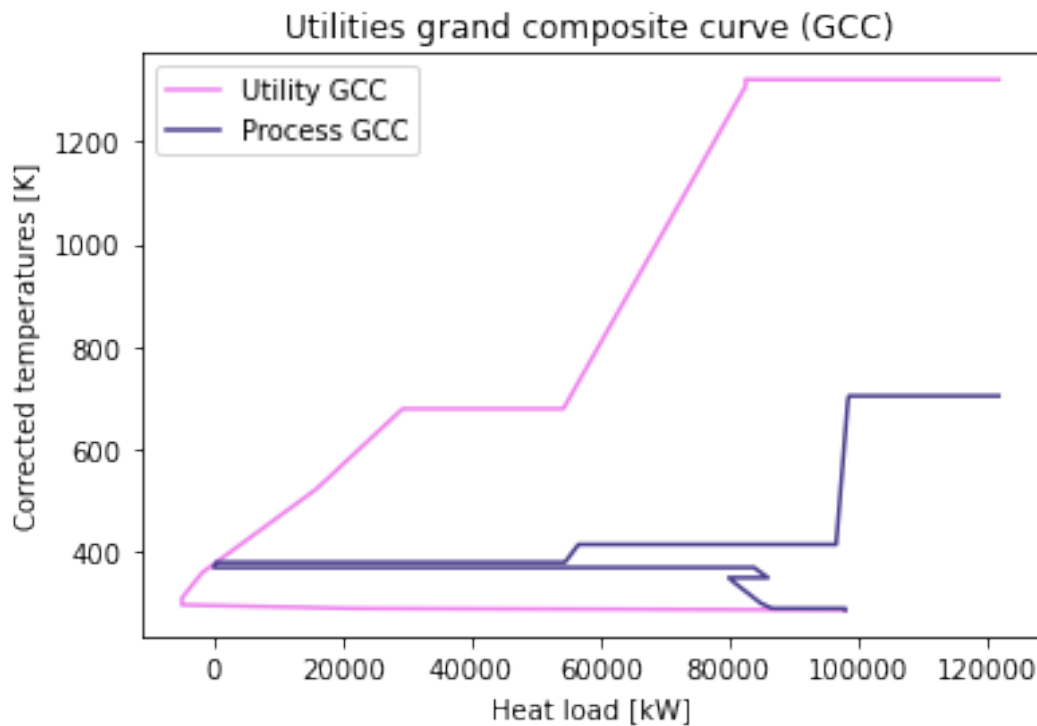


Figure 5.1: Grand composite curves of the mineralization process sub-system and the utilities sub-system, composed of EfW steam, cooling water and NG boiler.

Cooling tower power	Natural gas boiler (on LHV basis)
2015.7 kW _{el}	77501.6 kW _{th}

Table 5.2: Utilities sizes for the reference case of EfW steam, NG-fired boiler and cooling water tower for cold utility.

Improved case : addition of electrical heater, DHN and HP

In order to improve the environmental performance of integrated system, an electrically heated fluidized bed reactor for decomposition of the salts is considered, as well as heat pumping across the pinch point and hot utility service for heat excess below the pinch point (DHN). For minimization of environmental impact, the electrical heating of fluidized bed is selected over the NG-fired FB. In Figure 5.2, the effect of recovering the heat below the pinch point by pumping it above or exchanging it with the DHN is clearly observable. Table 5.3 reports the corresponding utilities sizes. The heat pump, selected for temperatures levels between 85 and 115°C, uses ammonia as working fluid. Its power input is 5.62 MW_{el} for an evaporator load of 38.98 MW_{th} at 87°C. Heat is provided between 112 and 138°C, including condensation (at 113°C) and sensible heat from the superheated fluid, for a total supply of 44.60 MW_{th}. The corresponding coefficient of performance (COP) of the heat pump is 7.94.

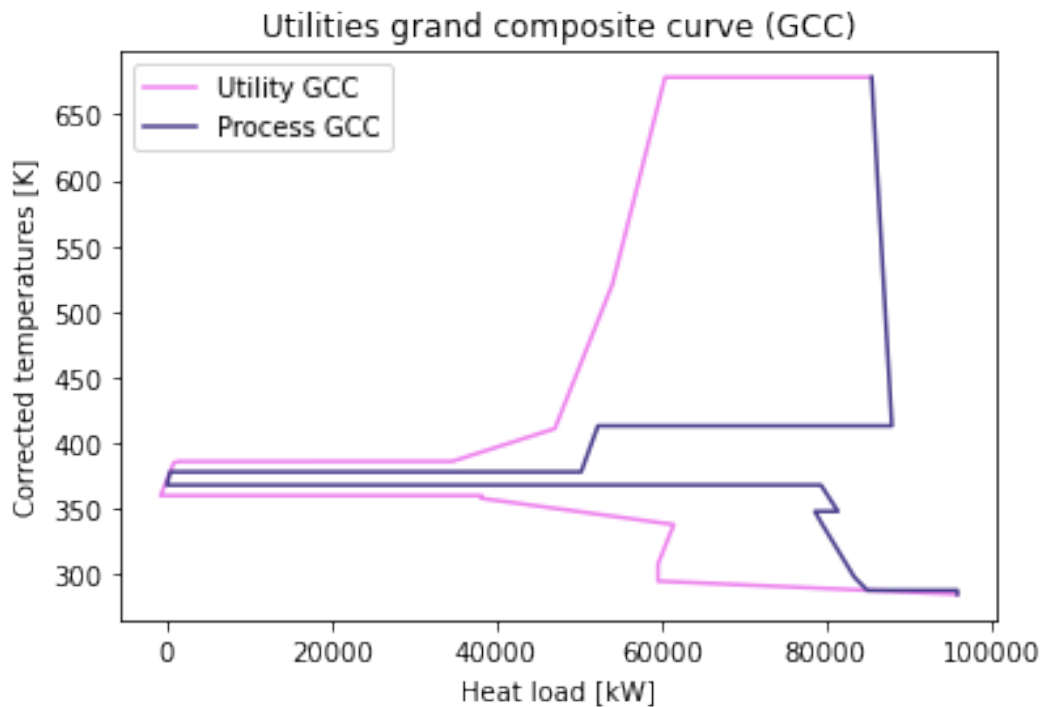


Figure 5.2: Grand composite curves of the integrated mineralization process, with heat pumping and DHN.

Power : kW _{el}			Heat : kW _{th}
HP	CW	FB	DHN
5'620	726.6	28'240	24'711.1

Table 5.3: Utilities sizes for the improved case, when an electrically heated fluidized bed reactor (FB), HP and DHN connection are additionally considered. No NG-fired boiler is selected.

Another way to visualize the improvement for the integrated system is through Figure 5.3. If utilities

and process are selected optimally, the grand composite curve of the whole integrated system tend to form more than one pinch point. This is obviously not the case for the reference case, but when DHN and HP are implemented two kinks appear, at 65 and 140°C.

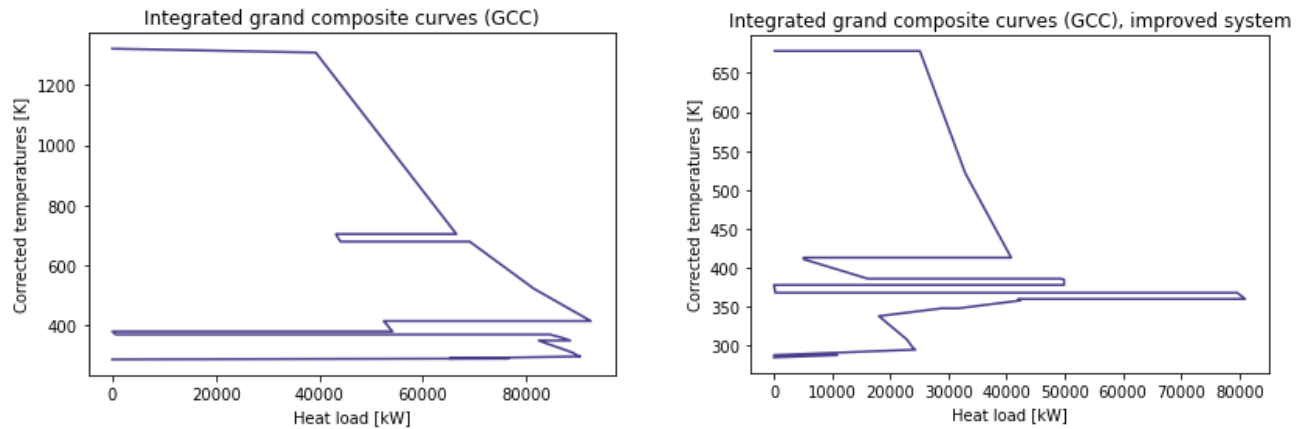


Figure 5.3: Grand composite curves of the total integrated system, when utilities are integrated to the process. *Left* : reference case with only EfW steam, cooling water and NG boiler. *Right* : environmentally improved case with addition of electrical fluid bed, DHN and HP.

Note that if the fluidized bed is forced as gas-fired reactor, and the heat pump and DHN are implemented as in the above, the utilities are sized as presented in Table 5.4.

Power : kW_{el}		Heat : kW_{th}	
HP	CW	CH ₄	DHN
5'570	726.6	29'554	24'711.1

Table 5.4: Utilities sizes when the fluidized bed reactor (FB) is gas-driven, and HP and DHN connection are considered. The heat equivalent for NG combustion is based on LHV basis.

5.3 Plant arrangement

The mineralization plant can be split in different sites in the case of land availability limitations or other factors constraining the unified siting, such as the dispersed nature of the resources. The possible plant sub-divisions, shown in the blocks of Figure 5.4, are assessed in order to determine the feasibility and profitability of reactor clustering. The proximity of the mineralization site to PCC off-taker is economically and environmentally beneficial, but is not assessed hereafter : the scope boundary is at the PCC gate.

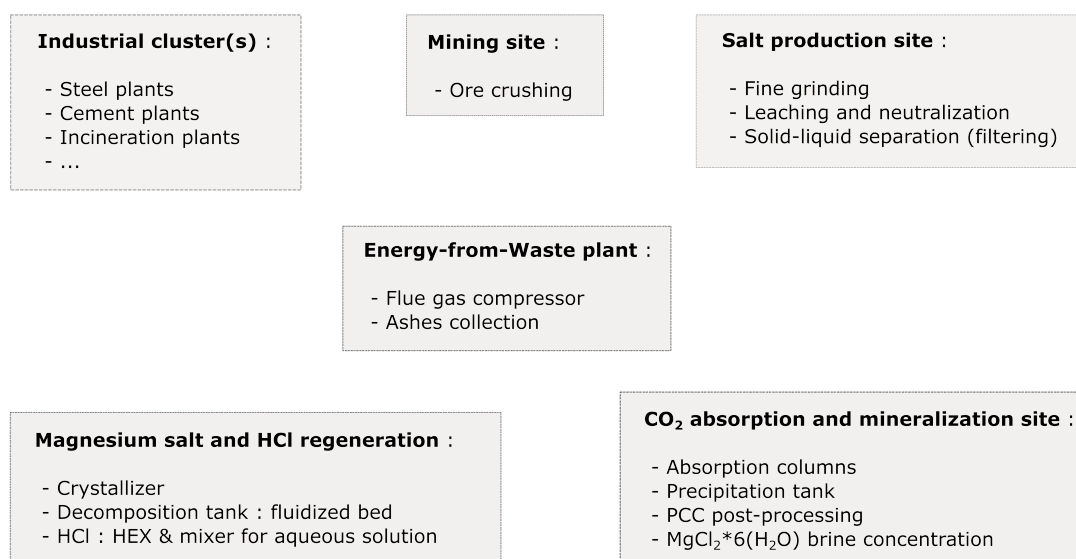


Figure 5.4: The distinguishable blocks of the mineralization pathway, which can be clustered in different sites.

In order to assess the most interesting configuration, all options are evaluated by optimizing for the most economic arrangement, taking into account mass and power demand balance, heat integration, transport of resources between the potential different locations and land price. The transportation mode for chemicals or alkaline material, with related cost and emission factor, may vary depending on the context, the available infrastructure and the type of good transported. If the mineralization pathway is distributed in different locations, the transport distance between EfW site and salt production site is assumed to be 75 km. Thereby, the mineralization site and the magnesium salts regeneration site might be located at either of the locations. However, given the high costs of flue gas pipelines if mineralization site and EfW site are separated, these are sited together. The distance to the closest mines is assumed as 400 km, accessible by train. The distance to other industries for alkaline waste supply is estimated for slags and CKD : for instance, the average distance of the 6 national cement plants to 5 distributed EfW plants (of relevant size) across Switzerland is ca. 125 km. The shipping costs and assumed transport distances for each resource are listed in Table 5.5.

In order to take into account the typically elevated land prices around the EfW plants in Switzerland, industrial land price is fixed at 250 CHF/m² for locations separated from the EfW, and this value is doubled if the unified mineralization plant is to be built on-site. The land footprint of the mineralization plant components is not disclosed for confidentiality reason.

	Resource	Transport mode	Transport cost CHF/ton-km	Transport distance, km
Salts slurry	CaCl ₂ (leached, 41-45%wt.)	Truck	0.052	75
	MgCl ₂ (hexahydrate)	Truck	0.067	75
	Mg(OH) ₂ flakes/slurry	Truck	0.131	75
	HCl solution 38%	Rubber lined trailer truck	0.04	75
Solids	Crushed rock minerals	Rail	0.113 - 0.146	400
	Cement kiln dust (CKD)	Truck	0.06	125
		Rail	0.113 - 0.146	125
	Slags	Truck	0.06	80
		Rail	0.113 - 0.146	80

Table 5.5: Summary of the assumptions regarding resources transportation logistics. Transport types, related cost (computed from Bina et al., 2014 and) and assumed distances for the optimization are listed for the main resources flows, if the plant is subdivided.

Findings

Based on the stated assumptions, the following results are observed :

- The initial fixed-investment cost for the total land footprint when the site is unified, although bigger, is of same order of magnitude than the annual operational cost related to transportation costs if salt production site and mineralization site (located at the EfW and regeneration site) are separated. Thus, the unified siting is the preferred option whenever possible.
- If the sites clustering is not avoidable for instance due to selection of mineral ore mining, or forced for other reason, the calcium salt production facility is placed at the mining location, and the magnesium salts regeneration is placed at the mineralization site. This split is motivated by heat integration opportunities and by the lower amount of goods that must be transported if compared to other arrangement options : ca. 120 t/h, whereas more than 130 t/h are transported if the magnesium salts regeneration site is placed at the calcium salt production site. Therefore, the transported resources are the HCl solution and CaCl₂.
- The calcium salt might be transported in anhydrous/hydrated crystal form, or aqueous solution (typically of maximum 42-45%wt. concentration). The optimization result show that although the transport quantities are multiplied by a factor of 2.5, the advantage of transporting the CaCl₂ in liquid form is the avoidance of high evaporation and crystallization heat after the leaching stage. A natural gas boiler utility for this heat supply exceeds by 2 orders of magnitude the transport emissions difference between both options, and by 1 order of magnitude the related transport cost. Thus, the transport of liquid CaCl₂ is thus both environmentally and economically more interesting.

Chapter 6

Mineralization scenarios

Based on the results obtained from the heat integration and plant arrangement analysis, this chapter presents specific scenarios of interest for the mineralization process integrated with an EfW plant. The scope for each scenario takes into account the flue gas as emitted at chimney stack of the EfW and the steam as produced at the outlet of the boiler, but generally leaves out other components of the EfW plant, unless stated and justified otherwise. To be completely consistent on a life-cycle approach, the shortfall implied on power grid injection, DHN and other (e.g. steam to partner industries) revenues for the EfW should be taken into account, but this analysis is left out of the scope.

The process main flows and energy requirements are as presented in Figure 4.2. The heat and cold utilities considered for the scenarios are as selected in the environmentally improved case of the heat integration, but forcing the gas-driven fluidized bed (see Table 5.4) due to the very large power capacity (28.2 MW) which would be required in the case of an electrically heated reactor. The scenarios, modeled and simulated in OpenModelica, are assessed on the basis of performance indicators described in Section 2.2.3.

6.1 Scenario 1 : Pure CaCl_2 intake

If the mineralization plant takes as input pure CaCl_2 , the salt production site is not required and the plant is considered on a unified site, as displayed in Figure 6.1. It is assumed that the salt is delivered either in aqueous solution or anhydrous crystal form, in which case it is dissolved with water to be fed as 42%wt. solution to the carbonation reactor. It is assumed that CaCl_2 is produced as by-product of the Solvay process (soda production) as reviewed in Section 3.4.1, and that the HCl produced can be commercialized as industrial grade product (38%wt.).

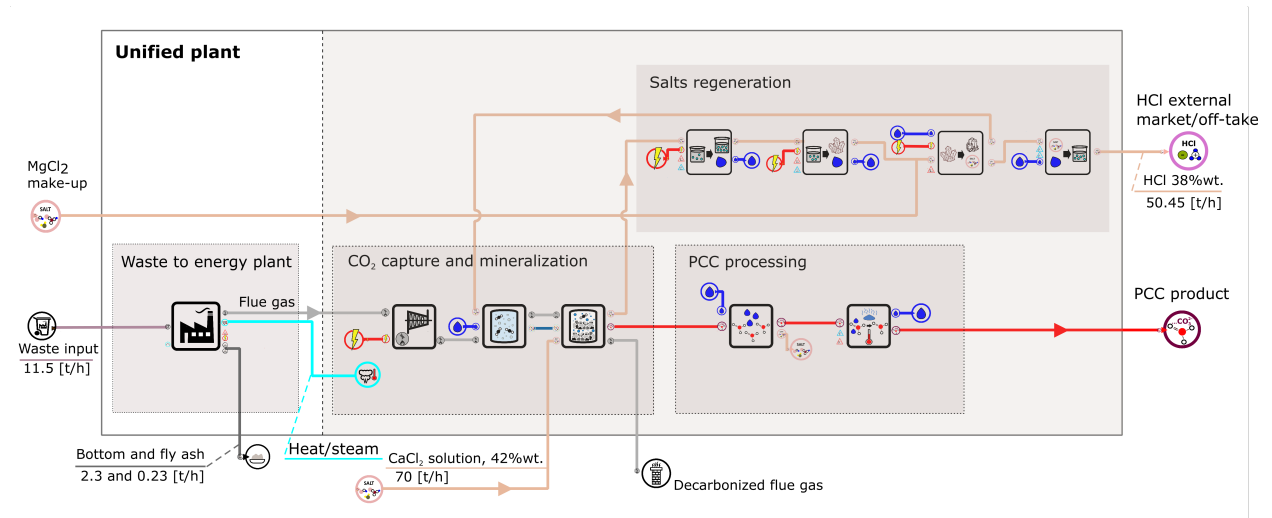


Figure 6.1: Scheme of the carbonation route using pure CaCl_2 as alkaline input.

6.2 Scenario 2 : Wollastonite-based mineralization

In the case of mineral grinding, wollastonite ore is the most appropriate naturally-occurring mineral for calcium source. This scenario is differing from the others in that it is very unlikely to be feasible in Switzerland : no exploited wollastonite mine is located at a distance lower than 400 km. In fact, even at continental scale, the potential of CO_2 mineralization with wollastonite is limited by its availability. Indeed, the wollastonite carbonation pathway requires $306.1 \text{ kton}_{\text{CaSiO}_3}/\text{y}$ for the reference plant size, whereas the current Finnish mining operations cover only 3% of that demand, and alternatively, the Kuovila and Kalkkimäki reserves would be consumed in less than 4 years (see Section 3.4). Considering the worldwide wollastonite production capacity, a scenario based on pure wollastonite for mineralization of $100 \text{ kton}_{\text{CO}_2}/\text{y}$ is also rather unlikely : the current worldwide production would supply only 4 of these plants. Nevertheless, this scenario is kept as fictive comparison basis, given that future exploitation of reserves is not excluded.

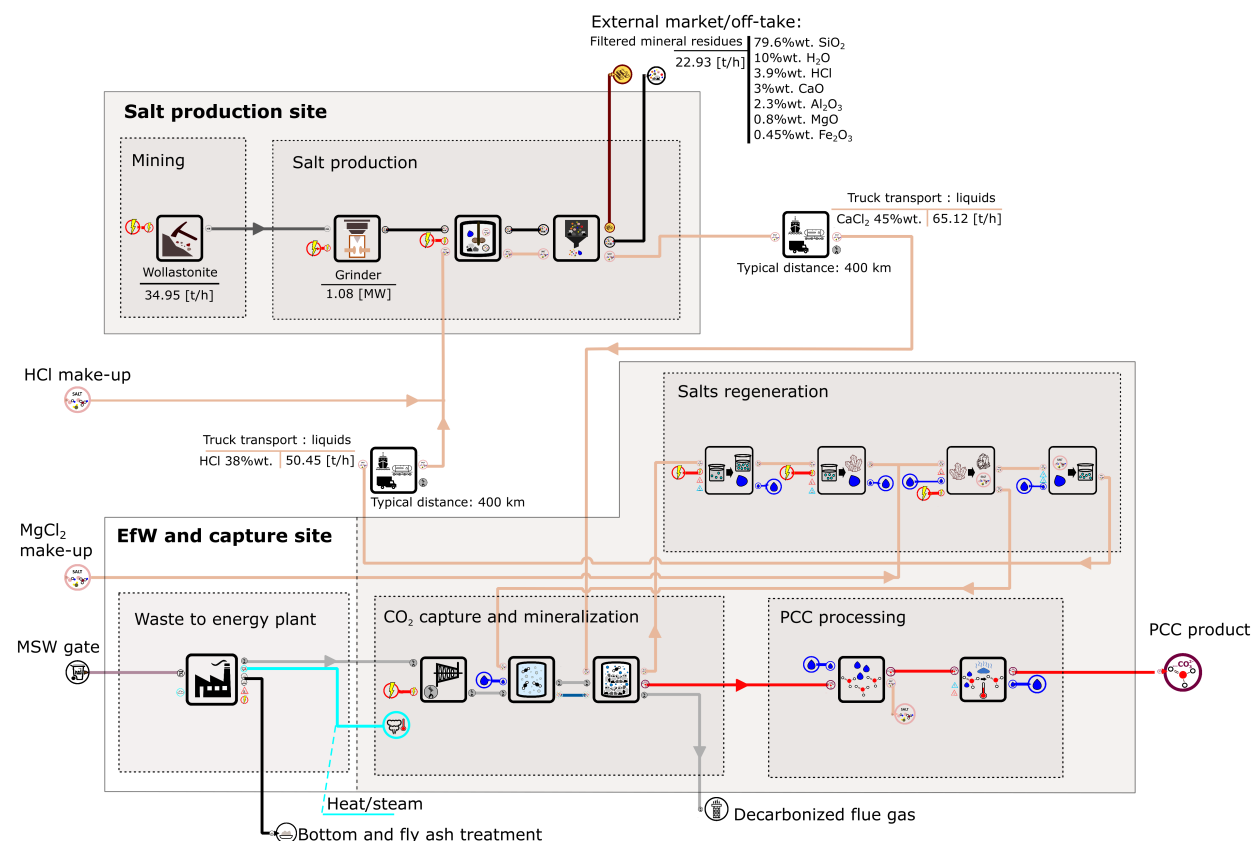


Figure 6.2: Scheme of the wollastonite carbonation route.

The salt production site is considered at the mining site for direct ore treatment (crushing, grinding, leaching and by-product reuse). The mineral residues after leaching consist majoritarily of silicon dioxide, which can be commercialized given the sufficient purity grades achieved (see Section 3.5). Hence, the displacement impact from state-of-the-art silicon dioxide is considered. The CaCl₂ produced (at 41-45%wt. solution concentration) and required HCl are transported between the EfW site and the mining site, over a hypothetical distance of 400 km.

6.3 Scenario 3 : Industrial alkaline waste utilization

If industrial wastes are to be used as alkaline input, there are no associated indirect environmental impacts as justified in 3.4.1. No displacement impact for avoided waste treatment is considered, given that it is assumed that most of these wastes are recycled in Switzerland. Due to the uncertainties around this exact recycling, the corresponding carbon offset is neither accounted for. Nevertheless, an indicative value for downstream emissions of leaching residues landfill is considered.

Using Table 3.3, the industrial waste with most potential in Switzerland are cement kiln dust, iron and steel slags, and municipal solid waste incineration ashes. None of these appear to be sufficient to supply a mineralization plant of 100 kton_{CO₂}/y capacity alone, hence a mix of these input material

must be considered. For instance, CaCl_2 effluents from the Hinwil plant might be mixed to CKD, avoiding the need for a salt production site. Alternatively, a mixture of different steel and iron slags might be fed to the fine grinder : this option is arbitrarily kept for the further analysis.

6.3.1 3a : Separated sites

If land availability restrictions (or other constraints) are assumed, the mineralization plant might be split into 2 sites : the salt production site and mineralization plant (including regeneration cycle), as depicted in Figure 6.3. The quantities of resources displaced between the 2 sites are similar to the scenario 2, but the slags transport from the steel plants to leaching process must be added, given that their transport is a direct cause of the mineralization pathway. This transport is assumed to be possible by train freight, over an average distance of 80 km, and corresponds to indirect CO_2 emissions of $551 \text{ t}_{\text{CO}_2}/\text{y}$.

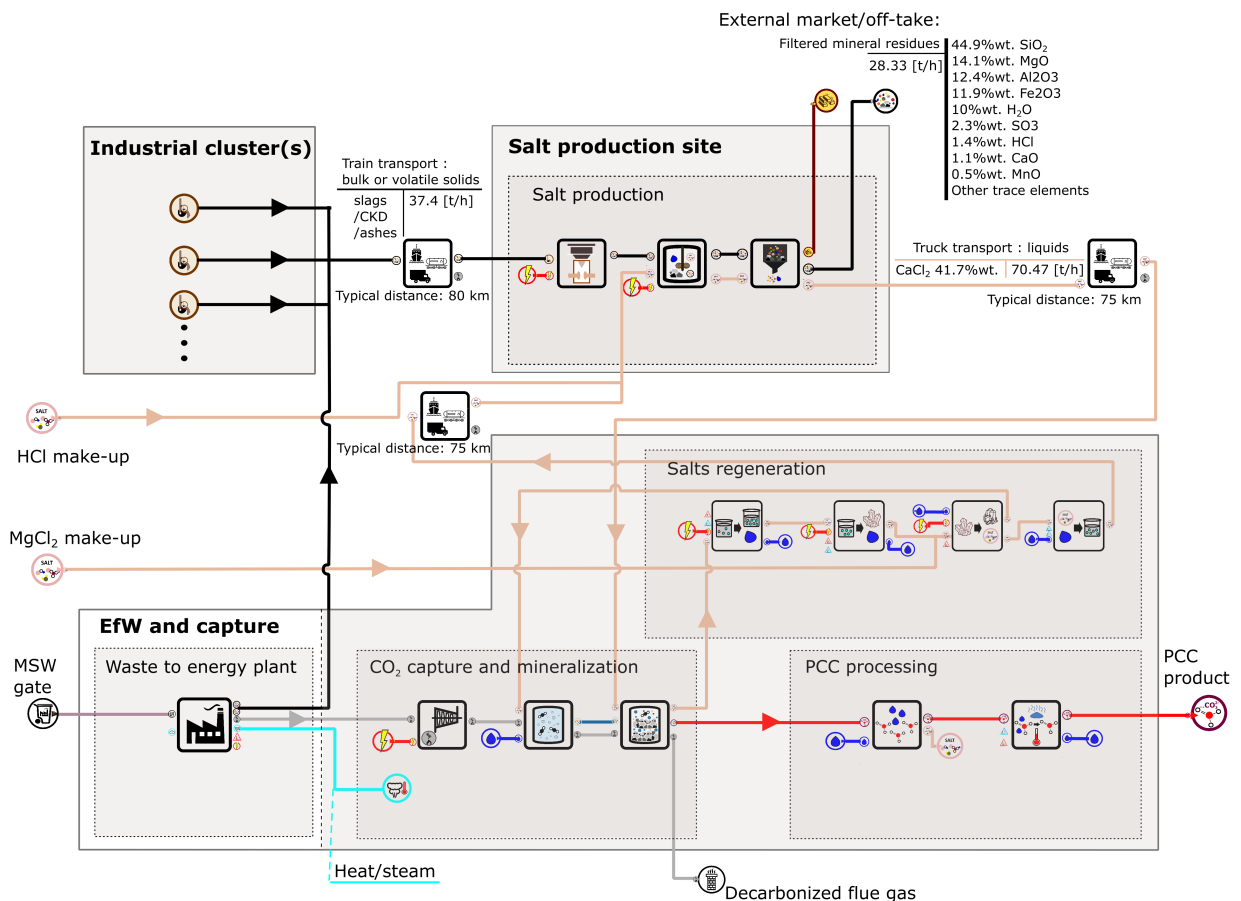


Figure 6.3: Scheme of an industrial waste carbonation route in the case of separated sites.

6.3.2 3b : Unified site

An alternative scenario is to consider the unified siting of the mineralization plant at the EfW site, in which case only the transportation of slags is required. As this scenario is very similar to scenario 3a in Figure 6.3, the scheme is not illustrated separately. Nevertheless, the process integration is modified on one aspect : the bottom ashes from the EfW boiler and the fly ashes separated from the flue gas may be directly reused on-site in the CaCl_2 production process. In this way, the slags requirement are reduced by 4.3% and the ashes downstream emissions, generated in the reference case of EfW normal operation (for which ashes are taken off to a treatment plant), are avoided. The latter implication on environmental balance and economics might be assessed using respectively the LCA results of Boesch et al., 2014 and the ash treatment cost reported by Zucha et al., 2020 (350-450 CHF/t_{FA}), but given the variability of actual reference downstream processing of the ashes, these implications are not taken into account in the following results

6.4 Scenario analysis

The results for environmental impact of mineralization routes are presented, as well as operational (OPEX) and total expenditures (TOTEX) over a year for the integrated process operation. The KPIs described in 2 are presented to set the basis for the discussion in Chapter 7.

6.4.1 Environmental performance

In a first step, the environmental impacts linked to heat and cold utilities are ignored in order to estimate the best possible decarbonization potential of each mineralization route. Figure 6.4 shows that for 101 kt_{CO₂}/y effectively mineralized, less than 44 kt_{CO₂}/y are emitted indirectly or directly for scenarios 3a and 3b. These emissions are composed predominantly by the gaseous CO₂ content still present in the decarbonized flue gas (25.4 kt_{CO₂}/y) and the indirect emissions linked to the power grid : 8.9 kt_{CO₂}/y for the mineralization site, and 1.3 or 2.7 kt_{CO₂}/y for respectively the slags grinding and the wollastonite grinding. The site separation in scenario 3a increases the transport emissions by 4.5 kt_{CO₂}/y with regards to scenario 3b. For the wollastonite-based scenario 2, the increased transport distance between EfW site and salt production site affects significantly the overall environmental impact (+20 kt_{CO₂}/y with regards to scenario 3a), indicating that mineralization pathway resources should not be transported over such distances if CO₂ emissions reduction is aimed. The displacement impact of SiO₂ by-product from the leaching process does not represent significant impact mitigation.

For scenario 1, the upstream emissions related to the production of CaCl_2 in the Solvay process make this route irrelevant for CO₂ capture purposes, even when considering the displacement emissions implied by the HCl by-product.

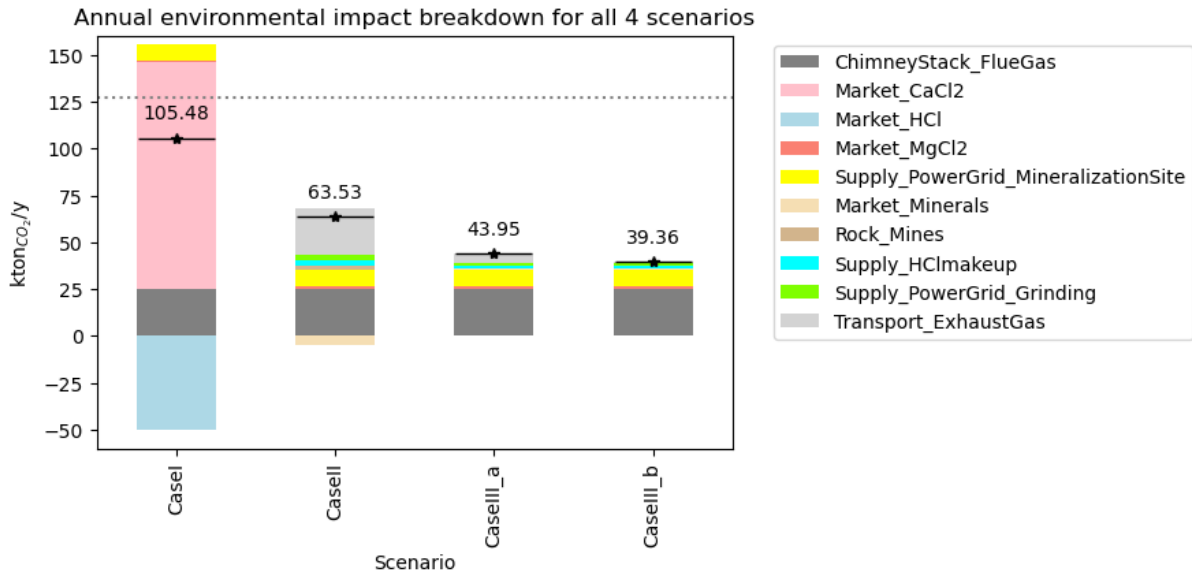


Figure 6.4: Environmental impact of the mineralization plant for each scenario, without heat and cold utilities. The dashed line indicates the total amount of CO₂ taken up by the process (hence contained in the EfW flue gas, accounting for both biogenic and non-biogenic CO₂) : 126.7 ktCO₂/y.

When considering the entire integrated system, the indirect emissions of the power requirements for the cooling tower and heat pump must be added, as well as the natural gas combustion emissions. Consequently, the environmental impact of scenario 2 approaches the quantity of CO₂ taken up through the EfW flue gas, as shown in Figure 6.5 by comparing with the dashed line. In the case of slags utilization, both scenarios 3a and 3b analyzed overall reduce the environmental burden of the EfW flue gas emissions by respectively 20.1% and 23.8%. This means that for a mineralization plant capacity of 101 ktCO₂/y, at most 26.9 ktCO₂/y may be effectively sequestered by the mineralization route studied, with the utilities implemented as considered in this work. The impact associated to natural gas combustion is largely dominant : it covers up to 53% of the overall system emissions.

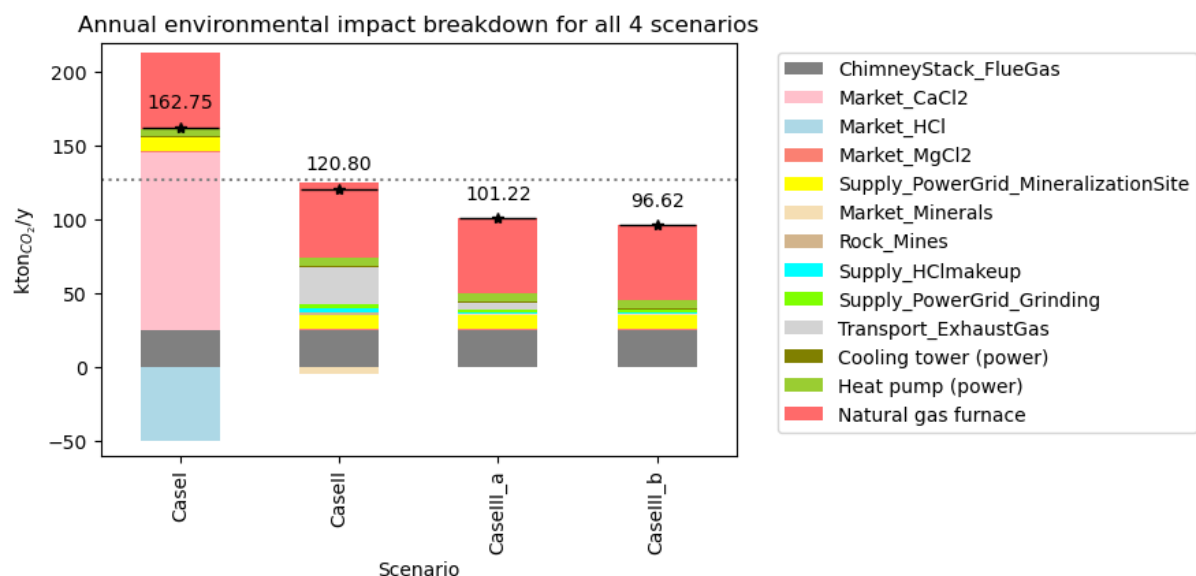


Figure 6.5: Environmental impact of the whole plant for each scenario, accounting for heat and cold utilities.

Indicatively, Figure 6.6 includes the corresponding displacement impact of PCC production. Due to the carbon intensive state-of-the-art production route of PCC, accounting for this displacement impact (330.5 ktCO₂/y generated for the same amount of PCC produced) would significantly override the emissions linked to direct and indirect emissions caused by the integrated mineralization pathway.

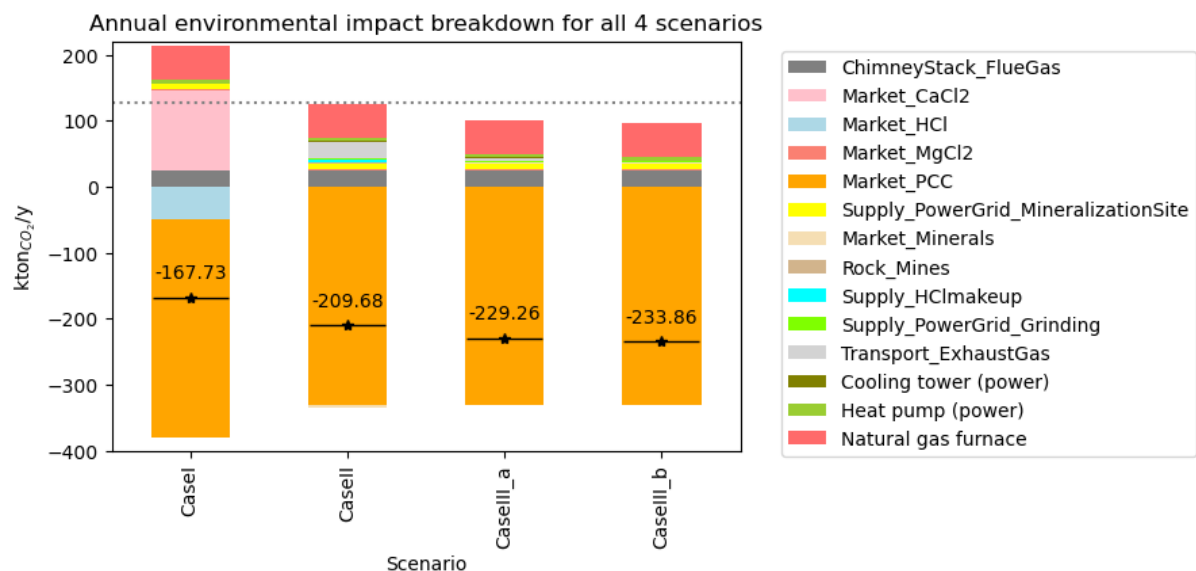


Figure 6.6: Environmental impact of the whole plant for each scenario, considering indicatively the displacement of PCC production.

6.4.2 Economic performance

The economic assessment of the mineralization routes discards the wollastonite-based scenario 2, due to the high ore price. Even if divided 3-fold to 100 CHF/t_{CaSiO₃}, the ore price per year would amount to 30 Mio. CHF/y, comparing to the entire annual operational costs for the other routes. The leaching process by-products, assumed to be sold at 20 CHF/t_{residues} in average (Wernet et al., 2016), form a revenue of only 4 Mio. CHF/y. Thus, the wollastonite-based pathway as considered in this work is economically nonviable.

The route based on pure CaCl₂ from the Solvay industry is very sensitive on commodity prices : for instance, a 1% increase in CaCl₂ crystals purchase cost induces a 0.98% increase of the total annual operational costs. The OPEX for each scenario is broken down in Figure 6.7, illustrating in particular the main operational cost components of scenarios 3a and 3b : the natural gas purchase price, and the PCC selling price. They respectively amount to +18.1 Mio. CHF/y and -23.2 Mio. CHF/y.

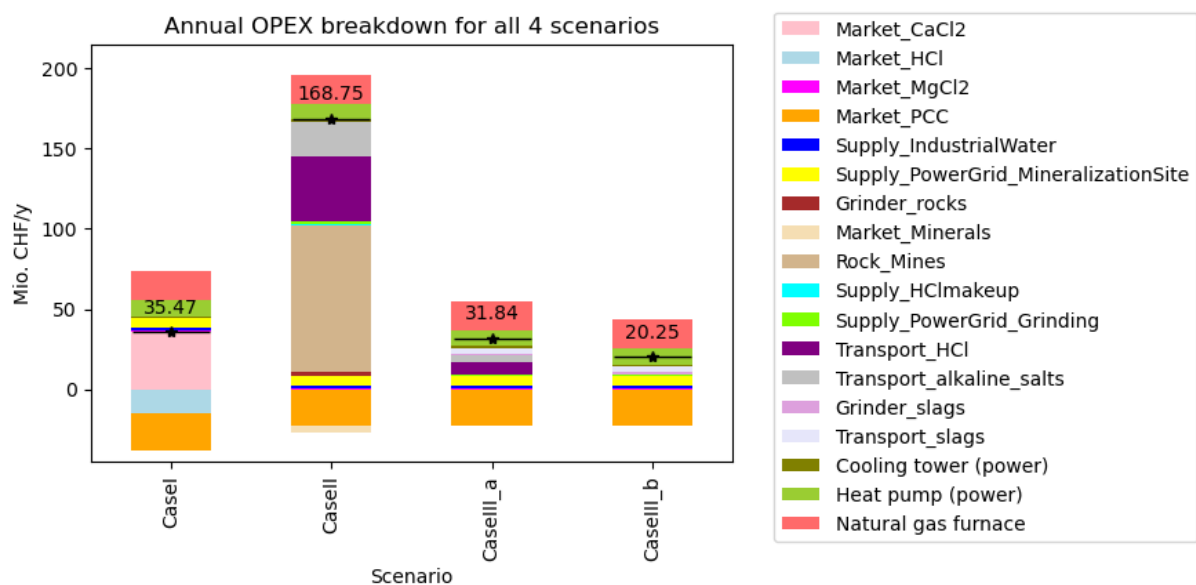


Figure 6.7: Operational expenditures of the whole plant for each scenario, accounting for heat and cold utilities.

The total mineralization plant expenditures breakdown, taking into account OPEX and annualized CAPEX for all processes and utilities, are compared in Figure 6.8. As compared to scenario 1 which has lowest purchased equipment capital cost (31.3 Mio CHF, taking into account the utilities), the addition of the salt production site represents 3-4 Mio. CHF more investment for the plant components before installation. The most economic pathway appears to be the slags utilization route, unified on one site (scenario 3b). To illustrate the sensitivity of the total annual expenditure to natural gas purchase price and PCC selling price, Table 6.1 reports the effect of a commodity price increase on the annual TOTEX of the mineralization routes for scenario 1, 3a and 3b.

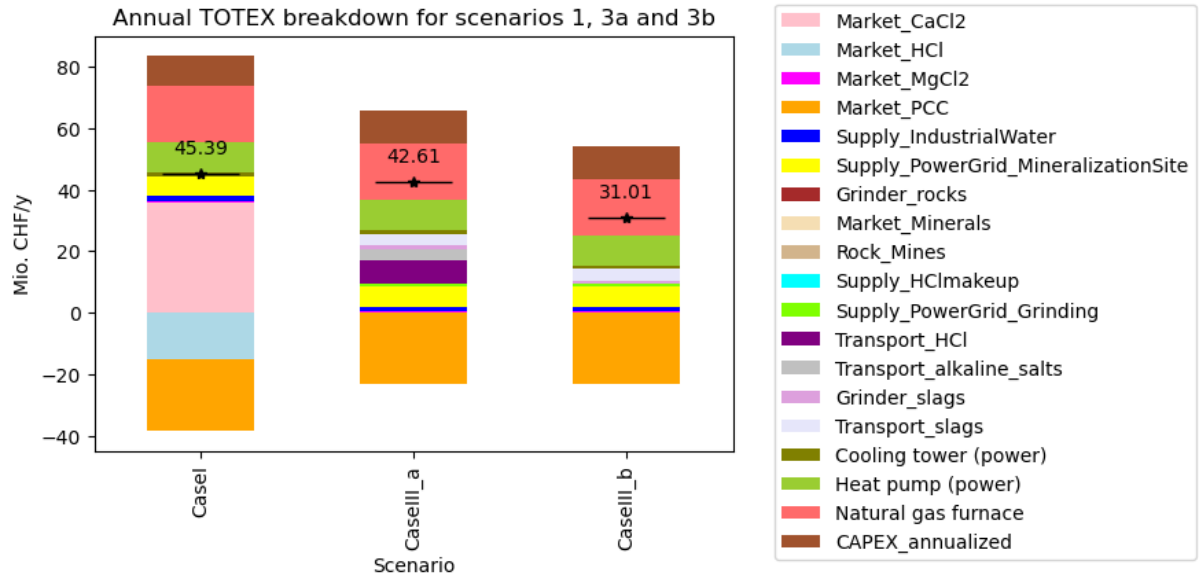


Figure 6.8: Total expenditures (OPEX and annualized CAPEX) of the whole plant for scenarios 1, 3a and 3b, accounting for heat and cold utilities. Scenario 2 is omitted given its significantly higher annual OPEX.

Commodity	1	3a	3b
NG	+0.40	+0.43	+0.58
PCC	-0.51	-0.54	-0.75

Table 6.1: Sensitivity of the plant annual TOTEX on key commodities purchase/selling price increase of 1%, in percentage.

6.4.3 Key performance indicators

KPI	1	2	3a	3b
Carbon intensity, $t_{CO_2,emitted}/t_{CO_2,FG}$	1.28	0.95	0.798	0.762
Specific cost, CHF/ $t_{CO_2,mineralized}$	447.7	1774.5	420.3	305.9
PCC break-even price, CHF/ t_{PCC}	295	876	284	234

Table 6.2: Key performance indicators for each scenario. *Note : here, the carbon intensity indicator does not take into account the displacement impact of PCC production.*

Chapter 7

Discussion

7.1 Integration in the industrial landscape

The interfaces of the magnesium cycle-based mineralization process studied are very diverse : magnesium and calcium salts, hydrochloric acid, water, minerals, heat and power are particularly represented streams. In terms of price and mass flows, the most important commodities to be exchanged with the external industries when the mineralization plant is located on a unified site are calcium containing resources (ca. 30-40 t/h for solids supply) and the calcium carbonate product (26.4 t/h). If the plant is sub-divided, the plant separation is done between the calcium salt production site and the EfW site (where CO₂ capture, mineralization and magnesium solvent regeneration take place), given the minimized transportation requirement of this configuration and heat recovery opportunities between processes. Although this splitting increases the annual emissions by only 4.6 t_{CO₂}/y, the magnesium chloride and hydrochloric acid transportation between both sites is significantly increasing the total annual expenditures of the plant (+37%). Therefore, the preferential plant arrangement for cost-effective mineralization in Switzerland is on a unified site.

Other important mass flows to be taken into account are clear water input, and waste water to be treated before discharge. These flows are present predominantly at the CO₂ absorption site and in particular for the PCC washing, given the input water quality requirement and waste water salts content. Left outside of the scope of this study, process optimization could likely lead to efficient reuse of effluent water (Yablonsky, Germain et al., 2018). For instance, condensed steam from the magnesium regeneration might be partly reused after heat recovery in the bubble column, or similarly, the chlorine content in the PCC washing waste water may be recovered for the process requirements. Regarding heat integration to the EfW plant, the steam utilization provides only ca. 45% of the entire mineralization heat demand when no recovery technology is implemented. It is however clear that the high evaporation and crystallization heat loads and waste heat represent a potential for energy recovery. The options for efficient process integration might include heat pumping and heat supply to the district heating network. For the improved system of Section 5.2, the DHN potential supply (24.7 MW_{th}) from the mineralization pathway is comparable to - or even exceeds - the indicative DHN supply from the reference EfW (14.3 MW_{th}, see Section 5.1). For this study, the remaining cold

requirement is fulfilled by cooling water, but smarter solutions might be investigated, such as Organic Rankine Cycle (ORC) for efficient reuse of waste heat at low temperature.

When implementing optimally these utilities, it is shown that the NG boiler is not required for heat supply, except for the magnesium salts decomposition FB reactor. Due to its temperature level (425°C) requirement, this process cannot be supplied only by EfW steam, which typically produces steam at <400°C due to corrosion in the boiler at higher temperatures. Solutions should be developed for providing this heat better than by natural gas combustion or electrical heating. Indeed, even with the rather low-carbon emission factor of the Swiss power grid, enabling to halve the corresponding NG emissions, the power load is significantly too big for this option to be competitive economically. Further developments could include the integration of high temperature biomass boiler (J. Li et al., 2015). Resulting challenges around biomass sources for feasibility at large scale would have to be assessed. Other process integration improvement might be achieved through better use of the EfW steam. If it is to be used only for the temperature levels of evaporation/crystallization, the steam could be used for turbine generation before, as done in most of the EfW plants equipped for power generation that also provide steam for other processes.

7.2 Process optimization

Process heat loads are shown to be very important due to the low magnesium chloride dehydrate decomposition reactor efficiency (50%). For increased decomposition temperature (up to 550-600°C), the decomposition efficiency of MgOHCl to Mg(OH)_2 over MgCl_2 is expected to increase (see Section 4.4). Evaporation and crystallization heat requirements might proportionately decrease, but higher operating temperature might in turn increase the decomposition reactor heat requirement not only due to increased sensible heat, but to endothermic side reactions such as Mg(OH)_2 dehydration to MgO , taking place at higher rates than at lower temperatures. Such process enhancement might be valuable to investigate given the potential for MER reduction, but too many unknowns remain for it to be analyzed in the present study : mainly, the temperature level, additional heat demand due to side reactions enabled by higher temperatures and the related decomposition efficiency increase.

Alternatively, in another attempt to reduce the high costs and energy requirements for the joint regeneration of the HCl and Mg(OH)_2 , the molten salt process described by Wendt et al., 1999 might be implemented. Working at lower temperatures (down to 250°C), the process would feature an even lower decomposition efficiency, resulting in a mixture of solids and melts of magnesium chlorides, hydroxychlorides and possibly, hydrates thereof, but the CO_2 dissolution in such salt brines is still not completely understood and might present advantages over the process studied in this study.

7.3 Decarbonizing the Energy-from-Waste plant

The mineralization pathway represents an effective CO_2 sequestration pathway only in some specific cases. Due to the upstream carbon intensive activities for the Solvay process, including energy-

intensive calcination of carbonates, the scenario 1 based on pure calcium chloride source is considered irrelevant for overall CO₂ capture if the process is approached in a holistic manner.

For a mineralization capacity of 101 kt_{CO₂}, the EfW emission reduction achieved at best is 30.1 kt_{CO₂}, in the case of steel industrial waste utilization (steel slags) on a unified mineralization plant arrangement (scenario 3b). The corresponding carbon intensity computed is 0.762 t_{CO₂,emitted}/t_{CO₂,FG}, which attests of the importance of energy sources of low carbon factor. The electricity mix of the Swiss grid is already relatively low, and a +1% variation of its emission factor would only induce a 0.16 kt_{CO₂}/y increase (in average, +14%) of the mineralization routes total environmental impact. In contrast, the natural gas combustion emissions might be reduced or avoided if the decomposition reactor heat is provided by a carbon-neutral source : the CO₂ mitigation could reach 81.3 kt_{CO₂}/y, closer to the actual amount of CO₂ mineralized.

Displacement of environmental impact

As shown in this work, the displacement impact of producing PCC by other means than the conventional route can in appearance dramatically shift the environmental balance of the mineralization pathway towards carbon sink. Nevertheless, these negative environmental impacts may be considered only if the carbonated product clearly replaces some part of the currently existing market. Indeed, for example in the case of much bigger mineralization plant scales, the carbonates would eventually overload the market and be landfilled. This scenario would imply that the negative environmental impact linked to PCC cannot be taken into account in the calculation of the mineralization carbon footprint. Therefore, this displacement impact cannot and should be accounted for in the CO₂ balance of the EfW flue gas decarbonization plant. Alternatively, the EfW might be considered as not decarbonized (or only partially), in which case the mineralization plant may be regarded as a carbon-neutral PCC production facility.

On a different approach, the mineralization process CO₂ emissions might be attributed to the function of PCC production, rather than the CO₂ capture function. From this point of view, the EfW could be considered fully decarbonized, including even the 20% of total CO₂ remaining in the clean flue gas CO₂. The PCC product carbon factor, calculated using the carbon intensity KPI and the PCC/CO_{2,in} mass ratio (where CO_{2,in} is the total CO₂ in the EfW flue gas), would be 0.416 kg_{CO₂}/kg_{PCC} (3-4x less than conventional PCC).

7.4 Profitability analysis

For the reference context assumed in this study, the CO₂ capture specific cost is high : it exceeds 300 CHF/t_{CO₂,mineralized} for all scenarios, high when compared to other studies but still performs better than other HCl-based routes (Sanna, Uibu et al., 2014). The specific cost for CO₂ effectively captured (taking into account the mineralization process emissions) is even higher given the high carbon intensity, indicating less economic profitability for this pathway than other mineralization processes (ranging from 25 to 258 €/t_{CO₂,avoided}, Huijgen, 2007). Nevertheless, the system's sensit-

ivity to PCC price is such that 234 CHF/t_{PCC} (+134%) is sufficient to break-even the annual TOTEX of the plant in scenario 3b. Considering the uncertainty about the carbonated product retail price, for instance if sold as "emission-free" PCC, the possibility for a profitable mineralization plant exists. This might be seen as a shift from main function of CO₂ capture to PCC production plant. It is here noteworthy to draw the attention on the similarities with the study from Teir et al., 2009, who find that the CO₂ mineralization process synthesizing pure hydromagnesite from serpentines might be suitable for valuable product manufacturing, but not for carbon sequestration purposes. As another comparison set-point, a CO₂ break-even price of around 95 CHF/t_{CO₂,captured} is reported by Zappa, 2014 for the *Slag2PCC* process using NH₄Cl.

7.5 Carbonfree Chemicals : process performance

Given the aforementioned results relaying on data available in free access, it is important to nuance the results with the performance achieved by the industrial partner Carbonfree Chemicals. If the novel developments materialize, the level of carbon intensity achieved result in a competitive carbon capture and sequestration method. While the developments cannot be fully disclosed at this stage and are therefore not part of the detailed analysis in this report, efforts are largely undertaken by the partner company to develop the design and integration of the mineralization process in the industrial landscape. Carbonfree Chemicals has allowed highlighting some of the planned improvements for the purpose of comparison with the previous analysis and information about potential improvements from the state-of-the-art.

Based on ASPEN simulations of full SkyCycle (proprietary implementation of the Mg-based mineralization process) performed by Carbonfree Chemicals and discussed in direct communication with the company, the carbon intensity of the mineralization process can be reduced under the following assumptions and process improvements:

- Low carbon intensity of electric grid (high penetration of renewables), such as in this example current carbon intensity in Switzerland of 0.108 kg_{CO₂}/kWh.
- Proprietary Carbonfree SkyCycle design of natural gas-fired decomposition reactors, allowing significant improvement of energy integration and process efficiency (Carbonfree Chemicals patent pending)
- Importantly, as also discussed extensively in this report, careful and realistic selection of feed-stock materials for mineralization is critical. In the latest developments, the process is improved by utilization of combination of two sources and processes for obtaining magnesium hydroxide and calcium chloride, requiring only 50% reliance on forced decomposition of MgCl₂, while maintaining required chloride balance. The proposed process consists of :
 - 50% passive dissolution : reacting spontaneously CaO (in ash or water) and dissolved magnesium (provided free from the process as by-product) to Mg(OH)₂(s) and CaCl₂(aq), from the own magnesium-chloride brine.

- 50% forced decomposition of MgCl_2 is processed to Mg(OH)_2 and CaCl_2 similar to the process described in this thesis.
- In this arrangement, passive dissolution allows full utilization of available low-cost ashes or other wastes, while reducing the HCl production and energy expenses related to the regeneration. Forced dissolution on the other hand allows balancing the process with addition of Mg ions. Chloride balance is maintained by conversion of acid to salts as required.
- The decarbonation operation consumes Mg(OH)_2 and CaCl_2 from stores and produces high-grade (1-10 μm) Precipitated Calcium-Carbonate product, of nearly 100% calcite quality. Purity grade achieved are typically 97-99%, and the shipped product is either dried to anhydrous form (0.1% water), or kept wet (72% by weight liquid). Optionally, edible grade product might be considered.

Based on these proprietary inputs under development, the potential for SkyCycle is to achieve carbon footprint of respectively :

- $0.75 \text{ kg}_{\text{CO}_2} / \text{kg}_{\text{CO}_2\text{-captured}}$ for dry shipped product,
- $0.62 \text{ kg}_{\text{CO}_2} / \text{kg}_{\text{CO}_2\text{-captured}}$ for wet shipped product,
- and $0.60 \text{ kg}_{\text{CO}_2} / \text{kg}_{\text{CO}_2\text{-captured}}$ for sequestered carbonates.

As comparison, the best result achieved in this thesis is a footprint of $96.62 \text{ kton}_{\text{CO}_2} / \text{y}$ (including $25.4 \text{ kton}_{\text{CO}_2} / \text{y}$ of flue gas CO_2 not absorbed), hence its carbon footprint in comparable units is $\frac{(96.62-25.4) \text{ kton}_{\text{CO}_2} / \text{y}}{101 \text{ kton}_{\text{CO}_2} / \text{y}} = 0.705 \text{ kg}_{\text{CO}_2} / \text{kg}_{\text{CO}_2\text{-captured}}$. The overall process carbon intensity reached by Carbonfree hence improves significantly the results shown in this thesis and compares favourably with alternative capture methods. In cases when carbon-intensive PCC production can be displaced, the additional carbon footprint reduction can be accounted as discussed above, resulting in up to 3.5:1 CO_2 saving ratio, with considered components of CO_2 saving per ton of CO_2 captured from flue gases:

- -1.0 tCO_2 removed from flue gas, and mineralized,
- -3.1 tCO_2 displacement of PCC production emissions
- $+0.6 \text{ tCO}_2$ expected CO_2 emissions of SkyCycle process.

Chapter 8

Conclusion

This study determined the mass and energy flows, as well as heat recovery potential and transportation logistics requirement of a magnesium salt-based mineralization plant of 101 kt_{CO₂}/y capacity integrated to the Energy-from-Waste context in Switzerland. The framework deployed enabled the analysis of different plant arrangement options and heat integration opportunities. The review of selected calcium sources and comparison through specific scenarios showed that the most cost-effective and least carbon-intensive route is the steel slags utilization. It achieves 23.8% decarbonization of the EfW plant, which might be further enhanced to >64% only by modifying the decomposition reactor heat supply to a renewable source. The wollastonite-based route is unlikely to be feasible in Switzerland, due to the distance to ore mines and the related mining price. The pathway based on pure calcium chloride supply from the Solvay process is not a sequestration pathway, due to the carbon-intensive upstream activities linked to its production. Both high specific cost and carbon intensity of all scenarios were shown to be strongly linked to natural gas combustion for the process, and PCC retail price of 234 CHF/t_{PCC} was found to be sufficient to offset the total plant expenditures considered. Overall, even if some profit from economies of scale might exist, the extension of this mineralization pathway to large scale application might be restrained by the alkaline sources available, as only 2-3 plants of the studied size might be based on industrial alkaline waste in Switzerland.

Further work on the magnesium salts-based mineralization process might focus on more detailed assessment of process heat integration, targeting minimal environmental impacts linked to hot and cold utilities and optimal energy efficiency. For more detailed scenario definitions, the assessment of transportation logistics could be improved by taking into account all fix and variable cost components. The equipment cost estimation may be refined by determining the exact type of reactors involved (material, pressure level, etc.). Synergies with other novel technologies may be investigated, such as thermochemical seasonal solar heat storage with MgCl₂·6H₂O (Zondag et al., 2010) or hot potassium carbon capture (L. Li et al., 2021). Daily, or even seasonal energy storage opportunities may be studied, given the relative simplicity of mineralization materials storage (chemicals and minerals). The mineralization pathway may also be considered as part of the EfW flue gas treatment (for instance as described in Carbonfree's patent Yablonsky, Stola et al., 2018), which feasibility and performance would have to be evaluated by process engineering.

Future improvements on the OpenModelica library and its framework will involve better interfacing and post-processing of the simulation, creation of new models for energy technologies as well as improvement of existing ones (e.g. refinement of thermal integration elements).

Bibliography

- AACE. (2005). Cost estimate classification system - as applied in engineering, procurement, and construction for the process industries, 10.
- Adham, K., Lee, C. & O'Keefe, K. (2012). Fluid bed dehydration of magnesium chloride, 49–53. <https://doi.org/10.1002/9781118359228.ch9>
- AluSuisse. (2015). *Alu zahlenspiegel* [Daten und Fakten 2014]. Retrieved June 17, 2022, from <https://alu.ch/download/diverses/Zahlen2015.pdf>
- Arce, G. L. A. F., Soares Neto, T. G., Ávila, I., Luna, C. M. R. & Carvalho, J. A. (2017). Leaching optimization of mining wastes with lizardite and brucite contents for use in indirect mineral carbonation through the pH swing method. *Journal of Cleaner Production*, 141, 1324–1336. <https://doi.org/10.1016/j.jclepro.2016.09.204>
- Assima, G. P., Larachi, F., Molson, J. & Beaudoin, G. (2013). Accurate and direct quantification of native brucite in serpentine ores—new methodology and implications for CO₂ sequestration by mining residues. *Thermochimica Acta*, 566, 281–291. <https://doi.org/10.1016/j.tca.2013.06.006>
- Assima, G. P., Larachi, F., Molson, J. & Beaudoin, G. (2014). Comparative study of five québec ultramafic mining residues for use in direct ambient carbon dioxide mineral sequestration. *Chemical Engineering Journal*, 245, 56–64. <https://doi.org/10.1016/j.cej.2014.02.010>
- Azdarpour, A., Asadullah, M., Mohammadian, E., Hamidi, H., Junin, R. & Karaei, M. A. (2015). A review on carbon dioxide mineral carbonation through pH-swing process. *Chemical Engineering Journal*, 279, 615–630. <https://doi.org/10.1016/j.cej.2015.05.064>
- Bains, P., Psarras, P. & Wilcox, J. (2017). CO₂ capture from the industry sector. *Progress in Energy and Combustion Science*, 63, 146–172. <https://doi.org/10.1016/j.pecs.2017.07.001>
- Bajpai, P. (2015). Generation of waste in pulp and paper mills. In P. Bajpai (Ed.), *Management of pulp and paper mill waste* (pp. 9–17). Springer International Publishing. https://doi.org/10.1007/978-3-319-11788-1_2
- Bakker, J. d., Peacey, J. & Davis, B. (2013). Thermal decomposition studies on magnesium hydroxy-chlorides [Publisher: Taylor & Francis]. *Canadian Metallurgical Quarterly*. <https://doi.org/10.1179/1879139512Y.0000000007>
- Ballirano, P., De Vito, C., Ferrini, V. & Mignardi, S. (2010). The thermal behaviour and structural stability of nesquehonite, MgCO₃·3H₂O, evaluated by in situ laboratory parallel-beam x-ray powder

- diffraction: New constraints on CO₂ sequestration within minerals. *Journal of Hazardous Materials*, 178(1), 522–528. <https://doi.org/10.1016/j.jhazmat.2010.01.113>
- Bang, J.-H., Lee, S.-W., Jeon, C., Park, S., Song, K., Jo, W. J. & Chae, S. (2016). Leaching of metal ions from blast furnace slag by using aqua regia for CO₂ mineralization [Number: 12 Publisher: Multidisciplinary Digital Publishing Institute]. *Energies*, 9(12), 996. <https://doi.org/10.3390/en9120996>
- Becker, H., Girardin, L. & Maréchal, F. (2010, January 1). Energy integration of industrial sites with heat exchange restrictions. In S. Pierucci & G. B. Ferraris (Eds.), *Computer aided chemical engineering* (pp. 1141–1146). Elsevier. [https://doi.org/10.1016/S1570-7946\(10\)28191-9](https://doi.org/10.1016/S1570-7946(10)28191-9)
- Becker, H. C. (Ed.). (2012). *Methodology and thermo-economic optimization for integration of industrial heat pumps*. EPFL. <https://doi.org/10.5075/epfl-thesis-5341>
- Beigi, S., Sobati, M. A. & Charkhi, A. (2015). An experimental investigation on drying kinetics of calcium carbonate. *Journal of Particle Science & Technology*, 1(3). <https://doi.org/10.22104/jpst.2015.219>
- Bertos, M. F., Li, X., R. Simons, S. J., D. Hills, C. & J. Carey, P. (2004). Investigation of accelerated carbonation for the stabilisation of MSW incinerator ashes and the sequestration of CO₂ [Publisher: Royal Society of Chemistry]. *Green Chemistry*, 6(8), 428–436. <https://doi.org/10.1039/B401872A>
- Bina, L., Binova, H., Brezina, E., Kumpost, P. & Padelek, T. (2014). Comparative model of unit costs of road and rail freight transport for selected european countries. *The Journal of business and social studies*, 3, 127–136.
- Boesch, M. E., Vadenbo, C., Saner, D., Huter, C. & Hellweg, S. (2014). An LCA model for waste incineration enhanced with new technologies for metal recovery and application to the case of switzerland. *Waste Management*, 34(2), 378–389. <https://doi.org/10.1016/j.wasman.2013.10.019>
- Boni, D. (2020). *Industrielle Schlackenaufbereitung – Status und Ziele* (No. 001). Stiftung Zentrum für nachhaltige Abfall- und Ressourcennutzung (ZAR). Hinwil. https://zar-ch.ch/fileadmin/user_upload/Contentdokumente/Oeffentliche_Dokumente/200102_ZAR_Schriftenreihe_001_Schlackenaufbereitung_Erkenntnisse_2019.pdf
- Bretscher, D., Heldstab, J., Rihm, B., Rogiers, N., Schappi, B., Sommerhalder, M., Stettler, C. & Weber, F. (2018). *Switzerland's greenhouse gas inventory* (National Inventory Report). Federal Office for the Environment FOEN, Climate Division.
- Bungener, L. G. S. (2016). *Energy efficiency and integration in the refining and petrochemical industries* (Doctoral dissertation). EPFL. <https://doi.org/10.5075/epfl-thesis-7038>
- Butun, H., Kantor, I. & Marechal, F. (2018). A heat integration method with multiple heat exchange interfaces. *Energy*, 152, 476–488. <https://doi.org/10.1016/j.energy.2018.03.114>
- Camison-Haba, S. & Clemente-Almendros, J. A. (2020). A global model for the estimation of transport costs. *Economic Research-Ekonomska Istraživanja*, 33(1), 2075–2100. <https://doi.org/10.1080/1331677X.2019.1584044>

- CemSuisse. (2022, June 16). *Portrait de l'industrie du ciment* [cemsuisse]. Retrieved June 16, 2022, from <https://www.cemsuisse.ch/fr/industrie-portraet/>
- Chang, R., Kim, S., Lee, S., Choi, S., Kim, M. & Park, Y. (2017). Calcium carbonate precipitation for CO₂ storage and utilization: A review of the carbonate crystallization and polymorphism. *Frontiers in Energy Research*, 5. Retrieved June 22, 2022, from <https://www.frontiersin.org/article/10.3389/fenrg.2017.00017>
- Chen, W., Li, W. & Zhang, Y. (2018). Analysis of thermal deposition of MgCl₂·6H₂O hydrated salt in the sieve-plate reactor for heat storage. *Applied Thermal Engineering*, 135, 95–108. <https://doi.org/10.1016/j.applthermaleng.2018.02.043>
- Chen, Z., Cang, Z., Yang, F., Zhang, J. & Zhang, L. (2021). Carbonation of steelmaking slag presents an opportunity for carbon neutral: A review. *Journal of CO₂ Utilization*, 54, 101738. <https://doi.org/10.1016/j.jcou.2021.101738>
- Chu, G., Li, C., Liu, W., Zhang, G., Yue, H., Liang, B., Wang, Y. & Luo, D. (2019). Facile and cost-efficient indirect carbonation of blast furnace slag with multiple high value-added products through a completely wet process. *Energy*, 166, 1314–1322. <https://doi.org/10.1016/j.energy.2018.10.128>
- Consortium, P. (2013). *ProMine data products* [European geological data infrastructure]. Retrieved June 11, 2022, from <https://www.europe-geology.eu/promine/>
- Constantz, B. R. & Bewernitz, M. A. (2019, February 5). *Carbon sequestration methods and systems* (U.S. pat. 10197747B2).
- Ordinance on the Avoidance and the Disposal of Waste (2015, December 4). Retrieved June 21, 2022, from <https://www.fedlex.admin.ch/destore/fedlex.data.admin.ch/eli/cc/2015/891/20220401/en/pdf-a/fedlex-data-admin-ch-eli-cc-2015-891-20220401-en-pdf-a.pdf>
- Couper, J. R. (2003). *Process engineering economics* [Google-Books-ID: qE6IZQnIjDUC]. CRC Press.
- d'Amore, F. & Bezzo, F. (2017). Economic optimisation of european supply chains for CO₂ capture, transport and sequestration. *International Journal of Greenhouse Gas Control*, 65, 99–116. <https://doi.org/10.1016/j.ijggc.2017.08.015>
- d'Amore, F. & Bezzo, F. (2020). Optimizing the design of supply chains for carbon capture, utilization, and sequestration in europe: A preliminary assessment. *Frontiers in Energy Research*, 8. Retrieved June 12, 2022, from <https://www.frontiersin.org/article/10.3389/fenrg.2020.00190>
- d'Amore, F., Romano, M. C. & Bezzo, F. (2021). Carbon capture and storage from energy and industrial emission sources: A europe-wide supply chain optimisation. *Journal of Cleaner Production*, 290, 125202. <https://doi.org/10.1016/j.jclepro.2020.125202>
- D'Antoni, M., Romeli, D. & Fedrizzi, R. (2014, September 16). *Techno-economic analysis of air-to-water heat rejection systems*. <https://doi.org/10.18086/eurosun.2014.07.06>
- Daval, D., Hellmann, R., Martinez, I., Gangloff, S. & Guyot, F. (2013). Lizardite serpentine dissolution kinetics as a function of pH and temperature, including effects of elevated pCO₂. *Chemical Geology*, 351, 245–256. <https://doi.org/10.1016/j.chemgeo.2013.05.020>

- Dickinson, S. R., Henderson, G. E. & McGrath, K. M. (2002). Controlling the kinetic versus thermodynamic crystallisation of calcium carbonate. *Journal of Crystal Growth*, 244(3), 369–378. [https://doi.org/10.1016/S0022-0248\(02\)01700-1](https://doi.org/10.1016/S0022-0248(02)01700-1)
- Dong, C., Song, X., Li, Y., Liu, C., Chen, H. & Yu, J. (2018). Impurity ions effect on CO₂ mineralization via coupled reaction-extraction-crystallization process of CaCl₂ waste liquids. *Journal of CO₂ Utilization*, 27, 115–128. <https://doi.org/10.1016/j.jcou.2018.05.023>
- Doucet, F. J. (2010). Effective CO₂-specific sequestration capacity of steel slags and variability in their leaching behaviour in view of industrial mineral carbonation. *Minerals Engineering*, 23(3), 262–269. <https://doi.org/10.1016/j.mineng.2009.09.006>
- Dri, M., Sanna, A. & Maroto-Valer, M. M. (2013). Dissolution of steel slag and recycled concrete aggregate in ammonium bisulphate for CO₂ mineral carbonation. *Fuel Processing Technology*, 113, 114–122. <https://doi.org/10.1016/j.fuproc.2013.03.034>
- Dwortzan, M. (2021). *Reducing industrial carbon emissions* [MIT news | massachusetts institute of technology]. Retrieved June 29, 2022, from <https://news.mit.edu/2021/reducing-emissions-decarbonizing-industry-0721>
- Ecke, H. (2003). Sequestration of metals in carbonated municipal solid waste incineration (MSWI) fly ash. *Waste Management*, 23(7), 631–640. [https://doi.org/10.1016/S0956-053X\(03\)00095-3](https://doi.org/10.1016/S0956-053X(03)00095-3)
- ECTA & CEFIC. (2011). GUIDELINE FOR MEASURING AND MANAGING CO₂ - ISSUE 1. Retrieved May 26, 2022, from <https://www.ecta.com/wp-content/uploads/2021/03/ECTA-CEFIC-GUIDELINE-FOR-MEASURING-AND-MANAGING-CO2-ISSUE-1.pdf>
- Eikeland, E., Blichfeld, A. B., Tyrsted, C., Jensen, A. & Iversen, B. B. (2015). Optimized carbonation of magnesium silicate mineral for CO₂ storage [Publisher: American Chemical Society]. *ACS Applied Materials & Interfaces*, 7(9), 5258–5264. <https://doi.org/10.1021/am508432w>
- Elbaz, A. A., Aboulfotoh, A. M., Dohdoh, A. M. & Wahba, A. M. (2019). Review of beneficial uses of cement kiln dust (CKD), fly ash (FA) and their mixture, 12.
- El-Hassan, H. (2020, October 1). *Accelerated carbonation curing as a means of reducing carbon dioxide emissions* [Publication Title: Cement Industry - Optimization, Characterization and Sustainable Application]. IntechOpen. <https://doi.org/10.5772/intechopen.93929>
- Eloneva, S. (2010). *Reduction of CO₂ emissions by mineral carbonation : Steelmaking slags as raw material with a pure calcium carbonate end product* [Accepted: 2012-08-28T11:53:42Z ISSN: 1795-4584]. Aalto-yliopiston teknillinen korkeakoulu. Retrieved June 6, 2022, from <https://aaltodoc.aalto.fi:443/handle/123456789/4876>
- Fagerlund, J. (2012). Carbonation of mg(OH)₂ in a pressurised fluidised bed for CO₂ sequestration [Accepted: 2012-02-16T11:40:44Z Publisher: Åbo Akademi - Åbo Akademi University]. Retrieved January 22, 2022, from <https://www.doria.fi/handle/10024/74477>
- Fagerlund, J. & Zevenhoven, R. (2011). An experimental study of mg(OH)₂ carbonation. *International Journal of Greenhouse Gas Control*, 5(6), 1406–1412. <https://doi.org/10.1016/j.ijggc.2011.05.039>

- Feng, B., Yong, A. K. & An, H. (2007). Effect of various factors on the particle size of calcium carbonate formed in a precipitation process. *Materials Science and Engineering: A*, 445-446, 170–179. <https://doi.org/10.1016/j.msea.2006.09.010>
- Feng, X. & Zhu, X. X. (1997). Combining pinch and exergy analysis for process modifications. *Applied Thermal Engineering*, 17(3), 249–261. [https://doi.org/10.1016/S1359-4311\(96\)00035-X](https://doi.org/10.1016/S1359-4311(96)00035-X)
- FOEN, F. O. f. t. E. (2021). *CO2 levy*. Retrieved June 19, 2022, from <https://www.bafu.admin.ch/bafu/en/home/themen/thema-klima/klimawandel-stoppen-und-folgen-meistern/schweizer-klimapolitik/co2-abgabe.html>
- FOEN, F. O. f. t. E. (2022a). *Agreement with managers of waste treatment installations*. Retrieved June 19, 2022, from <https://www.bafu.admin.ch/bafu/en/home/themen/thema-klima/klimawandel-stoppen-und-folgen-meistern/schweizer-klimapolitik/branchenvereinbarungen/zielvereinbarung-uvek-abfallverwertungsanlagen-ch.html>
- FOEN, F. O. f. t. E. (2022b). *Switzerland's greenhouse gas inventory*. Retrieved June 19, 2022, from <http://www.bafu.admin.ch/bafu/en/home/themen/thema-klima/klima--daten--indikatoren-und-karten/daten--treibhausgasemissionen-der-schweiz/treibhausgasinventar.html>
- François, M. & Irsia, B. (1989). Synep1 : A methodology for energy integration and optimal heat exchanger network synthesis. *Computers & Chemical Engineering*, 13(4), 603–610. [https://doi.org/10.1016/0098-1354\(89\)85044-6](https://doi.org/10.1016/0098-1354(89)85044-6)
- Fricker, K. J. & Park, A.-H. A. (2013). Effect of h₂o on mg(OH)₂ carbonation pathways for combined CO₂ capture and storage. *Chemical Engineering Science*, 100, 332–341. <https://doi.org/10.1016/j.ces.2012.12.027>
- Fritzson, P., Pop, A., Abdelhak, K., Ashgar, A., Bachmann, B., Braun, W., Bouskela, D., Braun, R., Buffoni, L., Casella, F., Castro, R., Franke, R., Fritzson, D., Gebremedhin, M., Heuermann, A., Lie, B., Mengist, A., Mikelsons, L., Moudgalya, K., ... Östlund, P. (2020). The OpenModelica integrated environment for modeling, simulation, and model-based development. *Modeling, Identification and Control: A Norwegian Research Bulletin*, 41(4), 241–295. <https://doi.org/10.4173/mic.2020.4.1>
- Gerdemann, S. J., O'Connor, W. K., Dahlin, D. C., Penner, L. R. & Rush, H. (2007). Ex situ aqueous mineral carbonation [Publisher: American Chemical Society]. *Environmental Science & Technology*, 41(7), 2587–2593. <https://doi.org/10.1021/es0619253>
- Giannoulakis, S., Volkart, K. & Bauer, C. (2014). Life cycle and cost assessment of mineral carbonation for carbon capture and storage in european power generation. *International Journal of Greenhouse Gas Control*, 21, 140–157. <https://doi.org/10.1016/j.ijggc.2013.12.002>
- Gislason, S. R. & Oelkers, E. H. (2014). Carbon storage in basalt. *Science*, 344(6182), 373–374. <https://doi.org/10.1126/science.1250828>
- GlobalCement. (2011). *Steel-slag: A supplementary cementitious material and basis for energy-saving cement*. Retrieved June 29, 2022, from <https://www.globalcement.com/magazine/articles/419-steel-slag-a-supplementary-cementitious-material-and-basis-for-energy-saving-cement#:~:text=Steel%2Dslag%20can%20be%20used,is%20around%2040%2D50%25.>

- Han, Y.-S., Ji, S., Lee, P.-K. & Oh, C. (2017). Bauxite residue neutralization with simultaneous mineral carbonation using atmospheric CO₂. *Journal of Hazardous Materials*, 326, 87–93. <https://doi.org/10.1016/j.jhazmat.2016.12.020>
- Hemmati, A., Shayegan, J., Bu, J., Yeo, T. Y. & Sharratt, P. (2014). Process optimization for mineral carbonation in aqueous phase. *International Journal of Mineral Processing*, 130, 20–27. <https://doi.org/10.1016/j.minpro.2014.05.007>
- Herzberg, C., Vidito, C. & Starkey, N. A. (2016). Nickel–cobalt contents of olivine record origins of mantle peridotite and related rocks [Publisher: De Gruyter]. *American Mineralogist*, 101(9), 1952–1966. <https://doi.org/10.2138/am-2016-5538>
- Highfield, J., Lim, H., Fagerlund, J. & Zevenhoven, R. (2012). Activation of serpentine for CO₂ mineralization by flux extraction of soluble magnesium salts using ammonium sulfate [Publisher: The Royal Society of Chemistry]. *RSC Advances*, 2(16), 6535–6541. <https://doi.org/10.1039/C2RA01347A>
- Hills, C. D., Tripathi, N. & Carey, P. J. (2020). Mineralization technology for carbon capture, utilization, and storage. *Frontiers in Energy Research*, 8. Retrieved June 16, 2022, from <https://www.frontiersin.org/article/10.3389/fenrg.2020.00142>
- Hu, C. W. & Ahmad, S. (1994). Total site heat integration using the utility system. *Computers & Chemical Engineering*, 18(8), 729–742. [https://doi.org/10.1016/0098-1354\(93\)E0019-6](https://doi.org/10.1016/0098-1354(93)E0019-6)
- Huang, Q., Lu, G., Wang, J. & Yu, J. (2011). Thermal decomposition mechanisms of MgCl₂·6H₂O and MgCl₂·H₂O. *Journal of Analytical and Applied Pyrolysis*, 91(1), 159–164. <https://doi.org/10.1016/j.jaap.2011.02.005>
- Huijgen, W. J. J., Ruijg, G. J., Comans, R. N. J. & Witkamp, G.-J. (2006). Energy consumption and net CO₂ sequestration of aqueous mineral carbonation [Publisher: American Chemical Society]. *Industrial & Engineering Chemistry Research*, 45(26), 9184–9194. <https://doi.org/10.1021/ie060636k>
- Huijgen, W. J. J. (2007). *Carbon dioxide sequestration by mineral carbonation: Feasibility of enhanced natural weathering as a CO₂ emission reduction technology*.
- Huntzinger, D. N., Gierke, J. S., Kawatra, S. K., Eisele, T. C. & Sutter, L. L. (2009). Carbon dioxide sequestration in cement kiln dust through mineral carbonation [Publisher: American Chemical Society]. *Environmental Science & Technology*, 43(6), 1986–1992. <https://doi.org/10.1021/es802910z>
- HZI. (2021, November 30). *Using separated CO₂ instead of sequestering it* [Hitachi zosen inova AG]. Retrieved June 25, 2022, from <https://www.hz-inova.com/using-separated-co2-instead-of-sequestering-it/>
- IPCC. (2005). *Carbon dioxide capture and storage*. Intergovernmental Panel on Climate Change (IPCC). Retrieved April 30, 2022, from https://www.ipcc.ch/site/assets/uploads/2018/03/srccs_who_lereport-1.pdf

- Jarvis, K., Carpenter, R. W., Windman, T., Kim, Y., Nunez, R. & Alawneh, F. (2009). Reaction mechanisms for enhancing mineral sequestration of CO₂. *Environmental Science & Technology*, 43(16), 6314–6319. <https://doi.org/10.1021/es8033507>
- Ji, L., Yu, H., Wang, X., Grigore, M., French, D., Gözükar, Y. M., Yu, J. & Zeng, M. (2017). CO₂ sequestration by direct mineralisation using fly ash from chinese shenfu coal. *Fuel Processing Technology*, 156, 429–437. <https://doi.org/10.1016/j.fuproc.2016.10.004>
- Jo, H., Lee, M.-G., Park, J. & Jung, K.-D. (2017). Preparation of high-purity nano-CaCO₃ from steel slag. *Energy*, 120, 884–894. <https://doi.org/10.1016/j.energy.2016.11.140>
- Jo, H., Park, S. H., Jang, Y. N., Chae, S. C., Lee, P. K. & Jo, H. Y. (2014). Metal extraction and indirect mineral carbonation of waste cement material using ammonium salt solutions. *Chemical Engineering Journal*, 254, 313–323. <https://doi.org/10.1016/j.cej.2014.05.129>
- Jones, J. & Yablonsky, A. (2020, March 10). *Carbon dioxide sequestration with magnesium hydroxide and regeneration of magnesium hydroxide* (U.S. pat. 10583394B2).
- Jones, J. D. (2014, June 3). *Removing carbon dioxide from waste streams through co-generation of carbonate and/or bicarbonate minerals* (U.S. pat. 8741244B2).
- Jones, J. D. & St, A. D. (2012, February 1). *Elimination du dioxyde de carbone de courants de déchets par cogénération de carbonates et/ou bicarbonates* (European pat. 2205341B1).
- Jones, J. D. & Yablonsky, A. (2016, June 7). *Carbon dioxide sequestration involving two-salt-based thermolytic processes* (U.S. pat. 9359221B2).
- Jones, J. D. & Yablonsky, A. (2021, January 27). *Séquestrations de dioxyde de carbone entraînant des procédés thermolytiques à base de deux sels* (European pat. 2590729B1).
- Kang, C.-U., Ji, S.-W. & Jo, H. (2022). Recycling of industrial waste gypsum using mineral carbonation [Number: 8 Publisher: Multidisciplinary Digital Publishing Institute]. *Sustainability*, 14(8), 4436. <https://doi.org/10.3390/su14084436>
- Kantor, I., Robineau, J.-L., Bütün, H. & Maréchal, F. (2020). A mixed-integer linear programming formulation for optimizing multi-scale material and energy integration. *Frontiers in Energy Research*, 8, 49. <https://doi.org/10.3389/fenrg.2020.00049>
- Kashani-Nejad, S., Ng, K. -W. & Harris, R. (2005). MgOHCl thermal decomposition kinetics. *Metalurgical and Materials Transactions B*, 36(1), 153–157. <https://doi.org/10.1007/s11663-005-0015-2>
- Kelemen, P., Aines, R., Bennett, E., Benson, S., Carter, E., Coggon, J., de Obeso, J., Evans, O., Gadikota, G., Dipple, G., Godard, M., Harris, M., Higgins, J., Johnson, K., Kourim, F., Lafay, R., Lambart, S., Manning, C., Matter, J., ... Wilcox, J. (2018). In situ carbon mineralization in ultramafic rocks: Natural processes and possible engineered methods. *Energy Procedia*, 146, 92–102. <https://doi.org/10.1016/j.egypro.2018.07.013>
- Kelemen, P., Benson, S. M., Pilorgé, H., Psarras, P. & Wilcox, J. (2019). An overview of the status and challenges of CO₂ storage in minerals and geological formations. *Frontiers in Climate*, 1. Retrieved May 27, 2022, from <https://www.frontiersin.org/article/10.3389/fclim.2019.00009>

- Kelley, K. K. (1945). *Energy requirements and equilibria in the dehydration, hydrolysis, and decomposition of magnesium chloride* [OCLC: 16934475]. U.S. G.P.O.
- Kemp, I. C. (2011, April 1). *Pinch analysis and process integration: A user guide on process integration for the efficient use of energy* [Google-Books-ID: gQMxilJQmV4C]. Elsevier.
- Kermani, M., Kantor, I. D. & Maréchal, F. (2019). Optimal design of heat-integrated water allocation networks [Number: 11 Publisher: Multidisciplinary Digital Publishing Institute]. *Energies*, 12(11), 2174. <https://doi.org/10.3390/en12112174>
- Kermani, M., Wallerand, A. S., Kantor, I. D. & Maréchal, F. (2018). Generic superstructure synthesis of organic rankine cycles for waste heat recovery in industrial processes. *Applied Energy*, 212, 1203–1225. <https://doi.org/10.1016/j.apenergy.2017.12.094>
- Kim, D. & Kim, M.-J. (2018). Calcium extraction from paper sludge ash using various solvents to store carbon dioxide. *KSCE Journal of Civil Engineering*, 22(12), 4799–4805. <https://doi.org/10.1007/s12205-017-0819-z>
- Kirsh, Y., Yariv, S. & Shoval, S. (1987). KINETIC ANALYSIS OF THERMAL DEHYDRATION AND HYDROLYSIS OF $\text{MgCl}_2 \cdot 6\text{H}_2\text{O}$ BY DTA AND TG, 16.
- Klammer, N., Engtrakul, C., Zhao, Y., Wu, Y. & Vidal, J. (2020). Method to determine MgO and MgOHCl in chloride molten salts [Publisher: American Chemical Society]. *Analytical Chemistry*, 92(5), 3598–3604. <https://doi.org/10.1021/acs.analchem.9b04301>
- Kodama, S., Nishimoto, T., Yamamoto, N., Yogo, K. & Yamada, K. (2008). Development of a new pH-swing CO_2 mineralization process with a recyclable reaction solution [Publisher: Elsevier]. *Energy*, 33(5), 776–784. Retrieved June 7, 2022, from <https://ideas.repec.org/a/eee/energy/v33y2008i5p776-784.html>
- Kustov, A. V., Berezin, M. B. & Berezin, B. D. (2007). Enthalpies and heat capacities of dissolution for calcium chloride and sodium oxalate. *Russian Journal of Inorganic Chemistry*, 52(1), 129–130. <https://doi.org/10.1134/S0036023607010238>
- Lackner, K. S., Butt, D. P. & Wendt, C. H. (1997). Progress on binding CO_2 in mineral substrates. *Energy Conversion and Management*, 38, S259–S264. [https://doi.org/10.1016/S0196-8904\(96\)00279-8](https://doi.org/10.1016/S0196-8904(96)00279-8)
- Lackner, K. S., Wendt, C. H., Butt, D. P., Joyce, E. L. & Sharp, D. H. (1995). Carbon dioxide disposal in carbonate minerals. *Energy*, 20(11), 1153–1170. [https://doi.org/10.1016/0360-5442\(95\)00071-N](https://doi.org/10.1016/0360-5442(95)00071-N)
- Lee, J. H. & Lee, J. H. (2021). Techno-economic and environmental feasibility of mineral carbonation technology for carbon neutrality: A perspective. *Korean Journal of Chemical Engineering*, 38(9), 1757–1767. <https://doi.org/10.1007/s11814-021-0840-2>
- Lehtinen, E., Paulapuro, H. & Gullichsen, J. (2000). *Papermaking science and technology. book 11, pigment coating and surface sizing of paper*. Fapet Oy. Retrieved June 9, 2022, from <https://research.aalto.fi/en/publications/papermaking-science-and-technology-book-11-pigment-coating-and-su>

- Lemmens, S. (2016). Cost engineering techniques and their applicability for cost estimation of organic rankine cycle systems. *Energies*, 9, 485. <https://doi.org/10.3390/en9070485>
- Li, J., Paul, M. C., Younger, P. L., Watson, I., Hossain, M. & Welch, S. (2015). Characterization of biomass combustion at high temperatures based on an upgraded single particle model. *Applied Energy*, 156, 749–755. <https://doi.org/10.1016/j.apenergy.2015.04.027>
- Li, L., Liu, W., Qin, Z., Zhang, G., Yue, H., Liang, B., Tang, S. & Luo, D. (2021). Research on integrated CO₂ absorption-mineralization and regeneration of absorbent process. *Energy*, 222, 120010. <https://doi.org/10.1016/j.energy.2021.120010>
- Li, T., Keener, T. C. & Cheng, L. (2014). Carbon dioxide removal by using mg(OH)₂ in a bubble column: Effects of various operating parameters. *International Journal of Greenhouse Gas Control*, 31, 67–76. <https://doi.org/10.1016/j.ijggc.2014.09.027>
- Linnhoff, B. & Hindmarsh, E. (1983). The pinch design method for heat exchanger networks. *Chemical Engineering Science*, 38(5), 745–763. [https://doi.org/10.1016/0009-2509\(83\)80185-7](https://doi.org/10.1016/0009-2509(83)80185-7)
- Liu, W., Teng, L., Rohani, S., Qin, Z., Zhao, B., Xu, C. C., Ren, S., Liu, Q. & Liang, B. (2021). CO₂ mineral carbonation using industrial solid wastes: A review of recent developments. *Chemical Engineering Journal*, 416, 129093. <https://doi.org/10.1016/j.cej.2021.129093>
- Liu, Y. & Naidu, R. (2014). Hidden values in bauxite residue (red mud): Recovery of metals. *Waste Management*, 34(12), 2662–2673. <https://doi.org/10.1016/j.wasman.2014.09.003>
- Maier, W., Lahtinen, R. & O'Brien, H. (2015, January 1). *Mineral deposits of finland* [Pages: 792].
- Maizland, L. (2021, November 12). *Global climate agreements: Successes and failures* [Council on foreign relations]. Retrieved June 25, 2022, from <https://www.cfr.org/background/paris-global-climate-change-agreements>
- Maroto-Valer, M., Fauth, D., Kuchta, M., Zhang, Y. & Andrésen, J. (2005). Activation of magnesium rich minerals as carbonation feedstock materials for CO₂ sequestration. *Fuel Processing Technology*, 86(14), 1627–1645. <https://doi.org/10.1016/j.fuproc.2005.01.017>
- Martinez-Zarzoso, I. & Nowak-Lehmann, F. D. (2007). Is distance a good proxy for transport costs? the case of competing transport modes [<https://doi.org/10.1080/09638190701527186>]. *The Journal of International Trade & Economic Development*, 16(3), 411–434. <https://doi.org/10.1080/09638190701527186>
- Mattila, H.-P., Grigaliūnaitė, I. & Zevenhoven, R. (2012). Chemical kinetics modeling and process parameter sensitivity for precipitated calcium carbonate production from steelmaking slags. *Chemical Engineering Journal*, 192, 77–89. <https://doi.org/10.1016/j.cej.2012.03.068>
- Mattila, H.-P. & Zevenhoven, R. (2014, January 1). Chapter ten - production of precipitated calcium carbonate from steel converter slag and other calcium-containing industrial wastes and residues. In M. Aresta & R. van Eldik (Eds.), *Advances in inorganic chemistry* (pp. 347–384). Academic Press. <https://doi.org/10.1016/B978-0-12-420221-4.00010-X>
- Mazzotti, M., Abanades, J., Allam, R., Lackner, K., Meunier, F., Rubin, E., Sanchez, J., Yogo, K. & Zevenhoven, R. (2005). Mineral carbonation and industrial uses of carbon dioxide. *IPCC Special Report on Carbon Dioxide Capture and Storage*, 319–338.

- McGrail, B. P., Spane, F. A., Amonette, J. E., Thompson, C. R. & Brown, C. F. (2014). Injection and monitoring at the wallula basalt pilot project. *Energy Procedia*, 63, 2939–2948. <https://doi.org/10.1016/j.egypro.2014.11.316>
- Meng, J., Liao, W. & Zhang, G. (2021). Emerging CO₂-mineralization technologies for co-utilization of industrial solid waste and carbon resources in china [Number: 3 Publisher: Multidisciplinary Digital Publishing Institute]. *Minerals*, 11(3), 274. <https://doi.org/10.3390/min11030274>
- Mikkelsen, M., Jørgensen, M. & C. Krebs, F. (2010). The teraton challenge. a review of fixation and transformation of carbon dioxide [Publisher: Royal Society of Chemistry]. *Energy & Environmental Science*, 3(1), 43–81. <https://doi.org/10.1039/B912904A>
- Mun, M., Cho, H. & Kwon, J. (2017). Study on characteristics of various extractants for mineral carbonation of industrial wastes. *Journal of Environmental Chemical Engineering*, 5(4), 3803–3821. <https://doi.org/10.1016/j.jece.2017.05.048>
- Nguyen, H. V., Nakarai, K., Pham, K. H., Kajita, S. & Sagawa, T. (2020). Effects of slag type and curing method on the performance of expansive concrete. *Construction and Building Materials*, 262, 120422. <https://doi.org/10.1016/j.conbuildmat.2020.120422>
- NipponSlagAssociation. (2003). *Types of iron and steel slag*. Retrieved June 16, 2022, from <https://www.slg.jp/e/slag/kind.html>
- O'Connor, W., Dahlin, D., Rush, G., Gerdemann, S., Penner, L. & Nilsen, D. (2005). Aqueous mineral carbonation: Mineral availability, pretreatment, reaction parametrics, and process studies [Publisher: US DOE]. <https://doi.org/10.13140/RG.2.2.23658.31684>
- OpenModelica. (2022). *Tools - OpenModelica*. Retrieved June 25, 2022, from <https://www.openmodelica.org/openmodelicaworld/tools>
- Oppermann, G., Othmar, A., Kodel, J., Jutzeler, M. & Büchler, M. (2020, September 18). *Leitfaden - fernwärme/fernkälte*. Verband Fernwärme Schweiz. Bern. Retrieved June 26, 2022, from http://www.fernwaerme-schweiz.ch/fernwaerme-franz/Dienstleistungen/Leitfaden_Fernwaerme_Fernkaelte_200918.pdf
- Oskierski, H. C., Dlugogorski, B. Z. & Jacobsen, G. (2013). Sequestration of atmospheric CO₂ in chrysotile mine tailings of the woodsreef asbestos mine, australia: Quantitative mineralogy, isotopic fingerprinting and carbonation rates. *Chemical Geology*, 358, 156–169. <https://doi.org/10.1016/j.chemgeo.2013.09.001>
- Osman, A. I., Hefny, M., Abdel Maksoud, M. I. A., Elgarahy, A. M. & Rooney, D. W. (2021). Recent advances in carbon capture storage and utilisation technologies: A review. *Environmental Chemistry Letters*, 19(2), 797–849. <https://doi.org/10.1007/s10311-020-01133-3>
- Ostovari, H., Müller, L., Mayer, F. & Bardow, A. (2022). A climate-optimal supply chain for CO₂ capture, utilization, and storage by mineralization. *Journal of Cleaner Production*, 360, 131750. <https://doi.org/10.1016/j.jclepro.2022.131750>
- Owais, M., Yazdani, M. R. & Järvinen, M. (2021). Detailed performance analysis of the wet extractive grinding process for higher calcium yields from steelmaking slags. *Chemical Engineering and Processing - Process Intensification*, 166, 108489. <https://doi.org/10.1016/j.cep.2021.108489>

- Pan, Z. & Zhao, C. Y. (2015). Dehydration/hydration of MgO/h₂O chemical thermal storage system. *Energy*, 82, 611–618. <https://doi.org/10.1016/j.energy.2015.01.070>
- Pedraza, J., Zimmermann, A., Tobon, J., Schomäcker, R. & Rojas, N. (2021). On the road to net zero-emission cement: Integrated assessment of mineral carbonation of cement kiln dust. *Chemical Engineering Journal*, 408, 127346. <https://doi.org/10.1016/j.cej.2020.127346>
- Peduzzi, E. (2015). *Biomass to liquids: Thermo-economic analysis and multi-objective optimisation* (Doctoral dissertation). EPFL, Lausanne. <https://doi.org/10.5075/epfl-thesis-6529>
- Peltonen, P. (2006). *The 27th nordic geological winter meeting* (Vol. 78) [Google-Books-ID: zwIgwW EACAAJ]. Geological Society of Finland.
- Perez-Lopez, R., Montes-Hernandez, G., Nieto, J., Renard, F. & Charlet, L. (2008). Carbonation of alkaline paper mill waste to reduce CO₂ greenhouse gas emissions into the atmosphere. *Applied Geochemistry*, 23(8), 2292–2300. <https://doi.org/10.1016/j.apgeochem.2008.04.016>
- PerlenPaperAG. (2022). *Company – perlen papier AG*. Retrieved June 16, 2022, from <https://www.perlen.ch/en/company/>
- Pootakham, T. & Kumar, A. (2010). A comparison of pipeline versus truck transport of bio-oil. *Biore-source Technology*, 101(1), 414–421. <https://doi.org/10.1016/j.biortech.2009.07.077>
- Priestnall, M. (2018, May 8). *Method and system of activation of mineral silicate minerals* (U.S. pat. 9963351B2).
- Prigione, V., Costa, G., Baciocchi, R., Hanchen, M. & Mazzotti, M. (2009). The effect of CO₂ and salinity on olivine dissolution kinetics at 120°C. <https://doi.org/10.1016/J.CES.2009.04.035>
- Prigione, V., Hänchen, M., Werner, M., Baciocchi, R. & Mazzotti, M. (2009). Mineral carbonation process for CO₂ sequestration. *Energy Procedia*, 1(1), 4885–4890. <https://doi.org/10.1016/j.egypro.2009.02.318>
- Prigione, V., Polettini, A. & Baciocchi, R. (2009). Gas–solid carbonation kinetics of air pollution control residues for CO₂ storage. *Chemical Engineering Journal*, 148(2), 270–278. <https://doi.org/10.1016/j.cej.2008.08.031>
- Quina, M. J., Bontempi, E., Bogush, A., Schlumberger, S., Weibel, G., Braga, R., Funari, V., Hyks, J., Rasmussen, E. & Lederer, J. (2018). Technologies for the management of MSW incineration ashes from gas cleaning: New perspectives on recovery of secondary raw materials and circular economy. *Science of The Total Environment*, 635, 526–542. <https://doi.org/10.1016/j.scitotenv.2018.04.150>
- Rager, J. M. F. (2015). *Urban energy system design from the heat perspective using mathematical programming including thermal storage* (Doctoral dissertation). EPFL, Lausanne. <https://doi.org/10.5075/epfl-thesis-6731>
- Ragnheiðardóttir, E., Sigurðardóttir, H., Kristjansdóttir, H. & Harvey, W. (2011). Opportunities and challenges for CarbFix: An evaluation of capacities and costs for the pilot scale mineralization sequestration project at Hellisheidi, Iceland and beyond. *International Journal of Greenhouse Gas Control*, 4(5), 1065–1072. <https://doi.org/10.1016/j.ijggc.2010.11.010>

- Rammelberg, H. U., Schmidt, T. & Ruck, W. (2012). Hydration and dehydration of salt hydrates and hydroxides for thermal energy storage - kinetics and energy release. *Energy Procedia*, 30, 362–369. <https://doi.org/10.1016/j.egypro.2012.11.043>
- Rausis, K., Ćwik, A., Casanova, I. & Zarebska, K. (2021). Carbonation of high-ca fly ashes under flue gas conditions: Implications for their valorization in the construction industry [Number: 11 Publisher: Multidisciplinary Digital Publishing Institute]. *Crystals*, 11(11), 1314. <https://doi.org/10.3390/cryst11111314>
- Ravikumar, D., Zhang, D., Keoleian, G., Miller, S., Sick, V. & Li, V. (2021). Carbon dioxide utilization in concrete curing or mixing might not produce a net climate benefit [Number: 1 Publisher: Nature Publishing Group]. *Nature Communications*, 12(1), 855. <https://doi.org/10.1038/s41467-021-21148-w>
- Rendek, E., Ducom, G. & Germain, P. (2006). Carbon dioxide sequestration in municipal solid waste incinerator (MSWI) bottom ash. *Journal of Hazardous Materials*, 128(1), 73–79. <https://doi.org/10.1016/j.jhazmat.2005.07.033>
- Renergia. (2020). *Jahresbericht 2020*. Renergia Zentralschweiz AG. Perlen. Retrieved June 26, 2022, from https://www.renergia.ch/__/frontend/handler/document/42/203/renergia_jahresbericht_2020_low_FINAL.pdf
- Renforth, P. (2019). The negative emission potential of alkaline materials [Number: 1 Publisher: Nature Publishing Group]. *Nature Communications*, 10(1), 1401. <https://doi.org/10.1038/s41467-019-09475-5>
- Romanov, V., Soong, Y., Carney, C., Rush, G., Nielsen, B. & Oconnor, W. (2015). Mineralization of carbon dioxide: A literature review. *ChemBioEng Reviews*, 2, 231–256. <https://doi.org/10.1002/cben.201500002>
- Romão, I., Nduagu, E., Fagerlund, J., Gando-Ferreira, L. M. & Zevenhoven, R. (2012). CO₂ fixation using magnesium silicate minerals. part 2: Energy efficiency and integration with iron-and steelmaking. *Energy*, 41(1), 203–211. <https://doi.org/10.1016/j.energy.2011.08.026>
- Romero-Mujalli, G., Hartmann, J. & Börker, J. (2019). Temperature and CO₂ dependency of global carbonate weathering fluxes – implications for future carbonate weathering research. *Chemical Geology*, 527, 118874. <https://doi.org/10.1016/j.chemgeo.2018.08.010>
- Rosa, L., L. Sanchez, D. & Mazzotti, M. (2021). Assessment of carbon dioxide removal potential via BECCS in a carbon-neutral europe [Publisher: Royal Society of Chemistry]. *Energy & Environmental Science*, 14(5), 3086–3097. <https://doi.org/10.1039/D1EE00642H>
- Ruedisueli, M., Romano, E., Eggimann, S. & Patel, M. K. (2022). Decarbonization strategies for switzerland considering embedded greenhouse gas emissions in electricity imports. *Energy Policy*, 162, 112794. <https://doi.org/10.1016/j.enpol.2022.112794>
- Said, A. (2017). *CO₂ sequestration by steelmaking slags for the production of precipitated calcium carbonate* (Doctoral dissertation). Aalto University, Finland. Aalto.
- Salman, M., Cizer, O., Pontikes, Y., Santos, R. M., Snellings, R., Vandewalle, L., Blanpain, B. & Van Balen, K. (Eds.). (2014). Effect of accelerated carbonation on AOD stainless steel slag for its

- valorisation as a CO₂-sequestering construction material [Num Pages: 14 Place: Lausanne Publisher: Elsevier Science Sa]. *Chemical Engineering Journal*. <https://doi.org/10.1016/j.cej.2014.02.051>
- Sanna, A., Uibu, M., Caramanna, G., Kuusik, R. & M. Maroto-Valer, M. (2014). A review of mineral carbonation technologies to sequester CO₂ [Publisher: Royal Society of Chemistry]. *Chemical Society Reviews*, 43(23), 8049–8080. <https://doi.org/10.1039/C4CS00035H>
- Sanna, A., Dri, M., Hall, M. R. & Maroto-Valer, M. (2012). Waste materials for carbon capture and storage by mineralisation (CCSM) – a UK perspective. *Applied Energy*, 99, 545–554. <https://doi.org/10.1016/j.apenergy.2012.06.049>
- Sanna, A., Hall, M. R. & Maroto-Valer, M. (2012). Post-processing pathways in carbon capture and storage by mineral carbonation (CCSM) towards the introduction of carbon neutral materials [Publisher: The Royal Society of Chemistry]. *Energy & Environmental Science*, 5(7), 7781–7796. <https://doi.org/10.1039/C2EE03455G>
- Sanna, A., Lacinska, A., Styles, M. & Maroto-Valer, M. (2014). Silicate rock dissolution by ammonium bisulphate for pH swing mineral CO₂ sequestration. *Fuel Processing Technology*, 120, 128–135. <https://doi.org/10.1016/j.fuproc.2013.12.012>
- Sanna, A., Wang, X., Lacinska, A., Styles, M., Paulson, T. & Maroto-Valer, M. M. (2013). Enhancing mg extraction from lizardite-rich serpentinite for CO₂ mineral sequestration. *Minerals Engineering*, 49, 135–144. <https://doi.org/10.1016/j.mineng.2013.05.018>
- Sarapaa, O., Ahtola, T., Reinikainen, J. & Seppanen, H. (2003). INDUSTRIAL MINERAL POTENTIAL IN FINLAND. *Geological Survey of Finland*, 8.
- Sari, R. M. (2014). General process plant cost estimating - engineering design guidelines. *Kolmetz Handbook of Process Equipment Design*, 22.
- Schorcht, F., Kourti, I., Scalet, B. M., Roudier, S. & Sancho, L. D. (2013). *Best available techniques (BAT) reference document for the production of cement, lime and magnesium oxide* (EUR 26129 EN). European Commission. Retrieved April 9, 2018, from https://eippcb.jrc.ec.europa.eu/sites/default/files/2019-11/CLM_Published_def_0.pdf
- Scialom, M. (2020, December 4). *CO₂ captured in tiles: Cambridge carbon capture pilot under way* [Cambridge independent] [Section: Business]. Retrieved June 14, 2022, from <https://www.cambridgeindependent.co.uk/business/co2-captured-in-tiles-cambridge-carbon-capture-pilot-under-way-9144043/>
- Seeger, M., Otto, W., Flick, W., Bickelhaupt, F. & Akkerman, O. S. (2011). Magnesium compounds [ISSN: 1435-6007 _eprint: https://onlinelibrary.wiley.com/doi/pdf/10.1002/14356007.a15_595.pub2]. *Ullmann's encyclopedia of industrial chemistry*. John Wiley & Sons, Ltd. https://doi.org/10.1002/14356007.a15_595.pub2
- Seifritz, W. (1990). CO₂ disposal by means of silicates [Number: 6275 Publisher: Nature Publishing Group]. *Nature*, 345(6275), 486–486. <https://doi.org/10.1038/345486b0>
- Shen, H. & Forssberg, E. (2003). An overview of recovery of metals from slags. *Waste Management*, 23(10), 933–949. [https://doi.org/10.1016/S0956-053X\(02\)00164-2](https://doi.org/10.1016/S0956-053X(02)00164-2)

- Shin, C. & Criss, C. M. (1979). Standard enthalpies of formation of anhydrous and aqueous magnesium chloride at 298.15 K. *The Journal of Chemical Thermodynamics*, 11(7), 663–666. [https://doi.org/10.1016/0021-9614\(79\)90032-6](https://doi.org/10.1016/0021-9614(79)90032-6)
- Simonetti, D., La Plante, E. C., Sant, G., Wang, B., Alturki, A. & Bustillos, S. (2019, July 18). *Fine calcium carbonate production by CO2 mineralization of industrial waste brines*. Univ. of Wisconsin, Madison, WI (United States). Retrieved June 16, 2022, from <https://www.osti.gov/biblio/1544762-fine-calcium-carbonate-production-co2-mineralization-industrial-waste-brines>
- Sinha, A. (2020, May 20). *Procédé mécano-chimique pour produire des nanoparticules exfoliées* (European pat. 3652109A1).
- Snaebjörnsdóttir, S., Gislason, R. & Oelkers, E. H. (2020). MINERAL STORAGE OF CO₂, 24.
- Snaebjörnsdóttir, S. Ó., Oelkers, E. H., Mesfin, K., Aradóttir, E. S., Dideriksen, K., Gunnarsson, I., Gunnlaugsson, E., Matter, J. M., Stute, M. & Gislason, S. R. (2017). The chemistry and saturation states of subsurface fluids during the in situ mineralisation of CO₂ and H₂S at the CarbFix site in SW-Iceland. *International Journal of Greenhouse Gas Control*, 58, 87–102. <https://doi.org/10.1016/j.ijggc.2017.01.007>
- Spinola, A. C., Pinheiro, C. T., Ferreira, A. G. M. & Gando-Ferreira, L. M. (2021). Mineral carbonation of a pulp and paper industry waste for CO₂ sequestration. *Process Safety and Environmental Protection*, 148, 968–979. <https://doi.org/10.1016/j.psep.2021.02.019>
- Sun, Y., Yao, M.-S., Zhang, J.-P. & Yang, G. (2011). Indirect CO₂ mineral sequestration by steelmaking slag with NH₄Cl as leaching solution. *Chemical Engineering Journal*, 173(2), 437–445. <https://doi.org/10.1016/j.cej.2011.08.002>
- Survey, U. G. (2020). *Mineral commodity summaries 2020*. Retrieved June 12, 2022, from <https://doi.org/10.3133/mcs2020>
- swissinfo.ch, (f. i. b. T. S. (2020). *Switzerland and EU link CO2 emissions trading schemes* [SWI swissinfo.ch]. Retrieved June 19, 2022, from https://www.swissinfo.ch/eng/politics/climate-and-emissions_switzerland-and-eu-link-co2-emissions-trading-schemes/45514934
- Syc, M., Simon, F. G., Hyks, J., Braga, R., Biganzoli, L., Costa, G., Funari, V. & Grosso, M. (2020). Metal recovery from incineration bottom ash: State-of-the-art and recent developments. *Journal of Hazardous Materials*, 393, 122433. <https://doi.org/10.1016/j.jhazmat.2020.122433>
- Système d'échange de quotas d'émission de l'UE (SEQE-UE)*. (2022). Retrieved June 19, 2022, from https://ec.europa.eu/clima/eu-action/eu-emissions-trading-system-eu-ets_fr
- Tanzer, S. E., Blok, K. & Ramírez, A. (2021). Curing time: A temporally explicit life cycle CO₂ accounting of mineralization, bioenergy, and CCS in the concrete sector [Publisher: The Royal Society of Chemistry]. *Faraday Discussions*, 230(0), 271–291. <https://doi.org/10.1039/D0FD00139B>
- Teir, S., Auvinen, T., Said, A., Kotiranta, T. & Peltola, H. (2016). Performance of separation processes for precipitated calcium carbonate produced with an innovative method from steelmaking slag and carbon dioxide. *Frontiers in Energy Research*, 4, 6. <https://doi.org/10.3389/fenrg.2016.00006>

- Teir, S., Eloneva, S., Fogelholm, C. J. & Zevenhoven, R. (2009). Fixation of carbon dioxide by producing hydromagnesite from serpentinite. *Applied Energy*, 86(2), 214–218. <https://doi.org/10.1016/j.apenergy.2008.03.013>
- Teir, S., Eloneva, S., Fogelholm, C.-J. & Zevenhoven, R. (2006). Stability of calcium carbonate and magnesium carbonate in rainwater and nitric acid solutions. *Energy Conversion and Management*, 47(18), 3059–3068. <https://doi.org/10.1016/j.enconman.2006.03.021>
- Teir, S., Eloneva, S., Fogelholm, C.-J. & Zevenhoven, R. (2007). Dissolution of steelmaking slags in acetic acid for precipitated calcium carbonate production. *Energy*, 32(4), 528–539. <https://doi.org/10.1016/j.energy.2006.06.023>
- Teir, S., Kettle, J., Harlin, A. & Sarlin, J. (2010). Production of silica and calcium carbonate particles from silicate minerals for ink jet paper coating and filler purposes: ACEME10 third international conference on accelerated carbonation for environmental and materials engineering [Place: Turku Publisher: Åbo Akademi]. *3th International Conference on accelerated carbonation for environmental and materials engineering*, 63–74.
- Teir, S., Revitzer, H., Eloneva, S., Fogelholm, C.-J. & Zevenhoven, R. (2007). Dissolution of natural serpentinite in mineral and organic acids. *International Journal of Mineral Processing*, 83(1), 36–46. <https://doi.org/10.1016/j.minpro.2007.04.001>
- Tock, L. (2013). *OSMOSE - tool for process integration and optimization* (Industrial Process and Energy Systems Engineering Ecole Polytechnique Fédérale de Lausanne) [Industrial Process and Energy Systems Engineering Ecole Polytechnique Fédérale de Lausanne]. Retrieved June 21, 2022, from https://www.epfl.ch/labs/ipese/wp-content/uploads/2018/07/intro_osmose.pdf
- Tomohiro, H. (2021). Latest developments in steelmaking capacity. *OECD Steel Committee*, 67. <https://www.oecd.org/industry/ind/latest-developments-in-steelmaking-capacity-2021.pdf>
- Turton, R., Shaeiwitz, J. A., Bhattacharyya, D. & Whiting, W. B. (2018). *Analysis, synthesis, and design of chemical processes* [OCLC: 1047957540].
- Uhlrich, G. D. & Wiley, J. (1984). *A guide to chemical engineering process design and economics* (Vol. 30) [eprint: <https://onlinelibrary.wiley.com/doi/pdf/10.1002/aic.690300636>]. Retrieved May 26, 2022, from <https://onlinelibrary.wiley.com/doi/abs/10.1002/aic.690300636>
- Ukwattage, N., P.G, R., Yellishetty, M., Bui, H. & Xu, T. (2014). A laboratory-scale study of the aqueous mineral carbonation of coal fly ash for CO₂ sequestration. *Journal of Cleaner Production*, 103. <https://doi.org/10.1016/j.jclepro.2014.03.005>
- UNCTAD. (2022). *UNCTADstat - united nations conference on trade and development database*. Retrieved June 30, 2022, from <https://unctadstat.unctad.org/EN/Index.html>
- Van, M. D., Quaghebeur, M. & Nielsen, P. (2020, March 25). *Procédé de production d'article lié comportant un matériau granulaire carbonaté, moulé en presse* (European pat. 2771305B9).
- Van Pham, T. H., Aagaard, P. & Hellevang, H. (2012). On the potential for CO₂ mineral storage in continental flood basalts – PHREEQC batch- and 1d diffusion–reaction simulations. *Geochemical Transactions*, 13, 5. <https://doi.org/10.1186/1467-4866-13-5>

- Velts, O., Uibu, M., Kallas, J. & Kuusik, R. (2011). Waste oil shale ash as a novel source of calcium for precipitated calcium carbonate: Carbonation mechanism, modeling, and product characterization. *Journal of Hazardous Materials*, 195, 139–146. <https://doi.org/10.1016/j.jhazmat.2011.08.019>
- Wallerand, A. S. (2018). *Integration of solar energy with industrial processes* (Doctoral dissertation). EPFL. Lausanne. <https://doi.org/10.5075/epfl-thesis-8635>
- Walters, J. (2016, February 15). *SkyMine beneficial CO2 use project*. Skyonic Corporation, Austin, TX (United States). <https://doi.org/10.2172/1241314>
- Wang, L., Sun, N., Tang, H. & Sun, W. (2019). A review on comprehensive utilization of red mud and prospect analysis [Number: 6 Publisher: Multidisciplinary Digital Publishing Institute]. *Minerals*, 9(6), 362. <https://doi.org/10.3390/min9060362>
- Wang, X. & Maroto-Valer, M. M. (2011a). Dissolution of serpentine using recyclable ammonium salts for CO2 mineral carbonation. *Fuel*, 90(3), 1229–1237. <https://doi.org/10.1016/j.fuel.2010.10.040>
- Wang, X. & Maroto-Valer, M. M. (2011b). Integration of CO2 capture and mineral carbonation by using recyclable ammonium salts. *ChemSusChem*, 4(9), 1291–1300. <https://doi.org/10.1002/cssc.201000441>
- Weibel, G., Zappatini, A., Wolffers, M. & Ringmann, S. (2021). Optimization of metal recovery from MSWI fly ash by acid leaching: Findings from laboratory- and industrial-scale experiments [Number: 2 Publisher: Multidisciplinary Digital Publishing Institute]. *Processes*, 9(2), 352. <https://doi.org/10.3390/pr9020352>
- Wendt, C. H., Butt, D. P., Lackner, K. S. & Ziock, H.-J. (1999). Thermodynamic considerations of using chlorides to accelerate the carbonate formation from magnesium silicates. *Greenhouse gas control technologies 4* (pp. 349–354). Elsevier. <https://doi.org/10.1016/B978-008043018-8/50056-4>
- Wernet, G., Bauer, C., Steubing, B., Reinhard, J., Moreno-Ruiz, E. & Weidema, B. (2016). The ecoinvent database version 3 (part i): Overview and methodology. *The International Journal of Life Cycle Assessment*, 21(9), 1218–1230. <https://doi.org/10.1007/s11367-016-1087-8>
- White, S. K., Spane, F. A., Schaef, H. T., Miller, Q. R. S., White, M. D., Horner, J. A. & McGrail, B. P. (2020). Quantification of CO2 mineralization at the wallula basalt pilot project [Publisher: American Chemical Society]. *Environmental Science & Technology*, 54(22), 14609–14616. <https://doi.org/10.1021/acs.est.0c05142>
- Woodall, C. M., McQueen, N., Pilorgé, H. & Wilcox, J. (2019). Utilization of mineral carbonation products: Current state and potential [eprint: <https://onlinelibrary.wiley.com/doi/pdf/10.1002/ghg.1940>]. *Greenhouse Gases: Science and Technology*, 9(6), 1096–1113. <https://doi.org/10.1002/ghg.1940>
- Xie, W.-H., Li, H., Yang, M., He, L.-N. & Li, H.-R. (2022). CO2 capture and utilization with solid waste. *Green Chemical Engineering*, 3(3), 199–209. <https://doi.org/10.1016/j.gce.2022.01.002>

- Xu, J., Li, T., Yan, T., Chao, J. & Wang, R. (2021). Dehydration kinetics and thermodynamics of magnesium chloride hexahydrate for thermal energy storage. *Solar Energy Materials and Solar Cells*, 219, 110819. <https://doi.org/10.1016/j.solmat.2020.110819>
- Yablonsky, A., Germain, A. & Stola, A. (2018, August 21). *Water recycling in a CO₂ removal process and system* (U.S. pat. 10052584B2).
- Yablonsky, A., Stola, A., Germain, A. & Jones, J. (2018, May 15). *Systems and methods for acid gas removal from a gaseous stream* (U.S. pat. 9968883B2).
- Yadav, V. S., Prasad, M., Khan, J., Amritphale, S. S., Singh, M. & Raju, C. B. (2010). Sequestration of carbon dioxide (CO₂) using red mud. *Journal of Hazardous Materials*, 176(1), 1044–1050. <https://doi.org/10.1016/j.jhazmat.2009.11.146>
- Yan, H., Zhang, J., Zhao, Y. & Zheng, C. (2013). CO₂ sequestration from flue gas by direct aqueous mineral carbonation of wollastonite. *Science China Technological Sciences*, 56(9), 2219–2227. <https://doi.org/10.1007/s11431-013-5318-y>
- Yi, H., Xu, G., Cheng, H., Wang, J., Wan, Y. & Chen, H. (2012). An overview of utilization of steel slag. *Procedia Environmental Sciences*, 16, 791–801. <https://doi.org/10.1016/j.proenv.2012.10.108>
- Yuen, Y. T., Sharratt, P. N. & Jie, B. (2016). Carbon dioxide mineralization process design and evaluation: Concepts, case studies, and considerations. *Environmental Science and Pollution Research*, 23(22), 22309–22330. <https://doi.org/10.1007/s11356-016-6512-9>
- Zappa, W. (2014). *Pilot-scale experimental work on the production of precipitated calcium carbonate (PCC) from steel slag for CO₂ fixation* (Doctoral dissertation). Aalto University, Finland. Aalto.
- Zevenhoven, R., Kohlmann, J. & Mukherjee, A. B. (2002). *Direct dry mineral carbonation for CO₂ emissions reduction in finland* [27th International Technical Conference on Coal Utilization & Fuel Systems Clearwater (FL)].
- Zevenhoven, R., Slotte, M., Åbacka, J. & Highfield, J. (2016). A comparison of CO₂ mineral sequestration processes involving a dry or wet carbonation step. *Energy*, 117, 604–611. <https://doi.org/10.1016/j.energy.2016.05.066>
- Zhan, B. J., Xuan, D. X., Poon, C. S. & Shi, C. J. (2016). Effect of curing parameters on CO₂ curing of concrete blocks containing recycled aggregates. *Cement and Concrete Composites*, 71, 122–130. <https://doi.org/10.1016/j.cemconcomp.2016.05.002>
- Zhang, J., Zhang, R., Geerlings, H. & Bi, J. (2010). A novel indirect wollastonite carbonation route for CO₂ sequestration [eprint: <https://onlinelibrary.wiley.com/doi/pdf/10.1002/ceat.201000024>]. *Chemical Engineering & Technology*, 33(7), 1177–1183. <https://doi.org/10.1002/ceat.201000024>
- Zhang, S., Zhuang, Y., Tao, R., Liu, L., Zhang, L. & Du, J. (2020). Multi-objective optimization for the deployment of carbon capture utilization and storage supply chain considering economic and environmental performance. *Journal of Cleaner Production*, 270, 122481. <https://doi.org/10.1016/j.jclepro.2020.122481>

- Zhang, T., Chu, G., Lyu, J., Cao, Y., Xu, W., Ma, K., Song, L., Yue, H. & Liang, B. (2022). CO₂ mineralization of carbide slag for the production of light calcium carbonates. *Chinese Journal of Chemical Engineering*, 43, 86–98. <https://doi.org/10.1016/j.cjche.2022.02.011>
- Zhang, X., Asselin, E. & Li, Z. (2021). CaCO₃ precipitation kinetics in the system CaCl₂–CO₂–mg(OH)₂–h₂O for comprehensive utilization of soda production wastes [Publisher: American Chemical Society]. *ACS Sustainable Chemistry & Engineering*, 9(1), 398–410. <https://doi.org/10.1021/acscuschemeng.0c07467>
- Zhao, Q., Liu, C.-j., Jiang, M.-f., Saxén, H. & Zevenhoven, R. (2015). Preparation of magnesium hydroxide from serpentinite by sulfuric acid leaching for CO₂ mineral carbonation. *Minerals Engineering*, 79, 116–124. <https://doi.org/10.1016/j.mineng.2015.06.002>
- Zhao, Y. & Vidal, J. (2020). Potential scalability of a cost-effective purification method for MgCl₂-containing salts for next-generation concentrating solar power technologies. *Solar Energy Materials and Solar Cells*, 215, 110663. <https://doi.org/10.1016/j.solmat.2020.110663>
- Zohdy, K., Kareem, M. & Abdel-Aal, H. (2013). Separation of magnesium chloride from sea water by preferential salt separation (PSS). *Int J Bioassays*, 2, 376–378.
- Zondag, H. A., Van Essen, V. M., Bleijendaal, L. P. J., Kikkert, B. W. J. & Bakker, M. (2010). Application of MgCl₂·6H₂O for thermochemical seasonal solar heat storage. Retrieved June 30, 2022, from <https://www.osti.gov/etdeweb/biblio/21369618>
- Zucha, W., Weibel, G., Wolffers, M. & Eggenberger, U. (2020). Inventory of MSWI fly ash in Switzerland: Heavy metal recovery potential and their properties for acid leaching [Num Pages: 13 Number: 12 Publisher: MDPI]. *Processes*, 8(12), 1668. Retrieved June 17, 2022, from <https://boris.unibe.ch/156328/>

Appendix A

***Carbonpathway* library documentation**

CarbonpathwayLibraryDoc

Last updated by | Julie Dutoit | 22. Juni 2022 at 14:39 MESZ

Contents

- [Structure](#)
- [Conventions](#)
- [Modeling/simulation best-practices](#)
- [Documenting the models](#)
- [Notes](#)

This file summarizes the models structure, conventions and best practices applied in the **Carbonpathway** library, in order to develop the most unified and structurally resembling models possible.

To open the library, the fastest way is to open the package.mo file in the Carbonpathway folder.

Structure




- Each package should be hierarchically stored into separated folders, to eliminate lag when saving changes and enable practical use with Git.
- Typically, a library package contains the models of interest
 - *_data_temp record file* listing the parameters of interest and their default value. Generally, this default value is null in order not to account values without actively selecting them as project assumptions (exceptions might be thermodynamic or physical properties of resources/components).
 - *_data sub-package with record files* that can be used to overwrite the template.
 - A "test" model can be included to have a determined system of the model, and a sub-package
 - *_Variations* can be added, containing extended versions of the main models in the package.

Conventions

- *Abbreviations* :
 - Mass flows : MF
 - Mass fraction : SO_x, Ar, H₂ (even for H₂ in H₂), etc. Convention : mass concentration in fraction for this Modelica library.
 - P : Pressure, T : Temperature, Density : Density,
 - Cost parameters : CapexA, CapexB, CapexC for CAPEX, MaintVar / MaintFix for Maintenance variable / fixed costs, EmissionFactor for variable Environmental impacts, etc.
 - Heat : ThermEff, SpecHeatIn, SpecHeatOut (and not SpecCool, which is reserved for Refrigeration terminology), TempHeatOut
 - Power/Electric energy : PowerEff, SpecElecIn, PowerType, Voltage
 - Unit efficiency : ElectrolyzerEff, CarbEffA, CarbEffB, CHPPowerEff, etc.

- Reactors : Temperature, Pressure, etc. : general data like this stands for the state inside the reactor (OD, very basic).
- ResidenceTime : Detention, retention, residence time in a volume.
- Resources/utilities prices : PowerRev, WaterCost, etc.
- *Units and sign* :
 - Base units : kg, J, Pa, degC, s, W
 - Flows going out of units are defined as negative, flows coming in are positive.
- *Economics* :
 - All buying/selling prices are given in absolute values. The end sign of a cash flow is positive if it is an expense, and negative if it is benefit. The sign is taken into account in the sink/source model.
 - Resource streams material cost/revenue prices are not stored in Streams_economics_temp anymore, but in their own data folder in order to be easily modulable.
 - _CashFlow variables contain the accumulation of a certain resource's OPEX array, so is in USD.
- *Connector attributes* : attributes variables of connectors are generally defined as stream variables, except for :
 - Gases connectors : Pressure
 - Power connector : PowerType and Voltage (defined systematically in power sink and source units, and they are separated by transformer)

Modeling/simulation best-practices

- Stream variables should have an uppercase for the 1st letter. In order for the name to be readable, it can and should contain several uppercases (e.g. ThermEff).
- In order to take into account the cost accounting structures (for which the connections are hidden), make sure to include the commented lines in the Accounting.mo file.
- The users should ensure they are using proper values stored in record files : always check the data templates to be aware of values taken into account.
- Relative paths are a somewhat trickier subject on OM : for images, the relative use of url (with "modelica://") can be used, but not for .txt files (see <https://openmodelica.org/forum/default-topic/1704-on-relative-file-paths> , <https://www.openmodelica.org/forum/default-topic/2573-relative-filepath>  and <https://build.openmodelica.org/Documentation/Modelica.Utilities.Files.loadResource.html>)  so the user might use *parameter String filedir = Modelica.Utilities.Files.loadResource("modelica://Carbonpathway")*.

Documenting the models

To document the models you can press the *i* icon (see figure below).

There are three different information displayed:

- **Header:**
 - Author : *yourName*
 - Version : *ModelVersion*

- as a convention use 0.x for unfinished models, and then the first denominator for major changes and the second for minor ones

Author : _
Version : _._

- **Information:**

- Description
 - You can describe your model in here
- Sources:
 - To link to references, add the DOI (preferably, as it is a permanent link) and the date.

Description:

Sources:

- **Revisions**, all separated by tabs:

0.0 xx.xx.xxxx John Wayne Comment

See the documentation template in the DocTemplate.txt.

The screenshot displays a software interface with two main panes. The left pane, titled 'CompleteModel_no_link', shows a code editor with the following content:

```

169 model CompleteModel_no_link "comment displayed in the info"
170 parameter Real InputA=222;
171 parameter Real InputB=111;
172 parameter Real test;
173
174 Real model_variable_C;
175 Real model_variable_B;
176 Real model_variable_A;
177
178 equation
179   model_variable_C = model_variable_A * 5 - model_variable_B * 6;
180   model_variable_A = InputA * 1.0;
181   // model_variable_A = InputA; does not work...
182   model_variable_B = InputB * 5;
183   annotation( ... )
184   </body></html>", revisions = "<html><head></
185   head><body>0.1<span class=\"Apple-tab-span\" style=\"white-

```

The right pane, titled 'Documentation Browser', shows the 'Example.CompleteModel_no_link' page. It includes sections for 'Information', 'Description', 'Sources', and 'Revisions'. The 'Revisions' section contains a table with the following data:

Version	Date	Author	Comment
0.1	01.03.2022	Rafael Graf	This model is not complete and does not work
0.2	24.03.2022	Rafael Graf	added some stuff
1.0	24.03.2022	Rafael Graf	First working model

Notes

- Heat connector : contain all data (for now : inlet and outlet T°, load for each state or state change) necessary to do the heat integration basics. Improvements could include addition of minimum approach temperature (DTmin) for HEX.